



KIT SCIENTIFIC REPORTS 7642

Tritium transport analysis in HCPB DEMO blanket with the FUS-TPC Code

Fabrizio Franza

Fabrizio Franza

Tritium transport analysis in HCPB DEMO blanket with the FUS-TPC Code

Karlsruhe Institute of Technology
KIT SCIENTIFIC REPORTS 7642

Tritium transport analysis in HCPB DEMO blanket with the FUS-TPC Code

by
Fabrizio Franza

Report-Nr. KIT-SR 7642

Hinweis

Die vorliegende wissenschaftliche Kurzdarstellung wurde im Auftrag des Umweltministeriums Baden-Württemberg durchgeführt.
Die Verantwortung für den Inhalt dieser Veröffentlichung liegt bei den Autoren.

Impressum

Karlsruher Institut für Technologie (KIT)
KIT Scientific Publishing
Straße am Forum 2
D-76131 Karlsruhe
www.ksp.kit.edu

KIT – Universität des Landes Baden-Württemberg und
nationales Forschungszentrum in der Helmholtz-Gemeinschaft



Diese Veröffentlichung ist im Internet unter folgender Creative Commons-Lizenz
publiziert: <http://creativecommons.org/licenses/by-nc-nd/3.0/de/>

KIT Scientific Publishing 2013
Print on Demand

ISSN 1869-9669
ISBN 978-3-7315-0012-4

Abstract

In thermonuclear fusion reactors, the fuel is an high temperature deuterium-tritium plasma, in which tritium is bred by lithium isotopes present inside solid ceramic breeder (e.g. Li-Orthosilicate) or inside liquid eutectic alloys (e.g. Pb-16Li alloy). In the breeding areas a significant fraction of the tritium produced is extracted out from the Breeding Zone by the He gas purging the breeding ceramic in the Helium Cooled Pebble Bed (HCPB) blanket concept or transported in solution by the owing alloy in the Helium Cooled Lead Lithium (HCLL) blanket concept.

Tritium produced in the breeding blanket by neutrons interacting with lithium nuclei can enter the metal structures, and can be lost by permeation to the environment. Tritium in metallic components should therefore be kept under close control throughout the fusion reactor lifetime, bearing in mind the risk of accidents and the need for maintenance.

In this study the problem of tritium transport in HCPB DEMO blanket from the generation inside the solid breeder to the release into the environment has been studied and analyzed by means of the computational code FUS-TPC (Fusion Devoted-Tritium Permeation Code). The code has been originally developed to study the tritium transport in HCLL blanket and it is a new fusion-devoted version of the fast-fission one called Sodium-Cooled Fast Reactor Tritium Permeation Code (SFR-TPC). The main features of the model inside the code are described. The code has the main goal to estimate the total tritium losses into the environment and the tritium inventories inside the breeder, inside the multiplier, inside the purge gas and the main coolant loops and inside the structural materials.

Different simulations of the code were performed by adopting the configuration of the European HCPB blanket for DEMO.

Total tritium losses from a generic fusion power plant, is often considered a key parameter to evaluate the tritium containment capabilities (added to tritium inventories) of a certain nuclear plant. Without any tritium control techniques, permeation can be quite significant, thus some tritium transport mitigation devices are required. The code is able to model and compute different tritium fluxes exchanged in the overall tritium system. A sensitivity study for the tritium losses and inventories is performed in this work.

Contents

Abstract.....	I
Figures	V
Tables.....	VII
Acronyms and Abbreviations.....	IX
1 Introduction.....	1
2 Description of HCPB DEMO Blanket.....	3
3 Description of the Model.....	7
3.1 Tritium Fluxes Extracted by TES and CPS	10
3.2 Isotope Exchange Rate.....	12
3.3 Permeation Fluxes.....	14
3.3.1 Theory on Hydrogen Isotopes Permeation.....	14
3.3.2 Tritium Permeation Flux through CPs Cooling Channels.....	17
3.3.3 Tritium Permeation Flux from Implanted Tritons onto First Wall.....	18
3.3.4 Tritium Permeation Flux though Steam Generator Tube Walls	20
3.4 Tritium Flux Associated to Helium Leaks.....	21
3.5 Tritium Losses and Inventories	21
3.5.1 Tritium Inventories.....	22
3.5.2 Tritium Losses into the Environment.....	26
4 Results and Discussions	27
4.1 Material Properties, Input Data and Main Assumptions.....	27
4.1.1 Definition of the Limiting Regime for Tritium Permeation	28
4.1.2 Material Properties Database	29
4.1.3 Input Data for the HCPB DEMO Blanket Operative Conditions.....	31
4.2 Results for the Operative Blanket Configuration.....	33
4.2.1 Tritium Concentrations and Partial Pressures Vs. Time	33

4.2.2	Tritium Inventories Vs. Time	35
4.2.3	Tritium Losses Vs. Time	37
4.3	Impact of the Main Assumptions on the Results	39
4.3.1	Oxidized Vs. Clean SG Walls Surfaces	39
4.3.2	Diffusion Vs. Surface-Limited Permeation Regime	42
4.3.3	Presence Vs. Absence of a FW Coating Layer	47
4.4	Main Parameters for Tritium Migration in HCPB DEMO Blanket	49
4.4.1	Tritium Losses and Inventories Vs. TES Efficiency.....	50
4.4.2	Tritium Losses and Inventories Vs. CPS Efficiency.....	51
4.4.3	Tritium Losses and Inventories Vs. CPS Recirculation Rate.....	52
4.4.4	Tritium Losses and Inventories Vs. PRF on CPs	55
4.4.5	Tritium Losses and Inventories Vs. PRF on SG Tubes	57
4.4.6	Overall Summary of the Parametric Study	59
	Summary and Conclusions	63
	References.....	71

Figures

Figure 2-1 Basic Layout of HCPB Breeder Blanket.....	4
Figure 2-2 Reference Scheme for Tritium Transport in HCPB Blanket.....	5
Figure 3-1 H ₂ Permeation Vs. Pressure through Ferritic Steel [11]	15
Figure 3-2 Overall Permeation Behavior of Hydrogen Gases through Metals [13].....	16
Figure 3-3 Fractional Tritium Release from Neutrons Irradiated Be [21]	25
Figure 4-1 Different Adsorption Constants in MANET Steels Vs. 1000/T.....	29
Figure 4-2 HT and HTO Concentrations in Purge Gas and Coolant Loops Vs. Time	34
Figure 4-3 HT Partial Pressures in Purge gas and Coolant Loops Vs. Time	35
Figure 4-4 Tritium Inventories Vs. Time.....	36
Figure 4-5 Tritium Losses Vs. Time.....	38
Figure 4-6 Tritium Losses Vs. Time for Clean and Oxidized SG Tubes Conditions.....	40
Figure 4-7 Tritium Inventories Vs. Time for Clean and Oxidized SG Tubes Conditions ..	41
Figure 4-8 Normalized Tritium Losses Vs. Time Vs. Permeation Regime.....	44
Figure 4-9 Tritium Inventories Vs. Time Vs. Permeation Regimes	46
Figure 4-10 Tritium Losses Vs. Time Vs. Thickness of FW Coating Layer.....	47
Figure 4-11 Total T Inventories Vs. Time Vs. Thickness of FW Coating Layer	48
Figure 4-12 Steady State T Losses and Inventories Vs. TES Efficiency.....	51
Figure 4-13 Steady State T Losses and Inventories Vs. CPS Efficiency.....	52
Figure 4-14 Steady State T Losses and Inventories Vs. CPS Recirculation Rate.....	53
Figure 4-15 Steady State T losses and Inventories Vs. PRF on CPs	56
Figure 4-16 Steady State T Losses and Inventories Vs. PRF on SG Tubes	58
Figure 4-17 Tritium Losses Vs. α_{CPS} Vs. PRF_{CP} Vs. $T k_{rec}$. in SG tubes	60

Tables

Table 2-1 Main Features of HCPB Blanket [8]	6
Table 3-1 Description of Tritium Fluxes in HCPB Blanket.....	8
Table 4-1 FUS-TPC Material Properties	30
Table 4-2 Geometric Input Data for Tritium Assessment in HCPB Blanket.....	31
Table 4-3 Main Features of Tritium System in HCPB DEMO Blanket	31
Table 4-4 FUS-TPC Input Data for FUS-TPC Simulations	32
Table 4-5 Steady State T Concentrations and Partial Pressures	34
Table 4-6 Steady State Tritium Inventories Vs. Time in all the Blanket Locations	36
Table 4-7 Steady State T Losses and Inventories for Clean and Oxidized SG Tubes	42
Table 4-8 Steady State Tritium Losses for all the Permeation Regime Scenarios	44
Table 4-9 Steady State Tritium Inventories for all the Permeation Regime Scenarios.....	45
Table 4-10 Steady State T Losses and Inventories Vs. Thickness of FW Coating Layer ...	48
Table 4-11 Summary Results of the Sensitivity Study	59

Acronyms and Abbreviations

- BU Breeding Unit
- CP Cooling Plate
- CPS Coolant Purification System
- EOL End Of Life
- FPP Fusion Power Plant
- FUS-TPC FUSion devoted-Tritium Permeation Code
- FW First Wall
- HCLL Helium Cooled Lead-Lithium
- HCPB Helium Cooled Pebble Bed
- HCS Helium Coolant System
- LOCA LOss of Coolant Accident
- PCS Power Conversion System
- R&D Research and Development
- PRF Permeation Reduction Factor
- SFR-TPC Sodium-Cooled Fast Reactor-Tritium Permeation Code
- SG Steam Generator
- TBM Test Blanket Module
- TBR Tritium Breeder Ratio
- TES Tritium Extraction System

1 Introduction

The management of tritium and the related transport analysis in the overall tritium cycle are key issues for DEMO and future fusion reactors. The most efficient way to provide tritium in steady state is to produce it directly inside the fusion reactor and to recover it. In order to achieve this goal, specific breeding blankets are used.

Tritium production occurs following the reactions: ${}^6\text{Li} + n \rightarrow {}^3\text{H} + {}^4\text{He} + 4.8 \text{ MeV}$ [1] and $n + {}^7\text{Li} \rightarrow {}^3\text{H} + {}^4\text{He} + n' - 2.5 \text{ MeV}$ [1]. The nuclear cross section of the first breeding reaction ${}^6\text{Li}(n, \alpha) {}^3\text{H}$ increases as the neutron energy decreases. Moreover, in a practical reactor, there are always some unavoidable neutron losses. For these reasons in fusion reactor breeding blanket some neutron multiplier and moderator is required (e.g. Beryllium in Helium Cooled Pebble Bed blanket and Lead in Helium Cooled Lead-Lithium blanket) by taking advantage from his interaction with fast neutrons which leads to the neutron multiplication reaction $(n, 2n)$, while lithium is needed for tritium breeding inside the fusion reactor. In particular, Beryllium has a great attitude to attenuate fast neutron.

Tritium is generated inside the breeder and moves with several mechanisms (e.g. permeation, adsorption, etc.) and potentially might reach the environment, giving a potential radiological hazard. Thus, the objective of this work is to evaluate the tritium inventories inside several components of the tritium management system in blanket (e.g. inside the breeder, inside Beryllium and inside the coolant loop) and the tritium losses into the environment, adopting a DEMO blanket configuration based on a solid breeder (e.g. lithium Orthosilicate Li_4SiO_4); the Helium Cooled Pebble Bed (HCPB) blanket. In this code, it has been adopted a simplified diffusion (or surface)-limited permeation model, with a series of simplifying and conservative assumptions, in order to solve the mass balance equations of different tritium species inside different HCPB blanket locations; however, more complicated models should be foreseen.

In order to perform this study, a tritium permeation analysis code (FUS-TPC) has been used. The code has been firstly developed in 2011 to analyze tritium transport in the European configuration of the HCLL blanket for DEMO [2]. FUS-TPC is a new simplified fusion-devoted version of the fast-fission one called SFR-TPC [3], developed to study tritium inventories and losses from Sodium-Cooled Fast Reactors (SFRs). The MATLAB computational tool was used to develop this code. The FUS-TPC is based on mass

1. Introduction

balance equation regarding various chemical forms of tritium (i.e. T^- , HT and HTO), coupled with a variety of tritium sources, sinks, and permeation models.

2 Description of HCPB DEMO Blanket

A detailed description of HCPB DEMO blanket design specifications is reported in Ref. [4].

The helium cooled pebble bed (HCPB) blanket is one of two concepts selected in the frame of the European Blanket Programme to be tested during the different ITER experimental phases.

The Helium Cooled Pebble Bed concept has been developed in Karlsruhe Institute of Technology (KIT, formerly Forschungszentrum Karlsruhe) starting from the nineties. The concept was proposed by M. Dalle Donne [5]; this concept has been successfully improved by Hermsmeyer in 1999 [6], and completely revised in 2003 by Hermsmeyer and Malang in the frame of the PPCS studies [7]. The DEMO HCPB Blanket 2003-2005 (Hermsmeyer et al.) is derived from the PPCS model B and is the last HCPB DEMO concept validated with neutronic, thermo-hydraulic and structural analyses.

The DEMO HCPB general design, is based on a ceramic breeder (lithium orthosilicate or metatitanate) and beryllium neutron multiplier in form of flat pebble beds, which are inserted into the blanket modules as a series of “breeder units” (BUs), separated each other by radial-toroidal and radial-poloidal stiffening plates. The Vacuum Vessel is covered by blanket modules.

The blanket thermal power, around 3000 MW_{th} (DEMO 2003), is extracted by the He primary coolant flowing at high pressure (8 MPa) through the first wall and blanket cooling plates made in EUROFER 97 martensitic steel. The inlet and outlet temperatures of the primary coolant are 300 and 500 °C. The HCPB Blanket concept is based on the following basic principles [4]:

- Use of a solid breeder in form of a pebble beds. Breeder ternary lithiated compound (Lithium Orthosilicate Li_4SiO_4 or Lithium Metatitanate Li_2TiO_3) have been considered for this function.
- Use of a neutron multiplier: Beryllium (or Be alloy) in form of a pebble bed. Beryllium is essential in this concept to reach Tritium Breeder Ratio (TBR) that are necessary for the self-sufficiently of the fusion reactor.
- Reduced Activation Ferritic Martensitic steel as structural material (EUROFER is under development in EU for the scope).
- Using of high pressure (~8 MPa) Helium for the cooling of the blanket. The Helium flows inside small channels realized in the structural material. The pebble beds are cooled indirectly by steel structures.

2. Description of HCPB DEMO Blanket

- The extraction of the tritium from the breeder materials is realized by an independent low pressure (0.1-0.2 MPa) Helium purge flow.
- The T generated in the pebble bed that can permeate into the Cooling Loop is considered a parasitic effect (that can have safety relevance for the future Fusion Power Plants FPP) and should be minimized using appropriate design and optimizing mass flow and chemical composition of the gasses (in both loops). Additional coating as anti-permeation barriers is not considered necessary for this concept. In any case the demonstration of this point is an objective of this study and of the ongoing R&D on this concept.

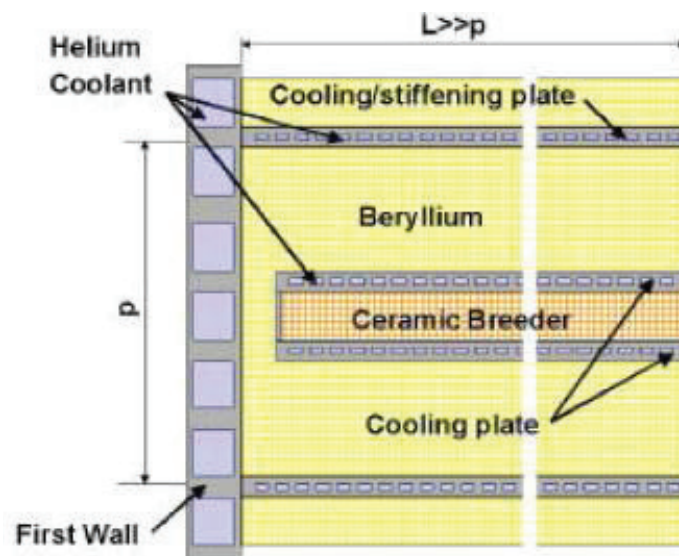


Figure 2-1 Basic Layout of HCPB Breeder Blanket

A simplified flow-diagram of the main tritium processing systems for this blanket concept is shown in Figure 2-2, while the main features of HCPB blanket for DEMO are reported in Table 2-1. These values are referred to the DEMO 2003 HCPB blanket, which is assumed to be the reference configuration for this study.

With reference to Figure 2-2, the first task of TES (Tritium Extraction System) is to extract tritium from the lithium ceramic beds and Be multiplier by a low pressure helium stream added with pure hydrogen. Then, TES accomplishes the function of tritium removal in the two main chemical forms, HT and HTO, from He. TES is a key step in the blanket tritium processing and, consequently, all possible process options to accomplish its function have to be deeply studied and compared on the basis of the envisaged operative conditions, taking into account their performance, reliability as well as industrial availability.

Although in all previous reference designs a He purge stream is added into the blanket modules, with the consequent decrease of the tritium partial pressure in the pebble beds,

however a non-negligible tritium permeation rate takes place in direction to the He primary cooling circuit (HCS, Helium Coolant System).

Consequently, an efficient CPS (Coolant Purification System) must be designed in order to carry out the primary function of tritium removal from He coolant.

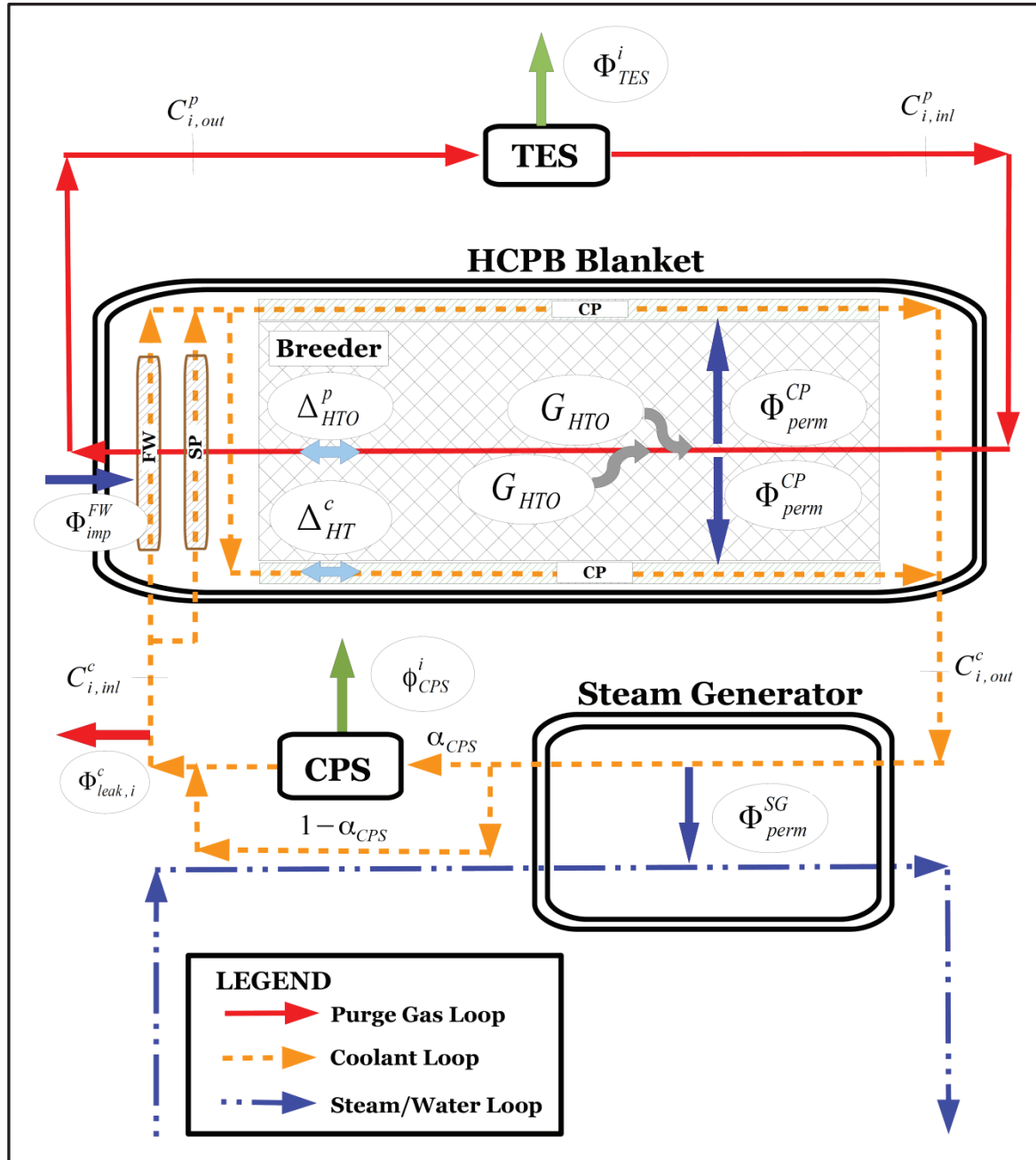


Figure 2-2 Reference Scheme for Tritium Transport in HCPB Blanket

The tritium removal from He coolant has also the beneficial effect to keep low the tritium inventory in HCS, minimising the tritium release into the reactor vault in case of ex-vacuum vessel LOCA and limiting the tritium release (He leaks + tritium permeation) into the secondary water-steam circuit through the steam generators. The present work is mainly developed by combining reference data coming from specifications of HCPB-

2. Description of HCPB DEMO Blanket

DEMO 1995, DEMO 2003 and DEMO model B of PPCS, since the tritium Cycle design remained basically the same.

Moreover, the results of this study are also meant to address the R&D efforts toward the right directions and to point out the most crucial issues related to tritium mobility in blanket components.

Blanket concept	HCPB
Fusion Power	~2500 MW
Blanket Thermal Power	~3000 MW
TBR	1.14
Blanket segmentation	Large modules
Structural Material	RAFM steel (EUROFER)
Coolant	Helium
Breeder	Solid Breeder (pebble beds) Li ₄ SiO ₄ (Li ⁶ enrich. 40%)
Coolant Pressure, Temperature in/out	8 MPa, 300/500 °C
Coolant mass flow rates	~ 2400 kg/s
T recovery method	Low pressure (1 bar) He purge loop
Maximum design temperatures	FW (steel) 548 °C CP (steel) 544 °C Breeder/multiplier 917/655 °C

Table 2-1 Main Features of HCPB Blanket [8]

3 Description of the Model

In this section the mathematical structure of the code will be illustrated, analyzing and highlighting the main features.

With reference to the tritium fluxes reported in Figure 2-2, is reported hereafter the system of differential equations describing the tritium mass balance inside the HCPB blanket, in which the integral balance of total amount $N_i^j(t)$ [mol] of tritium species i (with $i = HT$ and HTO) inside the j -th Helium loop (with $j =$ purge gas loop, coolant loop) is performed by means of the mass-averaged concentration $C_i^j(t)$ [mol/kg] = $N_i^j(t)/m_{He}^j$ where m_{He}^j is the Helium mass inside the loop j . Thus the tritium mass balance equations are given by:

$$\left\{ \begin{array}{l}
 \frac{dC_T^{br}(t)}{dt} = \dot{G}_v^{br} - \frac{C_T^{br}(t)}{\tau_{res}} \\
 \frac{dC_T^{Be}(t)}{dt} = (1 - f_r) \cdot \dot{G}_v^{Be} \\
 \frac{dC_{HT}^p(t)}{dt} = \frac{\dot{\Delta}_{HTO}^p(t) - \Phi_{perm}^{CP}(t) - \Phi_{TES}^{HT}(t)}{m_{He}^p} \\
 \frac{dC_{HTO}^p(t)}{dt} = \frac{\dot{G}_{HTO}(t) - \dot{\Delta}_{HTO}^p(t) - \Phi_{TES}^{HTO}(t)}{m_{He}^p} \\
 \frac{dC_{HT}^c(t)}{dt} = \frac{\Phi_{perm}^{CP}(t) + \Phi_{imp}^{FW}(t) - \Phi_{perm}^{SG}(t) - \dot{\Delta}_{HT}^c(t) - \Phi_{leak,HT}^c(t) - \Phi_{CPS}^{HT}(t)}{m_{He}^c} \\
 \frac{dC_{HTO}^c(t)}{dt} = \frac{\dot{\Delta}_{HT}^c(t) - \Phi_{leak,HTO}^c(t) - \Phi_{CPS}^{HTO}(t)}{m_{He}^c} \\
 C_i^j(0) = 0, \quad \text{with } i = T, HT, HTO, \quad j = br, Be, p, c
 \end{array} \right. \quad (3.1)$$

where the superscripts p and c are related to the purge gas and the Helium Coolant System (HCS) loops respectively, the subscripts br and Be to the breeder and Beryllium pebble beds respectively and the subscripts HT and HTO are related to the tritium hydride (HT) and tritiated water (HTO) respectively. All the tritium fluxes entering in the tritium mass balance of Eq. (3.1) and qualitatively described hereafter, are listed in Table 3-1.

3. Description of the Model

Tritium is generated inside the breeder in form of atomic tritium (T^-) with a local production rate \dot{G}_V^{br} and it is released into the purge gas with a time lag τ_{res} called tritium residence time (see § 3.5.1.3); due to the presence of oxygen and water inside the Li orthosilicate, tritium is assumed to be released into the purge gas almost totally in form of tritiated water HTO (\dot{G}_{HTO}). A smaller production rate \dot{G}_V^{Be} is also present in Beryllium pebble beds, in which large amounts of tritium can be retained and only a little fraction of produced tritium f_r is released from Be pebbles (see §.3.5.1.4). The release rate from the breeder $C_T^{br}(t)/\tau_{res}$ and the total tritium release into the purge gas \dot{G}_{HTO} are related by the following relationship:

$$\dot{G}_{HTO}(t) \left[\frac{mol}{s} \right] = \frac{C_T^{br}(t)}{\tau_{res}} \cdot V_{br} \quad (3.2)$$

where V_{breed} is the total volume of breeder inside the breeding blanket. Once tritium gets into the purge gas loop, due to the presence of swamping hydrogen inside purge Helium (with a swamping ratio fixed to 0.1 %), the chemical equilibrium $HT + H_2O \leftrightarrow H_2 + HTO$ (see § 3.2) takes place and a certain amount of HTO (Δ_{HTO}^P) gets converted into tritium hydride (HT).

Flux	Description
\dot{G}_{HTO} [mol/s]	Total tritium generation rate inside the breeder
\dot{G}_V^{br} [mol/cm ³ /s]	Local tritium generation rate inside breeder pebble beds
\dot{G}_V^{Be} [mol/cm ³ /s]	Total tritium generation rate inside Beryllium pebble beds
Φ_{imp}^{FW} [mol/s]	Flux of Tritons from the plasma through the FW cooling channels
Φ_{perm}^{CP} [mol/s]	HT permeated flux through CP channels
Φ_{perm}^{SG} [mol/s]	HT permeated flux through SG tubes
Φ_{TES}^i [mol/s]	Flux of tritium form i ($i = HT, HTO$) extracted by TES
Φ_{CPS}^i [mol/s]	Flux of tritium form i ($i = HT, HTO$) extracted by CPS
$\Phi_{leak,i}^c$ [mol/s]	Losses of tritium form i ($i = HT, HTO$) with coolant leakages
Δ_{HTO}^P [mol/s]	HTO Isotope exchange rate inside the BU from the purge gas side
Δ_{HT}^c [mol/s]	HT Isotope exchange rate inside the BU from coolant side

Table 3-1 Description of Tritium Fluxes in HCPB Blanket

In the purge gas loop, tritium is released from the breeder into the purge Helium mainly in form of HTO, and the presence of high hydrogen contents is needed to shift the HTO content into HT, which is much less worrying from the radiological point of view although is a permeable specie. The dose coefficients per unit of incorporation have been

evaluated at 1.8×10^{-15} Sv/Bq for HT inhalation and 1.8×10^{-11} Sv/Bq for ingested or inhaled HTO [10], thus, for the same ingested or inhaled amount of both species, the dose provided by HTO is 10000 times higher than the one coming from HT.

Since HT is a gaseous (and permeable) hydrogen species, a permeation flux ($\Phi_{\text{perm}}^{\text{CP}}$) across the Cooling Plates (CPs) placed between Beryllium and breeder pebble beds (see Figure 2-1 and Figure 2-2) occurs as well; this tritium permeation rate then reaches the primary coolant system (HCS). Moreover, the tritons coming from the Plasma and implanted into the First Wall (FW) can permeate into the HCS by means of the permeation flux through the FW cooling channels $\Phi_{\text{imp}}^{\text{FW}}$ (see § 3.3.3).

As reported in the Introduction, tritium is extracted from purge gas in Tritium Extraction System (TES), with a certain removal efficiency η_{TES} (see § 3.1) giving a total tritium extraction rate from the purge gas $\Phi_{\text{TES}} = \Phi_{\text{TES}}^{\text{HT}} + \Phi_{\text{TES}}^{\text{HTO}}$.

Following the tritium transport paths, the permeated tritium fluxes from FW ($\Phi_{\text{imp}}^{\text{FW}}$) and CPs ($\Phi_{\text{perm}}^{\text{CP}}$) get into the main coolant loop, in which, due to hydrogen and water addition for the oxidation control, the isotope exchange rate from HT to HTO ($\Delta_{\text{HT}}^{\text{c}}$) takes place, because of the same chemical equilibrium as considered for $\Delta_{\text{HTO}}^{\text{p}}$. In HCS, the tritium fluxes $\Phi_{\text{CPS}}^{\text{HT}}$ and $\Phi_{\text{CPS}}^{\text{HTO}}$ are extracted by re-circulating inside the Coolant Purification System (CPS) a certain fraction of total Helium mass flow rate inside the coolant loop α_{CPS} in which the tritium fluxes $\Phi_{\text{CPS}}^{\text{HT}}$ and $\Phi_{\text{CPS}}^{\text{HTO}}$ are extracted with a removal efficiency η_{CPS} (see § 3.1). Finally, a tritium permeation fluxes through the Steam Generator (SG) tubes walls ($\Phi_{\text{perm}}^{\text{SG}}$) gets into the steam circulating into the Power Conversion System (PCS), which is considered to be lost into the environment. As will be shown in the results, this tritium amount constitutes an important contribution to the total tritium losses.

Finally, a certain amount of tritium released into the environment due to He leakage from seals and material imperfections of the coolant circuit $\Phi_{\text{HT/HTO}}^{\text{leak}}$ and the tritium decay $\lambda_{\text{T}} \cdot C_{\text{HT/HTO}}^{\text{p/c}}$ must be considered. However, the tritium decay generates He³ atoms, which are responsible also of the nuclear reaction He³(n,p)H³ which is a source reaction for tritium and it should compensate losses due to tritons decay. Anyway this nuclear reactions has a relevant influence only at low energy neutrons (in the range of 0-2.27 eV [9]), that is quite off from the neutron energy spectrum involved in a breeding blanket (14.1 MeV), typically around the fast spectrum. Apparently the contribution of this reaction can be neglected and the decay should be considered in the tritium balance. However, tritium decay is usually negligible for short time periods but on longer time scales, the decay could provide also some benefits, especially in terms of T inventory. As a

matter of fact, inside Beryllium Pebbles Beds the fast neutrons are easily slowed down, thus making the nuclear reaction $\text{He}^3(n, p)\text{H}^3$ to easily take place. In conclusion, in order to keep the analysis as much conservative as possible, the tritium decay is neglected in the system of balance equations reported in Eq. (3.1).

From the mathematical point of view, the aim of the model is to express all the tritium fluxes listed above in terms of all the i -th tritium form average concentration (with $i = \text{HT}, \text{HTO}$) inside the j -th Helium loop (with $j = \text{purge, coolant}$) C_i^j [mol/kg_{He}] and solving this system of differential equations by finding all these time-dependent tritium concentrations which are averaged on their respective total purge and coolant Helium masses, m_{He}^p and m_{He}^c respectively. As shown hereafter, the differential equations entering in system of Eq. (3.1) can be non-linear, thus only a numerical solution can be found. In the following section all the already described tritium amounts are described from the mathematical point of view.

3.1 Tritium Fluxes Extracted by TES and CPS

The Tritium Extraction System (TES) is aimed to extract the tritium amount released from the solid breeder into the purge gas loop, whilst the Coolant Purification System (CPS) is aimed to purify a certain fraction of primary coolant mass flow rate α_{CPS} from tritium isotope forms. The aim of this section is to express as functions of all the concentrations unknowns entering into the tritium mass balance equation of Eq. (3.1) the two following (and important) tritium fluxes:

- Tritium extracted by TES Φ_{TES}^i (with $i = \text{HT}, \text{HTO}$);
- Tritium extracted by CPS Φ_{CPS}^i (with $i = \text{HT}, \text{HTO}$).

The first term is expressed as a function of the TES efficiency (η_{TES}^i), of the average tritium concentration of the i -th form in purge gas loop $C_i^p(t)$ and of the purge Helium mass flowrate (\dot{W}_{He}^p [kg/sec]). The TES efficiency is defined by tritium concentration at the inlet and the outlet of TES system (that is the outlet and the inlet i -th form concentration at the BU, $C_{\text{out},i}^p$ and $C_{\text{in},i}^p$ respectively as shown in Figure 2-2), which are linked to the average concentration in the purge gas loop C_i^p according to following equations:

$$\begin{aligned}
 C_i^p(t) &= \frac{C_{in,i}^p + C_{out,i}^p}{2} \\
 \eta_{TES}^i &= \frac{\Phi_{TES}^i}{W_{He}^p \cdot C_{out,i}^p(t)} = \frac{C_{out,i}^p(t) - C_{in,i}^p(t)}{C_{out,i}^p(t)} \Rightarrow C_{in,i}^p(t) = (1 - \eta_{TES}^i) \cdot C_{out,i}^p(t) \\
 C_{in,i}^p(t) &= \left[\frac{2 \cdot (1 - \eta_{TES}^i)}{2 - \eta_{TES}^i} \right] \cdot C_i^p(t)
 \end{aligned} \tag{3.3}$$

Given the above set of equations, the flux of tritium form i extracted by TES is defined as:

$$\Phi_{TES}^i(t) = W_{He}^p \cdot \frac{2 \cdot \eta_{TES}^i}{2 - \eta_{TES}^i} \cdot C_i^p(t) \tag{3.4}$$

The total tritium flux extracted from TES is obtained by summing the HT and HTO contribution.

As done for TES, the expression of tritium flux extracted from CPS is developed using the efficiency η_{CPS}^i (with $i=HT, HTO$) but also considering that only a fraction α_{CPS} of the total coolant flow rate (see Figure 2-2) is treated by CPS. Adopting the same approach used for Φ_{TES} we have the following set of equations, relating the inlet and the outlet concentration of the i -th form into and from the BU from the coolant side ($C_{in,i}^c$ and $C_{out,i}^c$ respectively) with the average concentration of the same form into the coolant loop C_i^c , the CPS efficiency η_{CPS} and the fraction of total mass flow rate re-circulated inside CPS α_{CPS} .

$$\begin{aligned}
 C_i^c(t) &= \frac{C_{in,i}^c + C_{out,i}^c}{2} \\
 C_{in,i}^c(t) &= (1 - \alpha_{CPS}) \cdot C_{out,i}^c(t) + \alpha_{CPS} \cdot (1 - \eta_{CPS}^i) \cdot C_{out,i}^c(t) \\
 C_{in,i}^c(t) &= \left[\frac{2 \cdot (1 - \alpha_{CPS} \cdot \eta_{CPS}^i)}{2 - \alpha_{CPS} \cdot \eta_{CPS}^i} \right] \cdot C_i^c(t)
 \end{aligned} \tag{3.5}$$

Given the above set of equations, the flux of tritium form i extracted by CPS is defined as:

$$\Phi_{CPS}^i(t) = W_{He}^c \cdot \frac{2 \cdot \alpha_{CPS} \cdot \eta_{CPS}^i}{2 - \alpha_{CPS} \cdot \eta_{CPS}^i} \cdot C_i^c(t) \tag{3.6}$$

As done for TES, the total tritium flux extracted from CPS is obtained by summing the HT and HTO contribution.

As shown in the results, the TES and CPS efficiencies have been represented by a unique parameter for each system (i.e. η_{TES} and η_{CPS}) without distinguishing between HT and HTO removal efficiencies. In general η_{TES}^{HT} can be different from η_{TES}^{HTO} (as well as η_{CPS}^{HT}

3. Description of the Model

and $\eta_{\text{CPS}}^{\text{HTO}}$) but in this study, since no more detailed values were available, only one efficiency value has been considered for TES and CPS systems. As it can be seen, these parameters affect the tritium losses and inventories assessment in a relevant manner, especially the CPS recirculation ratio α_{CPS} .

3.2 Isotope Exchange Rate

In the purge and coolant He loops, the following chemical equilibriums due to the H_2 and H_2O addition are assumed to be the most important ones:



Assuming an form exchange rate related to the HT specie for equilibrium 1 and for equilibrium 2 ($\dot{\Delta}_1^{\text{HT}}$ and $\dot{\Delta}_2^{\text{HT}}$ respectively), given the chemical equilibrium constants $K_{\text{eq},1}$ and $K_{\text{eq},2}$ the following relationships can be expressed as [9]:

$$K_{\text{eq},1}(T) = \frac{([\text{HT}]_{\text{eq}})^2}{[\text{H}_2]_{\text{eq}} \cdot [\text{T}_2]_{\text{eq}}} = \frac{p_{\text{eq},\text{HT}}^2}{p_{\text{eq},\text{H}_2} \cdot p_{\text{eq},\text{T}_2}} = \frac{(\dot{F}_{\text{in},\text{HT}}^j + \dot{\Delta}_1^{\text{HT}} - \dot{\Delta}_2^{\text{HT}})^2}{\left(\dot{F}_{\text{in},\text{H}_2}^j - \frac{\dot{\Delta}_1^{\text{HT}}}{2} + \dot{\Delta}_2^{\text{HT}}\right) \cdot \left(\dot{F}_{\text{in},\text{T}_2}^j - \frac{\dot{\Delta}_1^{\text{HT}}}{2}\right)} \quad (3.9)$$

$$K_{\text{eq},2}(T) = \frac{[\text{H}_2]_{\text{eq}} \cdot [\text{HTO}]_{\text{eq}}}{[\text{HT}]_{\text{eq}} \cdot [\text{H}_2\text{O}]_{\text{eq}}} = \frac{p_{\text{eq},\text{H}_2} \cdot p_{\text{eq},\text{HTO}}}{p_{\text{eq},\text{HT}} \cdot p_{\text{eq},\text{H}_2\text{O}}} = \frac{(\dot{F}_{\text{in},\text{H}_2}^j - \dot{\Delta}_1^{\text{HT}} + \dot{\Delta}_2^{\text{HT}}) \cdot (\dot{F}_{\text{in},\text{HTO}}^j + \dot{\Delta}_2^{\text{HT}})}{\left(\dot{F}_{\text{in},\text{HT}}^j + \frac{\dot{\Delta}_1^{\text{HT}}}{2} - \dot{\Delta}_2^{\text{HT}}\right) \cdot \left(\dot{F}_{\text{in},\text{H}_2\text{O}}^j - \dot{\Delta}_2^{\text{HT}}\right)} \quad (3.10)$$

where $[i]_{\text{eq}}$, $p_{\text{eq},i}$ and $\dot{F}_{\text{in},i}^j$ [mol/s] are the molar concentration at the chemical equilibrium, the partial pressures and the inlet molar flow rate of species i ($i = \text{HT}, \text{H}_2\text{O}, \text{H}_2, \text{HTO}$) respectively inside the j -th He loop (j =purge, coolant) and $\dot{\Delta}_k^{\text{HT}}$ [mol/s] is the HT isotope exchange rate of equilibrium k ($k=1, 2$). This exchange rates must be expressed as functions of tritium concentrations inside the He loops C_{HT}^{p} , $C_{\text{HTO}}^{\text{p}}$, C_{HT}^{c} , and $C_{\text{HTO}}^{\text{c}}$ and inserted inside the mass balance equation reported in Eq. (3.1).

Tritium molecular specie T_2 is usually considered to be a small portion of all the tritium forms present inside the system, since all the T_2 amount combine with hydrogen and leads to HT specie. In this isotope exchange model, the presence of T_2 is neglected, thus the T_2 concentration is immediately given by the chemical equilibrium constant of equilibrium 1 (see Eq. (3.9)) combining the HT concentration (computed in Eq. (3.1)) and H_2 concentration (fixed in this model). Therefore the isotope rate exchange of equilibrium 1 is considered negligible with respect the one in equilibrium 2 ($\Delta_1^{HT} \ll \Delta_2^{HT}$). With this simplifying assumption, the unique tritium isotope exchange rate considered in the tritium mass balance of Eq. (3.1) will be the one involved in the chemical equilibrium 2 (Eq. (3.8)), that is Δ_2^{HT} , which has to be defined both for the purge and the coolant loops.

In the purge gas loop, the considered isotope exchange rate will be the conversion rate from HTO to HT and H_2O , that is Δ_{HTO}^p . Thus, in order to estimate the isotope exchange rate inside the Breeding Unit (BU) Δ_{HTO}^p due to the mentioned chemical equilibrium reported in (3.8), the inlet molar flow rate of all the tritium chemical forms participating in this chemical equilibrium must be defined. Inside the BU from the purge gas side we find the following conditions:

$$\begin{aligned}
 \dot{F}_{in,HTO}^p &= \dot{W}_{He}^p \cdot C_{HTO,in}^p + \dot{G}_{HTO} \\
 \dot{F}_{in,H_2}^p &\gg \dot{\Delta}_{HTO}^p = \dot{W}_{He}^p \cdot C_{H_2,in}^p \\
 \dot{F}_{in,HT}^p &= \dot{W}_{He}^p \cdot C_{HT,in}^p \\
 \dot{F}_{in,H_2O}^p &= 0
 \end{aligned} \tag{3.11}$$

where the inlet concentrations in the HCPB blanket of the i -th form $C_{in,i}^p(t)$ are expressed as a function of the average concentration in the purge loop $C_i^p(t)$, obtained by averaging between the inlet and the outlet concentrations inside and outside the breeding unit (see § 3.1) as reported in Eq. (3.3), except for the hydrogen concentration, which is assumed to be at the BU entrance coincident to the one imposed by the swamping ratio $\chi_{H_2/He} = C_{H_2}[\text{at. fract}]$ (see Table 4-4 for values of swamping ratio in purge loop) in the purge circuit. According to these conditions and the equilibrium constant expression reported in Eq. (3.10), the isotope exchange rate in the purge gas loop Δ_{HTO}^p becomes:

$$\begin{aligned}
 \dot{\Delta}_{HTO}^p \left[\frac{mol}{s} \right] &= - \frac{\left(K_{eq,2}^p \cdot \dot{F}_{in,HT}^p + \dot{F}_{in,H_2}^p + \dot{F}_{in,HTO}^p \right)}{2 \cdot \left(K_{eq,2}^p - 1 \right)} + \\
 &+ \frac{\sqrt{\left(K_{eq,2}^p \cdot \dot{F}_{in,HT}^p + \dot{F}_{in,H_2}^p + \dot{F}_{in,HTO}^p \right)^2 + 4 \cdot \left(K_{eq,2}^p - 1 \right) \cdot \dot{F}_{in,HTO}^p \cdot \dot{F}_{in,H_2}^p}}{2 \cdot \left(K_{eq,2}^p - 1 \right)}
 \end{aligned} \tag{3.12}$$

3. Description of the Model

In the coolant loop, considering the feeding hydrogen and water flow rate \dot{F}_{in,H_2}^c and \dot{F}_{in,H_2O}^c fixed by oxidation control with a fixed ratio $\chi_{ox} = \dot{F}_{in,H_2}^c / \dot{F}_{in,H_2O}^c$, a tritiated water inlet flow rate null and all the permeated tritium flux from HCPB (ϕ_{perm}^{CP}) combining with fed hydrogen, we find the following conditions inside the HCPB BU from the coolant side:

$$\begin{aligned}
 \dot{F}_{in,HTO}^c &= \dot{W}_{He}^c \cdot C_{HTO,in}^c \\
 \dot{F}_{in,H_2}^c &\gg \dot{\Delta}_{HT}^c = \dot{W}_{He}^c \cdot C_{H_2,in}^c \\
 \dot{F}_{in,HT}^c &= \dot{W}_{He}^c \cdot C_{HT,in}^c + \phi_{perm,HT}^{CP} \\
 \dot{F}_{in,H_2O}^c &\gg \dot{\Delta}_{HT}^c = \dot{W}_{He}^c \cdot C_{H_2O,in}^c
 \end{aligned} \tag{3.13}$$

where the inlet concentrations inside the BU $C_{i,in}^c(t)$ are related to their respective average concentrations inside the coolant loop $C_i^c(t)$ expressed in the system of differential equations (3.1), according to the relationships defined in Eq.(3.5). According to these conditions, the isotope rate exchange in the HCPB blanket from the coolant side, is given by:

$$\dot{\Delta}_{HT}^c \left[\frac{mol}{s} \right] = \frac{K_{eq,2}^c \cdot \dot{F}_{in,HT}^c - \chi_{ox} \cdot \dot{F}_{in,HTO}^c}{K_{eq,2}^c + \chi_{ox}} \tag{3.14}$$

The oxidation ration $\chi_{ox} = \dot{F}_{in,H_2}^c / \dot{F}_{in,H_2O}^c$ is usually fixed to a certain value and is considered indispensable to produce an oxidation potential inside the Helium Coolant System capable of maintaining a thin and stable protective oxide layer on the primary side of the steam generator walls [16].

3.3 Permeation Fluxes

The tritium permeation fluxes entering in the total tritium mass balance are given by:

- Tritium permeation flux through Cooling Plates channels (ϕ_{perm}^{CP});
- Tritium permeation flux from implanted tritons into the First Wall (ϕ_{imp}^{FW});
- Tritium permeation flux through Steam Generator tube walls (ϕ_{perm}^{SG}).

3.3.1 Theory on Hydrogen Isotopes Permeation

Tritium atoms have a high mobility through high temperature structural materials, and the driving force of the permeation is characterized by the tritium partial pressure acting on a given material. Depending on the tritium partial pressures involved in the system, two possible extreme permeation models are available:

- Diffusion-limited model;
- Surface-limited model.

In the past many authors studied this net distinction between the two permeation regimes (e.g. Refs. [11], [12] and [13]) and they stated that for low tritium partial pressures the permeation is governed by surface limited model, whilst for high values the diffusion rules the mobility through structural materials. In principle, according to graphs reported in Figure 3-1 and Figure 3-2, when the system is characterized by low partial pressures, the diffusive model (proportional to \sqrt{p}) overestimates the permeated flux through a given wall, characterized by certain high and low pressures acting on it (p_h, p_l) and a given temperature T_w , with respect to the one estimated with surface-limited model (proportional to p). On the other hand, when the system is characterized by relatively high partial pressures (i.e. underlying the right lines of Figure 3-1), a surface-limited permeation model would overestimate the permeation flux through the same membrane at the same operative conditions.

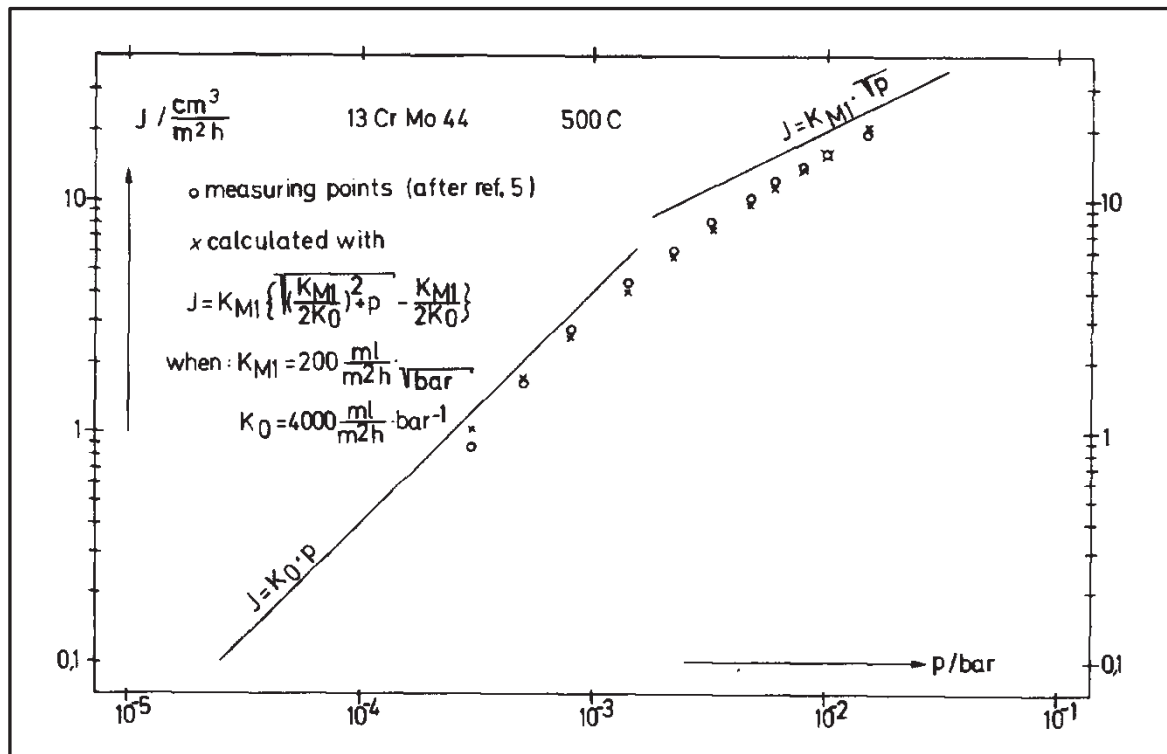


Figure 3-1 H₂ Permeation Vs. Pressure through Ferritic Steel [11]

The threshold value dividing the low and the high pressure areas probably depends on the operative conditions (e.g. structural materials, temperature, gas compositions, etc.) and, after a literature review, any consistent formulations or criteria have been found to establish this partial pressure. For example according to Ref. [12] this value has been stated to be around 10 Pa, while in Ref. [11] (as shown in Figure 3-1, this value is included between 10^{-3} and 10^{-2} bar (i.e. between 100 and 1000 Pa).

3. Description of the Model

In case of diffusive permeation model (at relatively high pressures) hydrogen migration through the metal membrane is limited primarily by hydrogen diffusion in the metal lattice while the surface processes (hydrogen adsorption, desorption) are considerably faster [14]. On the other hand, when a surface limited model is assumed, the diffusion through the membrane occurs fast enough, so that any concentration gradient is cancelled by diffusion.

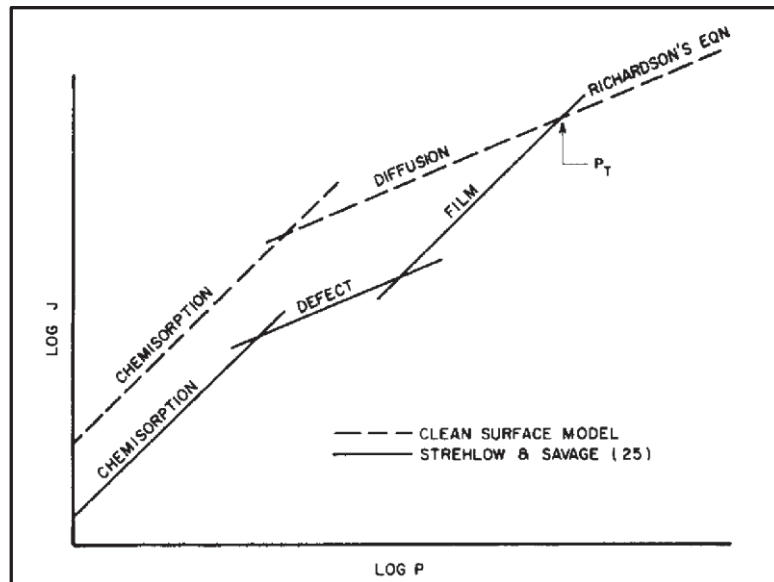


Figure 3-2 Overall Permeation Behavior of Hydrogen Gases through Metals [13]

Assuming a membrane of a certain material, with a given thickness Δx , an high partial pressure p_h and a low partial pressure p_l acting on each side respectively, the permeated flux through the membrane for the two limiting models are reported in Eqs. (3.15) and (3.16).

$$J_{perm}^{diff} \left[\frac{mol}{m^2 s} \right] = \frac{1}{PRF} \cdot \frac{D(T) \cdot K_S(T)}{\Delta x} \cdot (\sqrt{p_h} - \sqrt{p_l}) = \frac{P(T)}{\Delta x} \cdot (\sqrt{p_h} - \sqrt{p_l}) \quad (3.15)$$

$$J_{perm}^{surf} \left[\frac{mol}{m^2 s} \right] = \frac{\sigma k_1(T)}{2} \cdot (p_h - p_l) = \frac{\sigma k_2(T) \cdot (K_S(T))^2}{2} \cdot (p_h - p_l) \quad (3.16)$$

where:

- $D(T)$ [m^2/s] is the tritium diffusivity in the membrane;
- $K_S(T)$ [$mol/m^3/\sqrt{Pa}$] is solubility (or Sieverts) constant of tritium inside the membrane;
- $P(T)$ [$mol/m/sec/\sqrt{Pa}$] = $D(T) \cdot K_S(T)$ is the tritium permeability of the membrane (Richardson's law);
- $k_1(T)$ [$mol/m^2/s/Pa$] is the adsorption constants of tritium of the membrane surface;

- σ is the surface roughness factor, defined as the ratio of the real area to the geometric area of the surface;
- $k_2[\text{mol}/\text{m}^4/\text{s}]$ is the recombination constant of hydrogen onto the surface of the membrane;
- PRF is the Permeation Reduction Factor. Coating the membrane with an additional metallic layer (barrier) results in the reduced permeation if diffusion remains the rate limiting process [14]. This is why the PRF is not included in the expression defining the permeation flux through a membrane driven by surface-limiting rate. The experimental proof of the barrier efficiency is a relative reduction of the steady permeation flux measured at the identical conditions (p, T). Its definition is the ratio of the steady flux through the uncoated membrane versus the flux through the coated membrane.

From Eq. (3.16) can be derived the following relationship between Sieverts' constant, recombination and adsorption constant, defined as:

$$\sigma k_2(T) = k_{rec}(T) = \frac{\sigma k_1(T)}{K_S^2(T)} \quad (3.17)$$

From the tritium analysis point of view, it would be interesting to carry out the study by considering both models for permeation and check the influence of the adopted permeation regime on the results. As shown in the results the differences in terms of tritium losses and inventories are quite remarkable. As it will be seen in the next paragraph, the type of permeation regime (i.e. the assumed value of the adsorption constant) has a strong impact on the calculated tritium permeation rate into the HCS loop. In the following paragraphs the tritium permeation fluxes listed above will be mathematically described either using diffusion and surface limited models.

As assumed by [15], the effect of H₂ swamping in the purge stream as well as in the primary cooling circuit on the tritium permeation rate can be neglected, thus considering the HT partial pressure as the driving force of permeation and not the T₂ partial pressure coming from the chemical equilibrium between H₂ and T₂ (see equilibrium reaction (3.7)).

3.3.2 Tritium Permeation Flux through CPs Cooling Channels

The tritium permeation flux through the CP cooling channel walls given a specified CPs permeation area $A_{perm}^{CP}[\text{m}^2]$, a wall thickness $\Delta x_{CP}[\text{m}]$, a tritium permeability $P_{CP}[\text{mol}/\text{m}/\text{s}/\sqrt{\text{Pa}}]$ (defined at the CP wall average temperature $T_{av,w}^{CP}[\text{K}]$), a permeation reduction factor (PRF) PRF_{CP} , an adsorption constant σk_1^{CP} on the CP channel surface,

3. Description of the Model

the tritium partial pressure in the purge loop p_T^p [Pa] and a tritium partial pressure inside coolant loop p_T^c [Pa] is given by:

$$\Phi_{perm}^{CP} \left[\frac{mol}{s} \right]_{diff} = \frac{1}{PRF_{CP}} \cdot \frac{P_{CP}(T_{av,w}^{CP}) \cdot A_{perm}^{CP}}{\Delta x_{CP}} \cdot \left(\sqrt{p_{HT}^p} - \sqrt{p_{HT}^c} \right) \quad (3.18)$$

$$\Phi_{perm}^{CP} \left[\frac{mol}{s} \right]_{surf} = \frac{\sigma \kappa_2^{CP}(T_{av,w}^{CP}) \cdot (K_S^{CP}(T_{av,w}^{CP}))^2 \cdot A_{perm}^{CP}}{2} \cdot (p_{HT}^p - p_{HT}^c) \quad (3.19)$$

The HT partial pressure in the j -th loop p_{HT}^j ($j = \text{purge, coolant}$) and the corresponding T concentrations C_{HT}^j are related by means of Dalton's law for each, since tritium and Helium can be seen as a mixture of gaseous species. The Dalton's law describing the relationship between the i -th tritium form concentration and pressure (with $i = \text{HT, HTO}$) inside the j -th Helium loop (with $j = \text{purge, coolant}$) is defined as:

$$C_i^j \left[\frac{mol}{kg_{He}} \right] = \frac{1}{M_{He}} \cdot \frac{p_i^j}{p_{He}^j} \quad (3.20)$$

where M_{He} [kg/mol] is the He atomic weight, and p_{He}^j is the total Helium pressure in the j -th loop. Eq. (3.20) is derived considering that the molar fraction (then also the concentration) of a gaseous species inside a gaseous mixture is proportional to its partial pressure in it. Combining Eqs. (3.18)/(3.19) with (3.20) the permeation flux through the CP cooling channel can be expressed as a function of HT concentrations in purge and coolant loops $C_{HT}^p(t)$ and $C_{HT}^c(t)$ respectively, and put inside the tritium mass balance equations in Eq. (3.1).

3.3.3 Tritium Permeation Flux from Implanted Tritons onto First Wall

The contribution to the tritium permeation rate into HCS coming from ion implantation from the plasma into the first wall with the subsequent tritium diffusion towards the cooling channels of the first wall is often neglected (e.g. [15], [16]). In fact, taking into account the foreseen presence of tungsten as coating of the first wall (assumed to be equal to 2 mm [15], [16]), this second contribution to the tritium permeation into the coolant is negligible.

Tungsten is used as a 2 mm coating at the DEMO FW. Tritium (and Deuterium) coming from plasma implant into the reactor FW. A fraction of the implanted DT flux recycles back into plasma (recycling) at FW surfaces. The balancing part of the flux diffuses into the cooling circuit and/or builds-up a tritium a D-T inventory (solved and trapped) at the DEMO FW structure.

In the literature diverse tritium tracking calculations at the DEMO FW can be found. It is commonly noticed the large uncertainty of permeation rates. For DEMO -95 specifications values ranging from 6 to 60 g/d are usual (FW MANET). Main sources of uncertainty come from empirical parameters in the equations: value of sticking coefficient (or surface roughness factor already reported in Eq. (3.16)).

On the FW, tritium permeation and inventory assessment in the W-coating/EUROFER/coolant should be derived from a complete D-T recycling-permeation analysis for nearly steady-state plasma conditions (DEMO) or cyclic ion wall-loading (case of ITER-TBM).

From DEMO95 study, a tritium transport assessments on the FW (bare MANET) [16] estimated tritium into the HCS at FW ~ 18 g/d (with an uncertainties range of 2-60 g/d). Permeation assessment with 2 mm W-coating reduce such value below 0.1 g/d, and even below if recycling at W surface would be properly considered.

From this literature review, it can be pointed out that tritons implantation into the FW constitutes a problem from the permeated flux into the HCS only if no FW coating is foreseen.

In this study, a simplified estimation of the permeated flux is performed, in order to determine the influence of the FW on the total tritium losses. Assuming to have the FW characterized by a certain coating membrane facing the plasma defined by a thickness Δx_{coat} and a permeability $P_{coat}(T_{av}^{FW})$, and the main FW, defined by its thickness Δx_{FW} (separating the coating and the coolant channels) and its permeability $P_{FW}(T_{av}^{FW})$, the effective FW permeability $P_{eff}^{FW}(T_{av}^{FW})$ can be defined (assuming diffusion to be the rate limiting process for FW) as [14]:

$$\frac{\Delta x_{coat} + \Delta x_{FW}}{P_{eff}^{FW}} = \frac{\Delta x_{coat}}{P_{coat}} + \frac{\Delta x_{FW}}{P_{FW}} \quad (3.21)$$

Such membrane has been modeled as a membrane composed of two homogeneous layers. Effective permeability P_{eff}^{FW} is based on the sum of permeation resistances for each layer, analogous to the electrical resistors in series. In the results section a parametric study of tritium losses is carried out by varying the coating thickness, in order to show its influences on the tritium analysis (see § 4.3.3).

Assuming, then an effective permeability P_{eff}^{FW} , the tritium permeation flux through the FW cooling channel is given by:

$$\Phi_{imp}^{FW} \left[\frac{mol}{s} \right] = \frac{1}{PRF_{CP}} \cdot \frac{P_{eff}^{FW}(T_{av}^{FW}) \cdot A_{perm}^{FW}}{\Delta x_{coat} + \Delta x_{FW}} \left(\sqrt{\frac{J_{imp}^{FW}}{2 \cdot \sigma k_1^{coat}(T_{av}^{FW})}} - \sqrt{p_{HT}^c} \right) \quad (3.22)$$

3. Description of the Model

where J_{imp}^{FW} [T/m²/sec] is incident T ion flux from the plasma into the first wall, σk_1^{coat} is the adsorption constant of coating membrane and A_{perm}^{FW} is the permeation area onto the FW. The presence of a FW coating barrier is necessary in order to avoid large amount of implanted tritons into the main coolant but also to protect the FW from neutrons damages. The PRF on FW channels appearing in Eq. (3.22) is assumed to be coincident to the one on CPs (PRF_{CP}) because it is obtained from a formation of an oxidation layer by means of hydrogen and water addition with a certain molar ratio to the coolant circuit. Thus, except for neutrons and temperature influences on this coating layer, the assumption is that this PRF is maintained in all the blanket-side coolant loop (i.e. not in SG, where we have different temperatures and structural materials). As reported in the results, the differences in terms of tritium losses are quite remarkable with and without coating barriers.

3.3.4 Tritium Permeation Flux though Steam Generator Tube Walls

The tritium flux through SG tube walls Φ_{perm}^{SG} [mol/s] is obtained considering that the tritium concentration in water is negligible with respect to that in He. Therefore, considering for the SG a permeation area A_{perm}^{SG} [m²], a tubes thickness Δx_{SG} [m], a permeability of SG tube material P_{SG} [mol/m/s/ \sqrt{Pa}] (defined at the SG average tube walls temperature $T_{av,wall}^{SG}$ [K]) and a permeation reduction factor inside SG heat exchange walls (PRF_{SG}), the tritium permeation flux through SG tubes (in diffusion and surface limited model options) is given by:

$$\Phi_{perm}^{SG} \left[\frac{mol}{s} \right]_{diff} = \frac{1}{PRF_{SG}} \cdot \frac{P_{SG}(T_{av,w}^{SG}) \cdot A_{perm}^{SG}}{\Delta x_{SG}} \cdot \sqrt{p_{HT}^c} \quad (3.23)$$

$$\Phi_{perm}^{SG} \left[\frac{mol}{s} \right]_{surf} = \frac{\sigma k_2^{SG}(T_{av,w}^{SG}) \cdot (K_S^{SG}(T_{av,w}^{SG}))^2 \cdot A_{perm}^{SG}}{2} \cdot p_{HT}^c \quad (3.24)$$

where A_{perm}^{CP} [m²] is SG the permeation area, Δx_{SG} is the SG wall thickness, P_{SG} [mol/m/s/ \sqrt{Pa}] is the tritium permeability of SG tubes (defined at the SG tubes walls average temperature $T_{av,w}^{SG}$ [K]), PRF_{SG} is the permeation reduction factor (PRF) due to SG wall oxide layer, σk_1^{SG} is the adsorption constant of SG tubes surface and p_{HT}^c [Pa] is the HT partial pressure inside the coolant loop.

On SG tubes walls, is usually applied an oxidation layer aimed to keep the corrosion under control, thus reducing the tritium permeation of a certain PRF_{SG}. If permeation is dominated by surface phenomena, the reduction in terms of permeated tritium amounts

results in terms of a reduced adsorption constant σk_1^{SG} for oxidized SG tubes surfaces, which might be several order of magnitudes lower [16].

3.4 Tritium Flux Associated to Helium Leaks

Helium leakages from purge and coolant circuit can occur because of the presence of seals and material imperfections. In this study are considered only the leakages from the coolant circuit since the purge gas system it is assumed to be in a controlled and monitored environment, so the related to the leaked purge Helium has not to be considered and accounted in the tritium losses. Moreover, it is a relatively low pressure system, so the He leakages from this circuit are supposed to be negligible to ones found in the coolant loop.

For the evaluation of He leakage in the coolant circuit leakage data are reported in Gas Cooled Reactors field and they are taken as a reference for our purposes. Estimates of the rate of replenishment necessary to evaluate He leakage vary between 0.1% of total He inventory per day (0.1% inv./d) and one complete replenishment per year (100 % inv./yr.) [11], [16]. In this study, it is assumed that the leakage rate is the 0.1% of the He inventory inside the coolant loop M_{He}^c per day. However, these leakage values seem to be too pessimistic (22.6 kg/d are assumed to be lost considering an Helium inventory of order of 22.6 ton [16]), thus for the computation of the tritium losses related to helium leakage are assumed other values (2.5×10^{-3} mol/s = 0.864 kg/d) coming from more focused analysis on Helium circuit for breeding blankets [17]. Thus, the losses of *i*-th tritium form due to Helium leakage is deduced from the helium leak flowrate defined as the released Helium flowrate \dot{W}_{leak} [kg/s] and the *i*-th form concentration (*i* = HT, HTO) inside the coolant $C_i^c(t)$; it is defined as:

$$\Phi_{leak,i}^c(t) \left[\frac{mol}{s} \right] = \dot{W}_{leak} \cdot C_i^c(t) \quad (3.25)$$

The total tritium losses due to Helium leakage is obtained by summing the HT and HTO contribution.

3.5 Tritium Losses and Inventories

Tritium inventories and tritium losses are the key parameters in a tritium transport analysis.

Tritium inventories in this work are characterized by;

- tritium inventory inside the purge Helium (I_p [g]);

3. Description of the Model

- tritium inventory inside the primary coolant (I_c [g]);
- tritium inventories inside structural steels (Cooling plates, FW and SG tubes) (I_{steel} [g]);
- tritium inventory inside the breeder I_{br} [g];
- tritium inventory inside Beryllium pebbles I_{Be} [g].

Tritium losses are simply given by:

- Tritium permeation rate through Steam Generator tubes into the steam line Φ_{perm}^{SG} [Ci/d];
- Total tritium losses due to Helium leakage $\sum_i \Phi_{leak}^i$ [Ci/d] with $i = HT, HTO$.

3.5.1 Tritium Inventories

3.5.1.1 Tritium Inventories inside Purge and Coolant Loops

The first two terms are expressed by means of the average concentrations in purge loop $C_T^p = C_{HT}^p + C_{HTO}^p$ and the total average concentrations in the coolant loop $C_T^c = C_{HT}^c + C_{HTO}^c$, and are defined as:

$$I_p [g] = (C_{HT}^p(t) + C_{HTO}^p(t)) \cdot m_{He}^p \cdot M_T \quad (3.26)$$

$$I_c [g] = (C_{HT}^c(t) + C_{HTO}^c(t)) \cdot m_{He}^c \cdot M_T \quad (3.27)$$

where m_{He}^p and m_{He}^c are the total Helium inventories inside the purge and the coolant loops respectively and $M_T \approx 3$ [g/mol] is the atomic weight of tritium.

3.5.1.2 Tritium Inventory in Steels

Tritium inventories inside steels are characterized by the sum of inventories inside structural materials of the breeder (e.g. Cooling plates and First Wall) and those inside the SG tubes. These contributions are evaluated considering the average concentrations (C_{steel}^k [mol/m³]) and the volume (V_{steel}^k [m³]) of the k component steels (with $k = FW, CP, \text{ or } SG$) and the total tritium inventory inside steels I_{steel} [g] is given by:

$$I_{steel} [g] = \sum_k C_{steel}^k \cdot V_{steel}^k \cdot M_T \quad (3.28)$$

The average concentration C_{steel}^k is calculated averaging the concentrations acting on the m side of the k steel $C_{steel}^{k,m}$ [mol/m³] (with $m = \text{high or low tritium partial pressure side}$), which are evaluated by means of Sievert's law as follows:

$$C_{steel}^{k,m} \left[\frac{\text{mol}}{\text{m}^3} \right] = K_{S,steel}^k \left(T_{av,wall}^k \right) \cdot \sqrt{p_k^m} \quad (3.29)$$

where the p_k^m [Pa] is the tritium partial pressure acting on the m side of the k steels (derived from Dalton's laws reported in Eq. (3.20) using the HT concentrations C_{HT}^p and C_{HT}^c) and $K_{S,steel}^k$ [mol/m³/√Pa] is the Sievert's constant of tritium inside the k steels evaluated at k steels average temperature $T_{av,steel}^k$ (see Table 4-1 and Table 4-4 for values).

When we deal with CPs the high and the low tritium partial pressure are characterized by the one inside purge gas loop (p_T^p) and that inside the coolant (p_T^c) respectively, when $k = FW$, are respectively the equivalent implanted tritons partial pressure $J_{imp}^{FW}/(2 \cdot \sigma k_1^{coat})$ (see § 3.3.3) and the coolant partial pressure p_T^c and finally when $k = SG$ the high and the low tritium partial pressures are p_T^c and the inside steam/water loop $p_{HT}^{H_2O}$ respectively. This last partial pressure was assumed to be negligible with respect to p_T^c and therefore to p_T^p .

3.5.1.3 Tritium Inventory in Breeder Pebble Beds

The tritium concentration inside the breeder is obtained by solving the first equation of system of ODEs written in Eq. (3.1), which is uncoupled from the other equations and it can be easily integrated in time, giving the following analytical solution:

$$C_T^{br}(t) = \dot{G}_v^{br} \cdot \tau_{res}(T_{av}^{br}) \cdot \left(1 - \exp\left\{ -\frac{t}{\tau_{res}(T_{av}^{br})} \right\} \right) \quad (3.30)$$

where τ_{res} is the tritium residence time inside the breeder and it is strongly dependent on breeder temperature T_{av}^{br} (see Table 4-4 for values). The tritium inventory inside the breeder is simply derived multiplying the concentration inside it C_T^{br} (see Eq. (3.30)) by the total volume of breeder V_{br} [cm³] = $V_{br}^{BU} \cdot N_{BU}^{mod} \cdot N_{mod}$, and it is defined as:

$$I_{br}[g] = C_T^{br} \cdot (V_{br}^{BU} \cdot N_{BU}^{mod} \cdot N_{mod}) \cdot M_T \quad (3.31)$$

where V_{br}^{BU} , N_{BU}^{mod} and N_{mod} are the volume of breeder inside the Breeding Unit (BU), the number of BU inside a blanket module and the total number of modules (see Table 4-4 for values).

Although this model appears to be accurate and intuitive, since the temperature profiles into breeder pebbles bed are very important for tritium release another approach is adopted for tritium inventory inside the breeder. In fact, as reported in Table 4-1, the tritium residence into Li-Orthosilicate has an Arrhenius form, in which it is exponentially decreasing with the 1/T power of temperature. Therefore, if we have large temperature variations along the breeder profiles, assuming an average breeder temperature (as done for the model of Eq. (3.31) with T_{av}^{br}) might give high uncertainties to this important

3. Description of the Model

parameter. Thus, assuming to define the breeder volume with the coordinate \vec{r} and the temperature distribution on this domain $T(\vec{r})$, the total tritium inventory inside the breeder material can be defined as [18]:

$$I_{br} [g] = \int_{\Omega} \dot{m}(\vec{r}) \cdot \tau_{res}(T(\vec{r})) dV \quad (3.32)$$

where $\dot{m}(\vec{r})$ is the local tritium production rate and V is the breeder volume. From this relation, a simpler formula has been derived and it is defined as follows:

$$I_{br} [g] = \chi \cdot \frac{\dot{G}}{T_{max}^{br} - T_{min}^{br}} \cdot \int_{T_{max}^{br}}^{T_{min}^{br}} \tau_{res}(T) dT \quad (3.33)$$

where χ is geometry factor (0.3333 for DEMO geometry), \dot{G} [g/d] is the total tritium production rate (see Eq. (3.2)) and T_{max}^{br} and T_{min}^{br} are the maximum and the minimum temperatures in breeder material respectively.

As it can be seen, in this way it is possible to calculate the tritium inventory inside the breeder by taking into account of the operative temperature ranges.

3.5.1.4 Tritium Inventory in Beryllium Pebble Beds

The tritium inventory inside Beryllium pebbles is a crucial point for a tritium assessment of breeding blanket. As far as the beryllium is concerned, since 1999 the reference material grade has been considered the 1-mm pebbles produced by NGK with electrode rotating methods. The major design issue connected with the use of Be is its behavior under irradiation, mainly swelling and tritium inventory [19]. Lack in the database and in the modeling give large uncertainties in the design calculation of the EOL tritium inventory in Be in FPP conditions.

In spite of the progress made to better understanding the physic of the phenomena [20], the goal of producing a reliable code to support the designer in these choices, has not been achieved yet. An irradiation campaign to obtain data of Be at 3000 appm of helium in 2006 and 6000 appm helium in 2008 with temperatures in the range 500–700 °C has started in Petten in the frame of HIDOBE task. With these data the modeling should be improved and complementary an empirical extrapolation to the DEMO condition (18 000 appm) could be attempted.

A detailed analysis with irradiated Beryllium has been carried out in FZK [21], in which experimental data were supported by theoretical model implemented into the computational code ANFIBE, firstly developed in the years 1992-1995 [22]. In this study more improved models for tritium and helium kinetics in Beryllium were implemented in order to update the ANFIBE code from the version 0 to version 1 (see Figure 3-3).

The difficulties related to tritium release modeling in Beryllium, born from the presence of complex processes inside pebbles, in particular, atomic diffusion, precipitation into bubbles, bubble migration, growth, coalescence and for tritium also solubility, chemical trapping by impurities and surface recombination effects. All the efforts during the past years in trying to clarify the ideas on this issues were able to open questions but the issues are still open. Therefore, since the aims of this study are totally off from implementing detailed Helium and Tritium kinetics models, in a conservative way we consider a purely linear model, in which no-tritium sinks are considered and the tritium concentration inside the Beryllium is simply calculated considering a local production rate coming from neutronic analysis and a release rate obtained by simply fitting the results obtained with ANFIBE 1, considering the release fraction f_r (normalized to production at EOL) linearly dependent on the Beryllium temperature in the range 300-1300 K (see Figure 3-3).

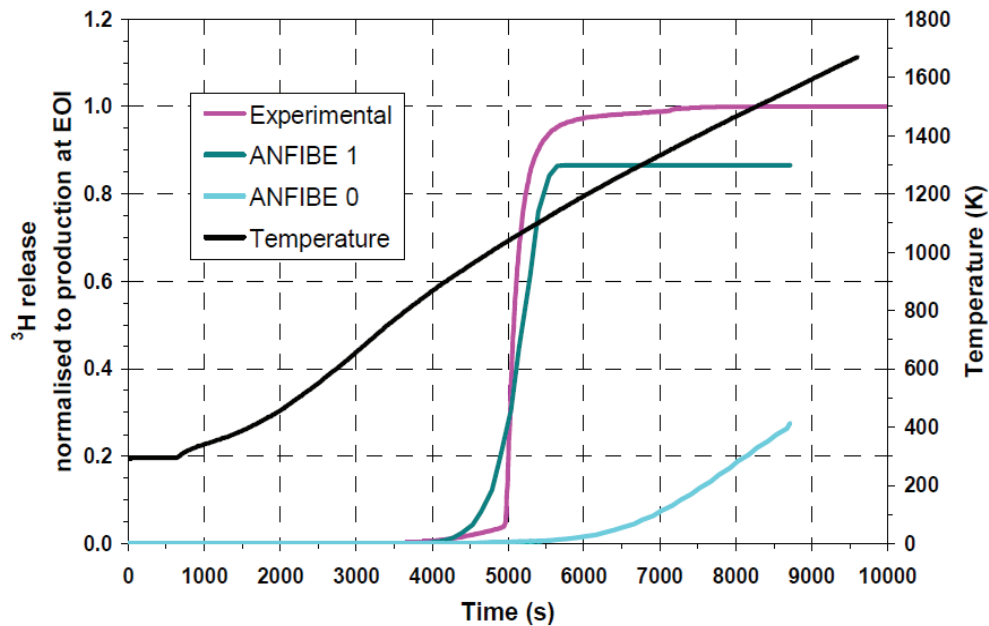


Figure 3-3 Fractional Tritium Release from Neutrons Irradiated Be [21]

According to this results we found the following linear fit of tritium release fraction, expressed as a function of average Beryllium temperature T_{av}^{Be} in Kelvin unit.

$$f_r(T_{av}^{Be}) = 0.2 + 0.00068 \cdot (T_{av}^{Be} - 300) \quad (3.34)$$

For an average Be temperature $T_{av}^{Be} = 655 \text{ }^\circ\text{C}$ (928 K), a fractional release $f_r = 0.627$, which is, as shown in Figure 3-3, in agreement with experimental data.

Finally, according to this very simplified and conservative model, the tritium concentration inside Be can be analytically obtained by integrating in time t the second differential equation reported in Eq. (3.1) and giving:

3. Description of the Model

$$C_T^{Be}(t) = (1 - f_r(T_{av}^{Be})) \cdot G_v^{Be} \cdot t \quad (3.35)$$

The tritium inventory inside Beryllium pebbles, is then defined as:

$$I_{Be}[g] = C_T^{Be} \cdot (V_{Be}^{BU} \cdot N_{BU}^{mod} \cdot N_{mod}) \cdot M_T \quad (3.36)$$

Given all the tritium inventories terms listed above, the total tritium inventory managed by the HCPB blanket I_{tot} is obtained by summing all the contributions, such as:

$$I_{tot}[g] = I_c + I_p + I_{steel} + I_{br} + I_{Be} \quad (3.37)$$

In the following section, many results will be reported for this amount of tritium, and, especially in section 4.3, the total tritium inventory is usually defined as the sum of only the first three terms, since the tritium inventories inside the breeder and inside the multiplier (see Figure 4-4), are mostly fixed by the temperature and the total tritium source and thus not influenced by the main assumptions for the SG tubes conditions, the adopted permeation models and the presence of the FW coating (see § 4.3).

3.5.2 Tritium Losses into the Environment

The two main paths for the tritium environmental release are:

- tritium permeation into the secondary circuit through the steam generator walls (see § 3.3.4);
- tritium losses associated to helium leakages from HCS due to the presence of seals and material imperfection (see § 3.4).

Therefore, tritium losses are given by summing the tritium permeation flux through SG walls Φ_{perm}^{SG} [mol/s] defined in Eqs.(3.23) and (3.24) and the tritium losses associated to helium leakages from coolant loop Φ_{leak}^c [mol/s] defined in Eq. (3.25). The choose to assume the permeation flux through SG tubes is conservative and is due to technical difficulties and economic unfeasibility of recovering tritium from water. Thus, tritium losses Φ_{tot} [Ci/d] are defined as:

$$\Phi_{tot} \left[\frac{Ci}{d} \right] = (\Phi_{perm}^{SG} + \Phi_{leak}^c) \cdot \frac{N_{Av} \cdot \lambda_T}{3.7 \times 10^{10}} \cdot N_{sec,d} \quad (3.38)$$

where $N_{sec,y}$ [sec/d] = 3600 · 24 = 86400 [sec/d] is the number of seconds per day, $N_{Av} = 6.022 \times 10^{23}$ [atoms/mol] is the Avogadro number and $\lambda_T = 1.7841 \times 10^{-9}$ [s⁻¹] is the tritium decay constant.

4 Results and Discussions

In this section the results of the mathematical model described in the previous sections will be reported. The tritium assessment is affected by different assumptions and operative conditions, as highlighted during the description of the model. Thus the objective is to show the relevance of the operation and design assumptions and condition, then followed by a parametric study in which the main design parameters for the Tritium System will vary in a reasonable range and the solution in terms of steady state tritium losses and inventories will be visualized.

The first operation is to define a reference DEMO HCPB blanket configuration (i.e. DEMO 2003 in this study, whose main features are listed in Table 2-1). Then, we need to assume a working point based on this configuration which is defined in terms of operative conditions (i.e. TES and CPS efficiencies, permeation surfaces conditions and regime, etc.). Finally, we range the most relevant parameters from that configuration.

4.1 Material Properties, Input Data and Main Assumptions

As already shown in 2011, the model described in chapter 2 has been implemented in a MATLAB code, named FUS-TPC. The code adopts the material properties database reported in Table 4-1, characterized by tritium transport properties in structural materials (e.g. permeabilities, solubility, adsorption constant, etc.) and chemical properties in Helium (e.g. chemical equilibrium constants described in Eqs. (3.9) and (3.10)). In Table 4-1 are reported all the material properties implemented into the code.

According to [16] the adsorption constant σk_1 of EUROFER is in the same range of values of MANET. Thus, for EUROFER structural materials the empirical adsorption constant for MANET will be chosen. It can be noticed that the adsorption constants for clean and oxidized INCOLOY surfaces differ from four orders of magnitudes, which is affecting very much the results, especially in terms of tritium permeation rate (then tritium losses) into the steam cycle (see § 3.5.2).

In Table 4-2, Table 4-3 and Table 4-4 are reported the adopted input data for the simulation and assumed to be corresponding as the nominal configuration parameters. The name of the variables are expressed with reference to the adopted ones in the description of the model, carried out in chapter 3.

Before reporting the results, important considerations must be reported about the choice of the permeation regime, which is highly affecting the nature of the results.

4.1.1 Definition of the Limiting Regime for Tritium Permeation

According to what reported in § 3.3.1, the tritium permeation is supposed to be controlled by surface-limited regime in case of low tritium partial pressures. According to Ref. [15] and to the calculated HT partial pressures reported in Figure 4-3, apparently the maximum values present into the tritium system, are the ones into the purge loop, which assume values of order of 1.6 Pa (design value at TES inlet for DEMO 2003), which is lower than 10 Pa, considered as the threshold value between surface and diffusion-limiting permeation regimes (see § 3.3.1). Indeed at low pressure values, the migration through structural materials is governed by surface phenomena, such as adsorption, recombination, dissociation, etc. and the diffusion is supposed to be much faster. Anyway as shown in Figure 3-1, assuming a diffusion-limited model instead of a surface-limited one at relatively low pressures, leads into an overestimation (thus conservative) of the permeation rate. In HCPB blanket the tritium permeation occurs into two main locations:

- through CPs Helium channels (from purge to primary coolant loop);
- through SG tubes (from primary to secondary coolant).

The first location is the one at maximum tritium partial pressure, and, in order to mitigate the tritium permeation into the coolant circuit, a coating layer (such as aluminum or erbium oxides [31]) can be applied in order to reduce the tritium permeation of a certain tritium Permeation Reduction Factor (PRF). However, as defined in § 3.3.1, a PRF has not to be considered in the surface-limited model defined in Eq. (3.16), since the membrane with an additional metallic layer (barrier) results in the reduced permeation if diffusion remains the rate limiting process [14]. Moreover, since a PRF is defined as a reduction of steady state permeation flux and since it is usually obtained experimentally at relatively high tritium/hydrogen partial pressure, it does not have any physical meaning to apply a PRF to a surface-limited permeation model. Indeed, the proper way to act in order to take into account of the presence of coating materials is to apply the correct surface properties for tritium related to oxidized or coated materials and not the one of the bare material reduced of a certain PRF.

Surface properties (i.e. adsorption and recombination constants) for EUROFER 97 (CP and FW materials) have some uncertainties [16], while data of oxidized INCOLOY

are well defined (see Table 4-1), since the application of an oxidation layer on SG tubes is performed on purposes for corrosion control. Summarizing the question issued for permeation limiting processes, for the current analysis the following assumption are adopted:

- tritium permeation regime through CP and FW is assumed to be diffusion governed with a certain PRF = 10 applied on the cooling channels surfaces (conservative choice).
- tritium permeation regime through SG tubes is assumed to be surface-limited, and the permeation rate is calculated adopting the adsorption/recombination constant for oxidized INCOLOY 800 reported in Table 4-1.

4.1.2 Material Properties Database

In Table 4-1 is reported the complete material properties database adopted in FUS-TPC code. In general tritium transport properties might be affected by large uncertainties. As an example, the adsorption constants $\sigma k_{1,EU}$ determined by E. Serra for MANET steels [24] reported in Table 4-1 (and adopted for this study) looks quite far from the one reported by same author three years later [25], that is: $\sigma k_1(T)[\text{mol}/\text{m}^2/\text{s}] = 5.56 \times 10^{-7} \exp(-19093/RT)$. In Figure 4-1 both adsorption constants relations are reported in the same Arrhenius plot. This wide range has also figured in Ref. [24].

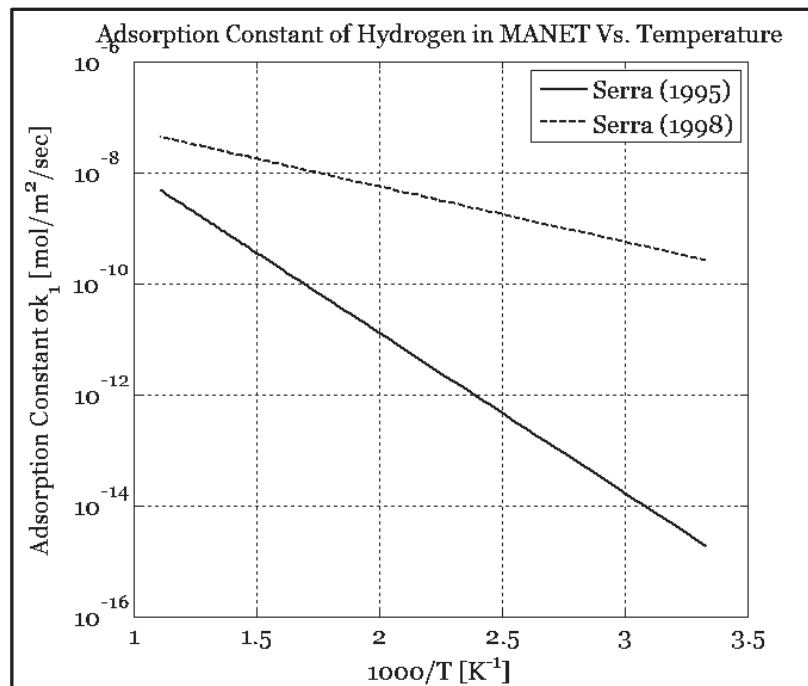


Figure 4-1 Different Adsorption Constants in MANET Steels Vs. 1000/T

4. Results and Discussions

Property	Expression	Ref.
T permeability for EUROFER 97	$P_{EU}(T) \left[\frac{mol}{m \cdot s \sqrt{Pa}} \right] = 1.8 \times 10^{-8} \exp\left(-\frac{39580}{RT}\right)$	[32]
T Sieverts' constant for EUROFER 97	$K_{S,EU}(T) \left[\frac{mol}{m^3 \sqrt{Pa}} \right] = 0.102 \cdot \exp\left(-\frac{23810}{RT}\right)$	[32]
T adsorption constant for EUROFER97 (clean surface)	$\sigma k_{1,EU}(T) \left[\frac{mol}{m^2 \cdot s \cdot Pa} \right] = 7.66 \times 10^{-6} \cdot \exp\left(-\frac{55217}{RT}\right)$	[24]
T permeability for INCOLOY 800	$P_{INC}(T) \left[\frac{mol}{m \cdot s \sqrt{Pa}} \right] = 3.94 \times 10^{-8} \exp\left(-\frac{55600}{RT}\right)$	[33]
T Sieverts' constant for INCOLOY 800	$K_{S,INC}(T) \left[\frac{mol}{m^3 \sqrt{Pa}} \right] = 0.102 \cdot \exp\left(-\frac{7800}{RT}\right)$	[33]
T adsorption constant for INCOLOY 800 (clean surface)	$\sigma k_{1,INC}^{clean}(T) \left[\frac{mol}{m^2 \cdot s \cdot Pa} \right] = 4.14 \times 10^{-6} \cdot \exp\left(-\frac{44300}{RT}\right)$	[33]
T adsorption constant for INCOLOY 800 (oxidized surface)	$\sigma k_{1,INC}^{ox}(T) \left[\frac{mol}{m^2 \cdot s \cdot Pa} \right] = 2.67 \times 10^{-10} \cdot \exp\left(-\frac{40100}{RT}\right)$	[33]
T recombination constant for INCOLOY 800 (clean surface)	$\sigma k_{2,INC}^{clean}(T) \left[\frac{m^4}{mol \cdot s} \right] = 4.0 \times 10^{-4} \cdot \exp\left(-\frac{28600}{RT}\right)$	[33]
T recombination constant for INCOLOY 800 (oxidized surface)	$\sigma k_{2,INC}^{ox}(T) \left[\frac{m^4}{mol \cdot s} \right] = 2.58 \times 10^{-8} \cdot \exp\left(-\frac{24500}{RT}\right)$	[33]
T permeability in TUNGSTEN	$P_W(T) \left[\frac{mol}{m \cdot s \cdot \sqrt{Pa}} \right] = 7.2 \times 10^{-8} \exp\left(-\frac{106300}{RT}\right)$	[25]
Constant of chemical equilibrium 1 (Eq. (3.9))	$K_{eq,1}(T) = 4.662 \cdot \frac{\left(1 - \exp\left\{-\frac{5986}{T}\right\}\right)}{\left(1 - \exp\left\{-\frac{4940}{T}\right\}\right)} \times$ $\times \left(1 - \exp\left\{-\frac{3548}{T}\right\}\right) \cdot \left(1 - \exp\left\{-\frac{176.3}{T}\right\}\right)$	[26]
Constant of chemical equilibrium 2 (Eq. (3.10))	$\log\{K_{eq,2}(T)\} = 0.292 \cdot \log(T) + \frac{336.5}{T} - 1.055$	[9]
Tritium residence time into Li4SiO4	$\tau_{res}(T)[h] = 1.28 \times 10^{-5} \exp\left(\frac{9729}{T}\right)$	[18]

Table 4-1 FUS-TPC Material Properties

The plot of Figure 4-1 was meant just to show that it is important to bear in mind that tritium properties in materials might be quite different between several experimenters.

4.1.3 Input Data for the HCPB DEMO Blanket Operative Conditions

In the three following tables are reported the sets of input data adopted for the normal HCPB tritium system configuration, which are representative of the results obtained in § 4.2. In Table 4-2 are reported all the geometrical data adopted in the model described in section 3, in Table 4-3 are summarized the main Tritium System features and in Table 4-4 is listed the complete set of input data adopted for the simulation.

Input	Input name [unit]	Value	Ref.
FW permeation area/thickness	$A_{\text{perm}}^{\text{FW}}[\text{m}^2]/\Delta x_{\text{FW+coat}}[\text{mm}]$	612/5.0	[27]/ [27]
CP permeation area/thickness	$A_{\text{perm}}^{\text{CP}}[\text{m}^2]/\Delta x_{\text{wall}}^{\text{CP}}[\text{mm}]$	13370/1.0	[16]/[4]
SG permeation area/thickness	$A_{\text{perm}}^{\text{SG}}[\text{m}^2]/\Delta x_{\text{SG}}[\text{mm}]$	40060/3	[16]/ [16]
FW/CP steels volume into BU	$V_{\text{steel,BU}}^{\text{FW+CP}}[\text{m}^3]$	205×10^{-5}	[28]
FW coating thickness	$\Delta x_{\text{coat}}[\text{mm}]$	2.0	[16], [15]
SG tubes volume	$V_{\text{steel}}^{\text{SG}}[\text{m}^3]$	11.36	[16]
Be pebbles volume in BU	$V_{\text{BU}}^{\text{Be}}[\text{m}^3]$	1208×10^{-5}	[28]
Breeder volume in BU	$V_{\text{BU}}^{\text{br}}[\text{m}^3]$	375×10^{-5}	[28]
Number of BUs per module	$N_{\text{BU}}^{\text{mod}}$	9×9	[28]
Total number of modules	N_{mod}	162	[29]

Table 4-2 Geometric Input Data for Tritium Assessment in HCPB Blanket

Parameter	Input name [unit]	Value
Tritium forms released from breeder	----	HTO mainly
TES efficiency	η_{TES}	0.90
CPS efficiency	η_{CPS}	0.95
CPS coolant recirculation	α_{CPS}	0.1 %
Permeation regime in CP He channels	-----	Diffusion-limited
Permeation regime in SG tubes	-----	Surface-limited
SG tubes conditions	-----	Oxidized
FW coating material	---	TUNGSTEN
FW coating thickness	$\Delta x_{\text{coat}}[\text{mm}]$	2.0
PRF on CP cooling channels	PRF_{CP}	10

Table 4-3 Main Features of Tritium System in HCPB DEMO Blanket

4. Results and Discussions

Input	Input name [unit]	Value	Ref.
Local tritium production in breeder	G_v^{br} [T/cm ³ /s]	1.0×10^{13}	[4]
Local tritium production in Be	G_v^{Be} [T/cm ³ /s]	$1.813 \times 10^{11*}$	[29]
Tritium implantation rate on FW	J_{imp}^{FW} [T/m ² /s]	3.0×10^{20}	[27]
Purge Helium mass flow rate	\dot{W}_{He}^p [kg/s]	0.4	[15],[16]
Purge Helium total mass	m_{He}^p [kg]	15 [†]	---
Purge Helium pressure	p_{He}^p [MPa]	0.1	[15],[16]
Swamping ratio in purge gas	$\chi_{H_2/He}$ [—]	0.1%	[15],[16]
TES efficiency	η_{TES}	0.90	[15]
CPS efficiency/Coolant Recirculation	η_{CPS}/α_{CPS}	0.95/0.1 %	[15]
Primary Coolant mass flow rate	\dot{W}_{He}^c [kg/s]	2400	[15],[16]
Primary Coolant total mass	m_{He}^c [kg]	22600	[15],[16]
Primary Coolant pressure	p_{He}^c [MPa]	8	[15],[16]
Coolant leakage rate	\dot{F}_{leak} [mol/s]	2.5×10^{-3}	[17]
Oxid. control H ₂ /H ₂ O ratio in cool. loop	χ_{H_2/H_2O} [—]	$\approx 40^\ddagger$	[16]
FW/CP material	---	EUROFER 97	[15],[16]
SG material	---	INCOLOY 800	[15],[16]
FW coating material	---	TUNGSTEN	[15],[16]
FW coating thickness	Δx_{coat} [mm]	2.0	[15],[16]
PRF on CP cooling channels	PRF_{CP}	10 [§]	[16]
PRF on SG tube	PRF_{SG}	10 ^{**}	---
He coolant average temperature	$T_{av,He}^c$ [K]	673	
FW average temperature	$T_{av,w}^{FW}$ [K]	698	[30]
CP channels average Temperature	$T_{av,w}^{CP}$ [K]	693	[30]
SG tubes wall average Temperature	$T_{av,w}^{SG}$ [K]	667 ^{††}	[16]
Beryllium pebbles average Temperature	T_{av}^{Be} [K]	823	[30]
Breeder Average/Min/Max temperature	$T_{av}^{br} / T_{min}^{br} / T_{max}^{br}$ [K]	973/573/1193	[30]

Table 4-4 FUS-TPC Input Data for FUS-TPC Simulations

* This value has been obtained from 3D MCNP transport and FISPACT inventory calculations using 20° torus sector. Globally, in 3.1 t of beryllium pebbles, 218 g of tritium at $t_{EOL} = 40000$ h are generated

† This value comes from non-published internal technical notes

‡ This value is obtained subdividing two references value of H₂ and H₂O partial pressure values inside the HCS, assumed to be able to ensure proper oxidation conditions onto SG walls (1500 Pa for H₂ and 36 Pa for H₂O).

§ Conservative choice and valid if diffusion limited permeation regime is adopted

** Arbitrary and conservative choice and valid if diffusion limited permeation regime is adopted

†† Average value between average Helium temperature and average water temperature inside the SG

4.2 Results for the Operative Blanket Configuration

Hereafter, are reported the representative results, considering a typical operative configuration of the entire “Tritium System in Blanket”, given by the main assumptions about the permeation limiting processes performed in the last paragraphs and the set of input data defined in Table 4-2, Table 4-3 and Table 4-4. The results will be then commented and compared with the ones obtained other two tritium transport studies performed for HCPB blanket configuration (Refs. [15] and [16]), assumed to be the reference ones to evaluate the quality of this work.

4.2.1 Tritium Concentrations and Partial Pressures Vs. Time

In this section, the results related to tritium concentrations and partial pressures are visualized. In Figure 4-2 are reported the time evolution of tritium HT and HTO concentrations inside the Purge Gas and the Coolant Loops respectively, while in Figure 4-3 the time behavior of HT partial pressures are visualized. Moreover, in order to summarize the results showed in these two plot, in Table 4-5. are reported the steady state values for all of these concentrations.

The HT and HTO steady state average concentrations inside the purge gas loop are observed to be 8.751 ppm for HT and 0.231 ppm for HTO. According to Eq. (3.3) and to the reference scheme visualized in Figure 2-2, these values correspond to 15.45 ppm and 0.4 ppm at TES entrance/BU outlet respectively. Therefore, it seems that the obtained concentrations are as a first approximation quite in accordance with the ones reported by other tritium transport assessment for HCPB blanket [15] (14.5 ppm for HT and 0.5 ppm for HTO). The calculated values are presumably lower than ones reported in this reference study probably because the assessment were performed considering purely surface-limited permeation model. Moreover, the obtained molar ratio between HTO and HT species inside the purge gas loop is 2.63 %, which is quite in agreement with the value reported in Ref [15] (i.e. 3.2 %).

The steady state HT concentration value into HCS (0.023 ppm), appears to be as well in agreement with the one reported in the same tritium analysis [15] (i.e. 0.08 ppm for HT at SG inlet). Moreover, in this reference study, the indicated average value between the inlet and the outlet CPS HT concentration is about 0.05 ppm, while for HTO it is assumed that no HTO is present. In our assessment HTO concentration is calculated and as shown in the results HTO is present in the HCS with an HTO/HT molar ratio equal to 5%.

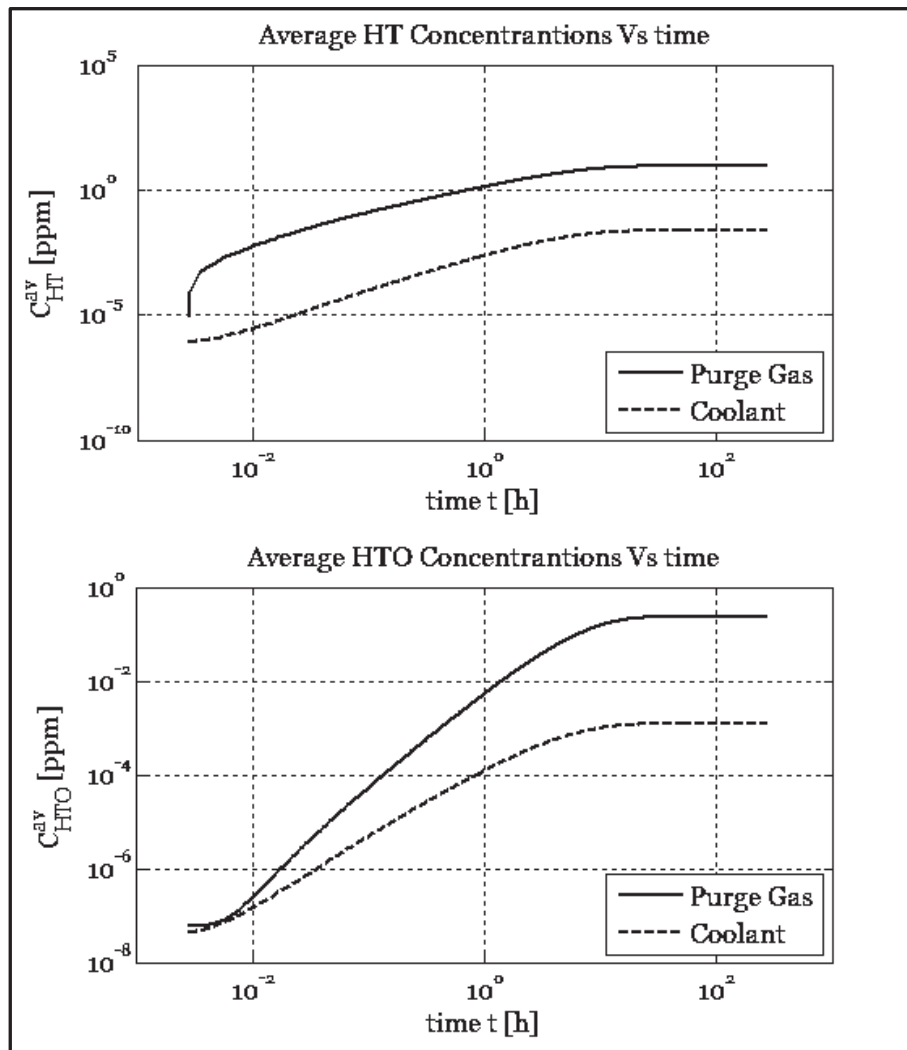


Figure 4-2 HT and HTO Concentrations in Purge Gas and Coolant Loops Vs. Time

Parameter	Variable Name [unit]	Value
HT Concentration in Purge gas Loop	C_{HT}^P [ppm]	8.751
HTO Concentration in Purge Gas Loop	C_{HTO}^P [ppm]	0.231
HT Concentration in Coolant Loop	C_{HT}^C [ppm]	0.023
HTO Concentration in Coolant Loop	C_{HTO}^C [ppm]	0.0012
HT Partial Pressures in Purge Gas Loop	p_{HT}^P [Pa]	0.96
HT Partial Pressure in Coolant Loop	p_{HT}^C [Pa]	0.185

Table 4-5 Steady State T Concentrations and Partial Pressures

Looking at time evolutions for HT and HTO in both purge gas and coolant loops, it can be noticed that HTO is “delayed” with respect HT in purge gas, while in coolant loop they HT and HTO concentrations seem to grow with the same growth rate. These time

behavior might be related to numerical issues. In fact, if we change the numerical integration method (i.e. by choosing a different MATLAB ODE solver), we get different initial time evolutions with the same steady state values.

In Figure 4-3 are reported the time evolution of HT partial pressure inside the purge gas and the coolant loops respectively (see also Table 4-5 for the steady state values). As already mentioned in §4.1.1, the foreseen HT partial pressure into the purge loop to be adopted for TES design (inlet HT partial pressure) is assumed to be 1.6 Pa, which is in accordance with the obtained results (the calculated average HT partial pressure of 0.96 Pa corresponds, according to Eq. (3.3), to an inlet HT partial into TES equal to 1.63 Pa). Therefore, the partial pressures inside the purge loop appear to be in accordance with results already published. Concerning the HT partial pressures into HCS, the reference value reported in [15] is essentially defined as 0.6 Pa, which is as a first approximation, close to the one calculated in this study (0.185 Pa). Finally, it can be stated that purge and coolant loops, have different time scales in the tritium response, that is of order of 4 hours for the purge loop and of order of 1.6 days for the coolant loop.

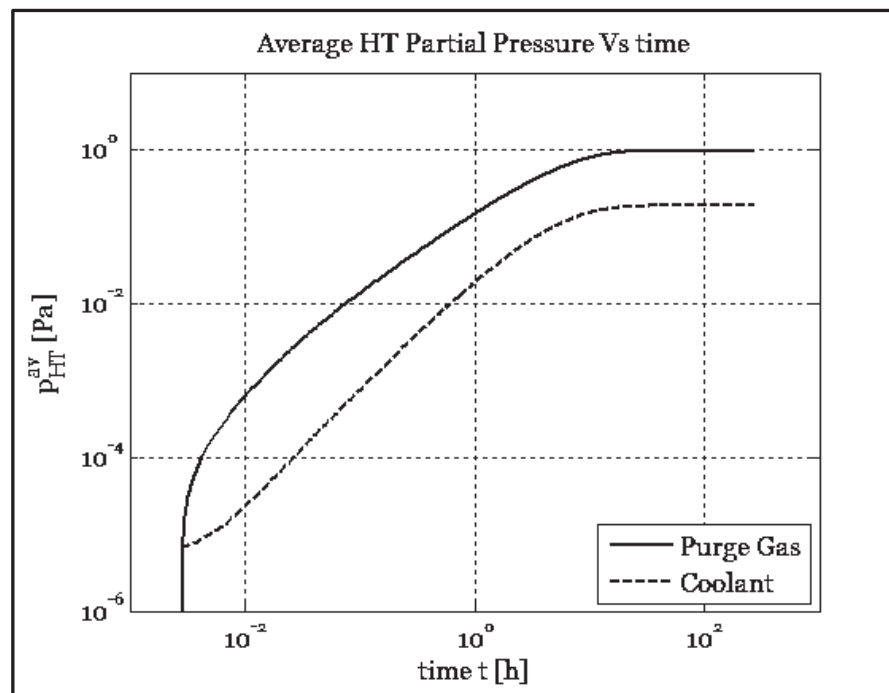


Figure 4-3 HT Partial Pressures in Purge gas and Coolant Loops Vs. Time

4.2.2 Tritium Inventories Vs. Time

In Figure 4-4 all the tritium inventories contributions described in § 3.5.1 are visualized in the same graphical area and in Table 4-6 the related steady state values are listed. As already mentioned, the tritium inventory inside Beryllium is a crucial point and

4. Results and Discussions

it is still an open issue. At End Of Life (EOL = 4 years) the tritium inventory is close to 1 kg, which is a large amount of tritium. As reported in § 3.5.1 this tritium inventory profile was obtained by a linear model in time with a given local production rate G_v^{Be} [T/cm³/s] and a release fraction $f_r(T_{av}^{Be})$ obtained by best fitting with average Be pebbles T_{av}^{Be} temperature the results obtained by ANFIBE 1 code and supported by lasts experimental results.

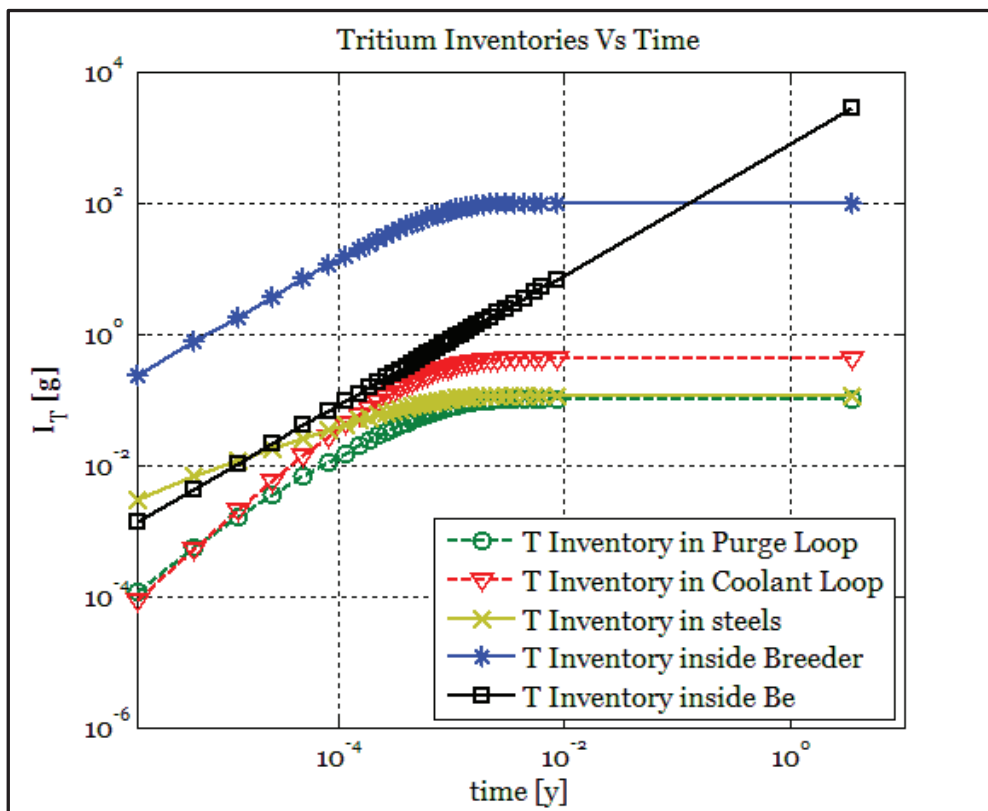


Figure 4-4 Tritium Inventories Vs. Time

Parameter	Variable Name [unit]	Value
T Inventory in Breeder	I_{br} [g]	99.19
T Inventory in Beryllium	I_{Be} [g]	2777
T Inventory in Purge Gas Loop	I_p [g]	0.101
T Inventory in Coolant Loop	I_c [g]	0.4033
T Inventory in Steels	I_{steel} [g]	0.1153

Table 4-6 Steady State Tritium Inventories Vs. Time in all the Blanket Locations

In this section was reported just for completeness and to show anyway a conservative estimation of this quantity but it does not constitutes a reliable matter of consideration

since, as mentioned, the tritium and helium kinetics related to retention inside Be are still complicated to be well described and modeled.

The second most important term is the tritium inventory inside the ceramic breeder, where the tritium is generated. At EOL, the total inventory of tritium inside the breeder is about 99 g.

Tritium inventories inside all the blanket components (i.e. purge gas coolant loops, Beryllium and breeder pebbles beds) are important in case of accident. For instance, in case of one or more coolant pipes failures, if we assume (conservatively) to release all the tritium amount inside the coolant loop, it can be seen from Table 4-6 that the maximum releasable tritium amount is about 40 mg. Concerning the releasable tritium quantity from purge gas, it must be pointed out that all the purge system it is supposed to be in a protected and well confined environment, thus the released quantity into the environment in case of accident can be lower than one indicated in Table 4-6 (i.e. about 10 mg).

Tritium inventory inside steels are important for shutdown and decommissioning phases. In this case the tritium amount inside the considered structural materials in contact with tritium contaminated Helium are of order of 10 mg of tritium, which is again not worrying from radiological problems.

In conclusion, the most relevant inventory terms for radiological safety are the ones for breeder and Be pebble beds.

4.2.3 Tritium Losses Vs. Time

Tritium losses into the environment is a very important quantity in a tritium assessment of a fusion reactor breeding blanket, since it indicates the potential radiological risks related to tritium contamination during the normal condition of the plant. As reported in Ref. [5], 20 Ci/d is considered as the allowable tritium environmental release value. In Figure 4-5 are visualized the results for total tritium losses into the environment which have been obtained according to the mathematical description reported in § 3.5.2, where the total tritium losses Φ_{tot} is given by the sum of total permeation rate into the steam cycle $\Phi_{\text{perm}}^{\text{SG}}$ and the tritium release rate associated to the helium leakages from the main coolant circuit $\Phi_{\text{leak},i}^{\text{c}}$.

As shown in the results the allowable environmental tritium release is well accomplished with the given tritium system configuration described by the sets of data reported in Table 4-2, Table 4-3 and Table 4-4, giving a tritium losses value around 2 Ci/d (i.e. 1.929 Ci/d). This result was quite expected since the HT partial pressure into

4. Results and Discussions

the main coolant system (see Figure 4-3) is about 0.18 Pa, which is lower the one found in Ref. [15], that is the maximum partial pressure value above which the permeation flux into the HCS is larger than 20 Ci/d (fixed to 0.6 Pa).

As reported in § 4.2.3, tritium losses are also characterized by tritium amount released with Helium leakage from the coolant loop. This term is usually smaller with respect the permeation rate into the HCS. In this study it is of order of 7.8%.

As already mentioned in § 3.3.1 and in the previous paragraph, the surface conditions either for CP channels and for SG tubes are impacting significantly the numerical results. Here, are reported the tritium losses results, considering the CP helium channels to be coated with $PRF_{CP} = 10$, oxidized SG tube walls and a recirculation rate 0.1% inside the CPS. It must be pointed out that $PRF=10$ on CPs He channels is a more conservative value than ones coming from literature for EUROFER 97 (e.g. $15 \div 80$ [31]), or the ones adopted in previous tritium transport assessment ($PRF=1 \div 100$ [32], [35]).

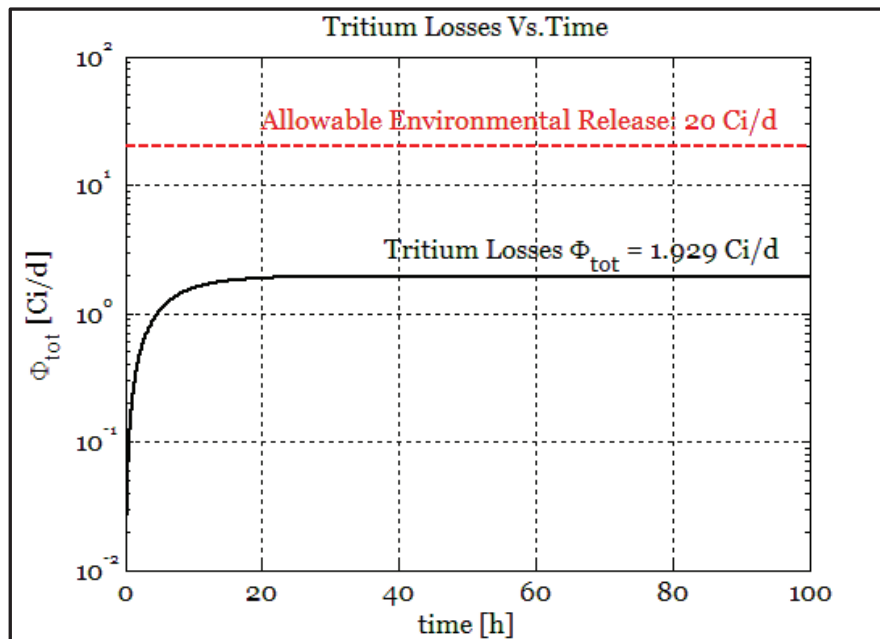


Figure 4-5 Tritium Losses Vs. Time

It has to be noticed also that for the SG walls, a surface limited permeation model was assumed and the surface properties for tritium in INCOLOY 800 membrane were taken considering the surfaces to be oxidized. This is not the most conservative choice, since, according to the adsorption/recombination constants for INCOLOY 800 reported in Table 4-1 the values for clean and oxidized surfaces differ one from each other of about four orders of magnitude. As reported in § 3.2, in HCS an oxidation layer for SG tubes is provided by hydrogen and water addition. The oxidation layer on SG tubes (and its

implication on tritium assessments) is anyway an open issue. The problem comes from the uncertainties of the oxygen potential into HCS, thus of the resulting protection layer. However, as reported in Table 4-1, adsorption/recombination constants values for oxidized INCOLOY surfaces were taken from [16]. It can be seen that both constants are reduced by four order of magnitudes with respect to bare materials samples.

4.3 Impact of the Main Assumptions on the Results

The tritium transport model derived in this study for HCPB DEMO blanket has been described in section 3 and the main results have been reported in § 4.2, considering a certain set of input data and some modeling and technological assumptions (see § 4.1, Table 4-2, Table 4-3 and Table 4-4), which are to be considered representative for the operative conditions of the tritium system. As a matter of fact, as reported in § 4.2 many assumptions and different hypothesis have been taken in order to carry out the analysis. These assumptions are either related to modeling aspects (e.g. diffusion Vs. surface-limited permeation model) and technological aspects (e.g. presence of a given coating barriers on the FW surface).

In order to show the importance and the impacts of these assumptions on the results (in terms of tritium losses and inventories inside the main components of the tritium system), in this paragraph will be reported the total tritium losses and inventories, by considering the following conflicts inside this tritium transport study:

- Oxidized Vs. Clean SG tubes surfaces;
- Diffusion Vs. Surface limited model;
- Presence Vs. Absence of a FW protection layer.

Before reporting the results, it must be pointed out that the tritium inventories reported hereafter (defined as the total tritium inventories), are given by considering only the contribution of tritium inventory inside the purge loop, inside the coolant loop and inside the steels, according to the model reported in § 3.5.1.

4.3.1 Oxidized Vs. Clean SG Walls Surfaces

As already stated in § 4.1, the results reported in plots from Figure 4-2 to Figure 4-5 have been obtained considering the surface conditions for the SG tube walls as they are kept oxidized, thus with a certain oxidation layer. This choice has been taken because for the previous set of results we wanted a certain set of conditions which are representative of the nominal and operative conditions of the plant. However, as shown in Table 4-1 the

surface constants (adsorption and recombination constants) are quite different between the two conditions (about four orders of magnitude), thus the differences on the results are supposed to be markedly high.

Anyway at a certain time of plant operation, the SG walls are supposed to assume a given oxidation layer given by hydrogen and water addition to the coolant circuit. So the objective is to show what are the effects in terms of tritium losses and inventories, if we assume an adsorption or recombination constant (keeping a surface-limited model for permeation through the SG pipes) for clean tubes instead of that for oxidized tubes, adopted for the previous set of results reported in § 4.2, assuming the same set of parameters reported in Table 4-3. In Figure 4-6 and Figure 4-7 are reported the tritium losses and the tritium inventories for both SG tubes conditions respectively.

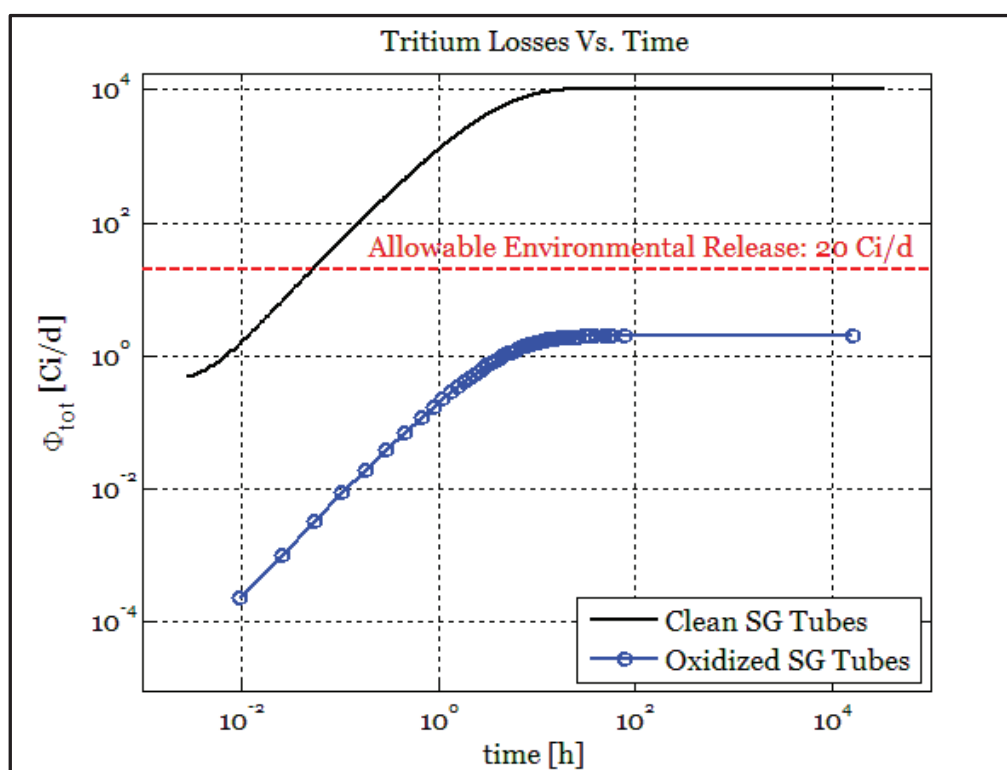


Figure 4-6 Tritium Losses Vs. Time for Clean and Oxidized SG Tubes Conditions

As shown in Figure 4-6, the differences from tritium losses obtained considering clean and oxidized SG tubes (as expected) are relevant. The steady state tritium losses for oxidized SG tubes are equal to 1.94 Ci/d (coincident to the values reported in Figure 4-5), while the total steady state tritium losses related to clean SG tube walls are about three orders of magnitude larger (about 10430 Ci/d), which is also much larger than the allowable limit (assumed to be equal to 20 Ci/d). This huge difference is due to

remarkable difference in tritium surface properties for both conditions (i.e. adsorption and recombination constants).

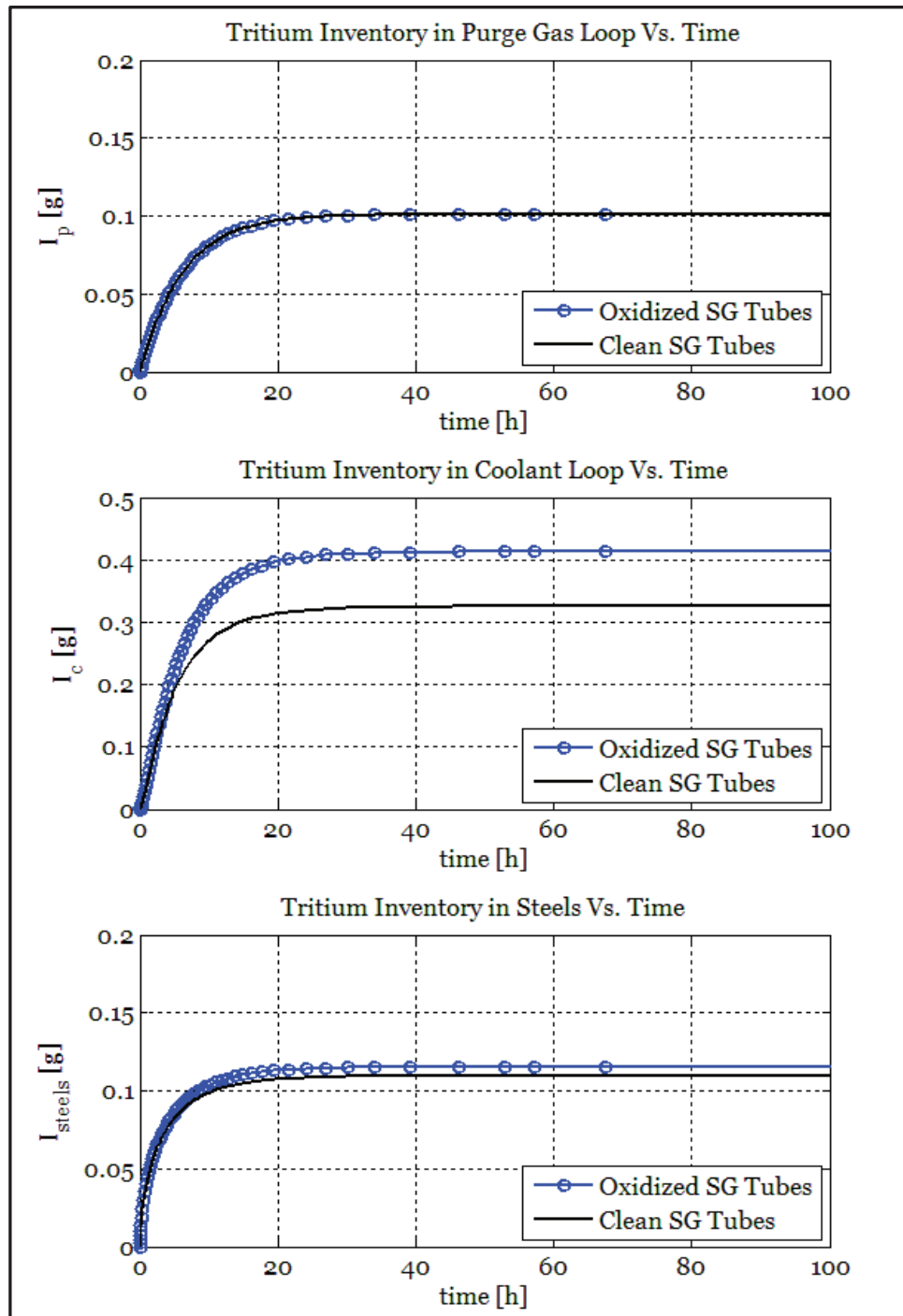


Figure 4-7 Tritium Inventories Vs. Time for Clean and Oxidized SG Tubes Conditions

Anyway, in order to have more reliable data in case of oxidized SG walls, further literature data for adsorption and recombination constants are needed. For this analysis only the expressions reported in Table 4-1 related to oxidized surfaces have been used.

Concerning the tritium inventories the difference are not so relevant as in the tritium losses results. As shown in Figure 4-7, between the two limiting SG tube surfaces conditions only the inventories in purge gas and coolant loops and steels are visibly varying (see Table 4-7 for values) whilst the other terms considered in the models (i.e. breeder and Be pebbles) are absolutely insensitive with respect to these conditions, as illustrated also by the mathematical structure of the model described in Chapter 3. The T concentration in breeder and Be are mathematically uncoupled from the others, thus not affected from the permeation conditions through the SG pipes).

Parameter	Oxidized SG Tubes	Clean SG Tubes
T Losses [Ci/d]	1.929	10430
T Inventory in Purge Gas Loop [g]	0.1074	0.1072
T Inventory in Coolant Loop [g]	0.412	0.324
T Inventory in Steels [g]	0.1153	0.109

Table 4-7 Steady State T Losses and Inventories for Clean and Oxidized SG Tubes

Summarizing the obtained results as regard the impact of the SG tubes conditions on the results, it is immediately clear that the SG tubes conditions must be well controlled, and the performances in terms of reduction of tritium permeation fluxes should be investigated with more detailed experimental campaign or models.

4.3.2 Diffusion Vs. Surface-Limited Permeation Regime

As reported in § 3.3.1, for the tritium permeation flux through structural materials two main models are available: 1) diffusion-limited and 2) surface-limited permeation models. As already described there, the right criteria defining the model to be adopted is not yet well defined. From many experimental campaigns it can be seen that at low pressures values (some authors [12] stated below than 10 Pa), the permeation through a membrane of a structural material seems to be better described by a surface-limited model, in which the relationship between the permeated flux and the partial pressure is linear.

As discussed in § 3.3 we need to express the permeation fluxes as a function of the permeable concentrations (basically only HT) inside the purge and the coolant loop, and to put these permeation fluxes into the mass balance equation reported in Eq. (3.1). The permeation fluxes present into our system, as reported in the scheme of Figure 2-2, are given by: 1) the permeation flux through the Cooling Plates (CPs) helium channels and 2) the permeation flux through the SG pipes. We have also the permeation flux of the

implanted tritons onto the FW, but it is considered in this study to be described only as a diffusive flux.

In Eqs. (3.18) and (3.19) are reported the expressions for permeation fluxes through cooling channels of CPs in case of diffusion and surface-limited permeation regime respectively, while in Eqs. (3.23) and (3.24) are reported the same expressions for tritium permeation flux through the SG pipes.

According to these theoretical options, four possible combinations are available to describe the permeated fluxes through CPs and SG walls, such as:

- Diffusion model through CPs He channels, Diffusion model through the SG pipes;
- Diffusion model through CPs He channels, Surface model through the SG pipes;
- Surface model through CPs He channels, Diffusion model through the SG pipes;
- Surface model through CPs He channels, Surface model through the SG pipes.

For each of these options, we find different results in terms of tritium losses and inventories, as reported in plots of Figure 4-8 and Figure 4-9. In order to make the comparison between all the possible combination meaningful, each curves has been obtained by considering the set of input data reported in Table 4-2, Table 4-3, Table 4-4 and all the permeation surfaces to be clean and without any oxidation layer or permeation coating. Since the objective is to compare the impact of the permeation models on the Tritium migration assessment, the tritium losses results are visualized by normalizing the obtained T losses curves for all four cases with the steady state value of the first case (i.e. Diffusion-Limited regime through the CP He channels and Diffusion-Limited through the SG Tubes), while the actual values are reported in Table 4-8. As reported on the results, the steady state tritium losses ranges between 42427 to 913 Ci/d, which is a wide range between the models. There is a factor of 47 between the highest and the lowest T losses curves (i.e. Diffusion-Diffusion and Surface-Surface for CPs-SG respectively), which are the two limiting cases. In our reference configuration system (whose features are reported and described in § 4.1) we assumed diffusion-limited permeation for through the CPs and surface-limited model for permeation flux through SG pipes (assuming oxidized surfaces). From plot of Figure 4-8 we notice that the diffusion model tends to overestimate the permeation fluxes, and the pure diffusive permeation model (i.e. the curve with circles) is the one with higher values, whilst the pure surface permeation model (the curve with triangles) is the lowest one. This is in agreement with the literature investigation reported in § 3.3.1, concerning the influence of the adopted model on the permeation flux. This very wide range in tritium losses

4. Results and Discussions

results, suggests to improve the efforts from R&D point of view in this topic, either with more focused experimental campaigns or with more detailed models.

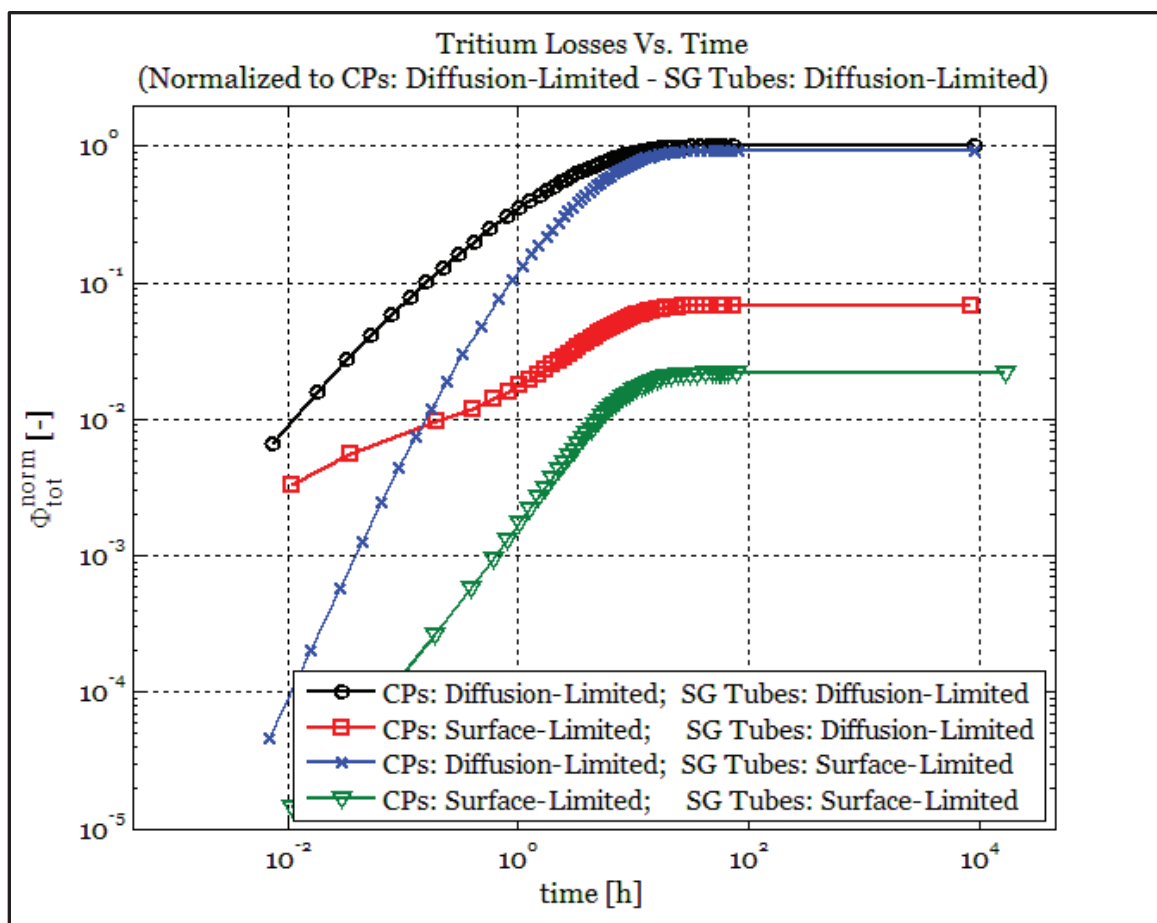


Figure 4-8 Normalized Tritium Losses Vs. Time Vs. Permeation Regime (Clean Surfaces for Surface-Limited and $PRF_{CP/SG} = 1$ for Diffusion-Limited)

Permeation Regime		Steady State Tritium Losses	
CPs	SGs Tubes	Actual [Ci/d]	Normalized on Case <i>a</i>
a) Diffusion-Limited	Diffusion-Limited	42427	1
b) Diffusion-Limited	Surface-Limited	39149	0.922
c) Surface-Limited	Diffusion-Limited	2877	0.067
d) Surface-Limited	Surface-Limited	913	0.021

Table 4-8 Steady State Tritium Losses for all the Permeation Regime Scenarios (Clean CPs/SG Tube for Surface-Limited and $PRF_{CP/SG} = 1$ for Diffusion-Limited)

The results for tritium inventories in purge gas, coolant and steels (i.e. the same locations as those indicated for the impact of SG surface conditions and as reported in § 4.3.1 and Figure 4-7) related to all the permeation model options are reported in plot of Figure 4-9 and Table 4-9. For these parameters the behavior looks as similar as the one

for tritium losses. In fact, the tritium inventories for pure diffusion permeation model (i.e. case *a*) and the tritium inventories for diffusive model on CPs and surface model for permeation through SG pipes (i.e. case *b*), are almost coincident for all the considered blanket locations. This means that the assumed permeation regime through the SG tubes does not strongly affect the T inventories results if diffusion remains the limiting process on CPs. In fact, if we assume surface-limited regime through CPs (i.e. cases *c* and *d*), the T inventories are markedly varying from the previous cases, especially in coolant loop, where the T inventory ranges among cases *a*, *b*, *c* and *d* by a factor of 219. The T inventories in Purge Gas and steels are not so affected by the permeation regime. In particular, for Purge gas we find T inventories between all the cases almost coincident, whilst for T inventory in steels we have large variations between cases *c* and *d* from cases *a* and *b* and smaller differences appear between case *c* and *d*.

Summarizing the reported results in Table 4-8 and Table 4-9 and plots of Figure 4-8 and Figure 4-9 it can be seen that the permeation regime assumed on CPs and SG tubes impact the results both on T losses and inventories. In particular, the assumption on the permeation regime through CPs seems to have a stronger impact than the one on SG tubes, especially on T inventory in coolant.

Permeation Regime		Tritium Inventories [g]		
CPs	SGs Tubes	Purge Gas	Coolant	Steels
a) Diffusion-Limited	Diffusion-Limited	0.09804	1.207	0.1511
b) Diffusion-Limited	Surface-Limited	0.0981	1.22	0.1516
c) Surface-Limited	Diffusion-Limited	0.1019	0.0055	0.0696
d) Surface-Limited	Surface-Limited	0.1019	0.02846	0.07728

Table 4-9 Steady State Tritium Inventories for all the Permeation Regime Scenarios (Clean CPs/SG tubes for Surface-Limited and $PRF_{CP/SG} = 1$ for Diffusion-Limited)

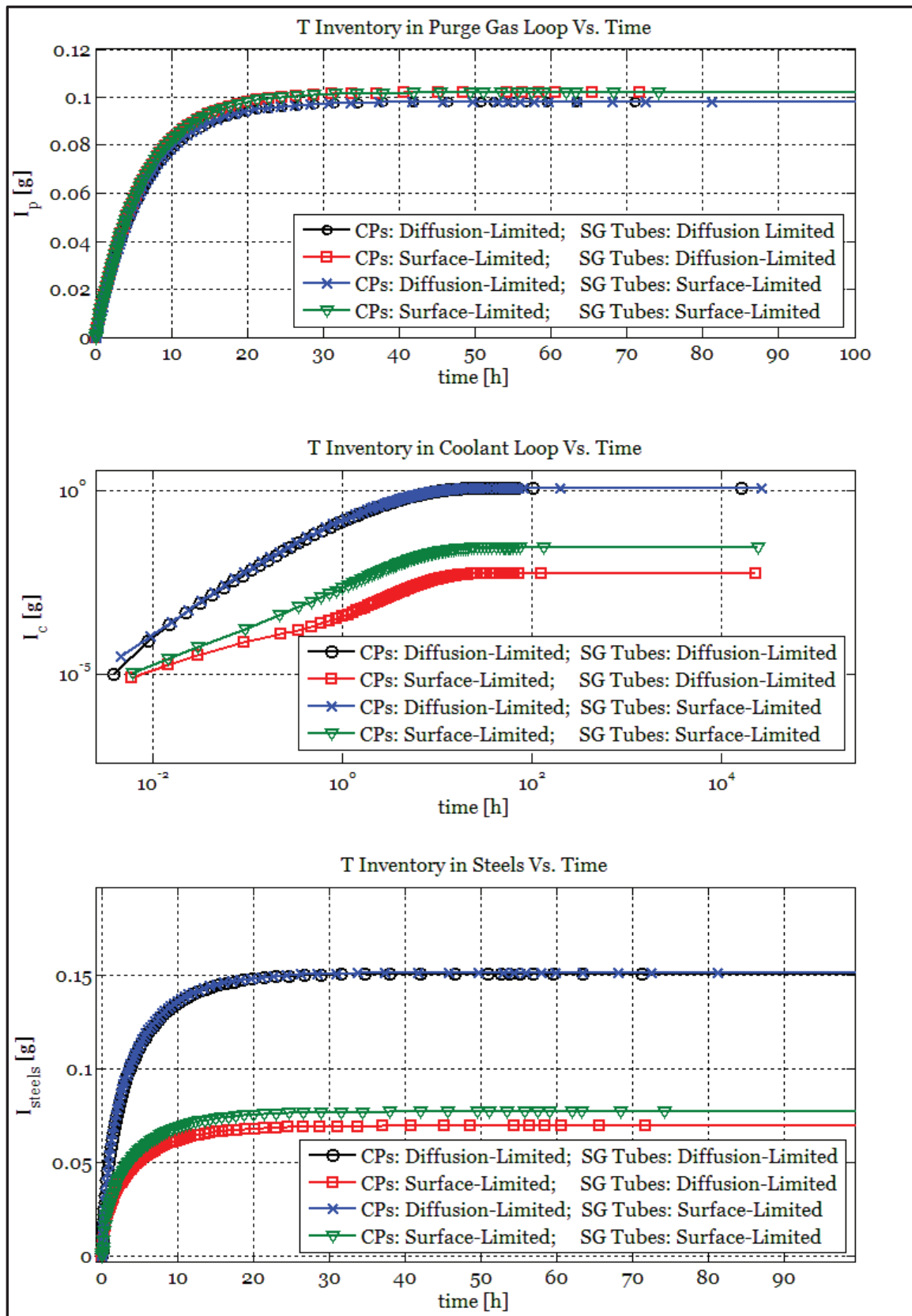


Figure 4-9 Tritium Inventories Vs. Time Vs. Permeation Regimes (Clean Surfaces for Surface-Limited and $PRF_{CP/SG} = 1$ for Diffusion-Limited)

4.3.3 Presence Vs. Absence of a FW Coating Layer

As reported in § 3.3.3, the presence of a FW protection layer, characterize an open issue for tritium assessment in fusion reactors. The tritium contribution coming from unburnt tritons implanted to the FW surface, permeating through the FW and getting into the cooling channels (thus the main coolant system) is usually neglected if a certain protection layer on the FW surface is foreseen (see § 3.3.3 for values and literature review).

As already showed, the permeation flux of tritons coming from the plasma through the FW channels (see Table 4-4 for implantation rate values), has been modeled considering two homogenous membranes characterized by the coating layer with a certain thickness Δx_{coat} and the bare FW material (i.e. EUROFER97 or MANET) characterized by a thickness t_{FW} . An effective permeability $P_{\text{eff}}^{\text{FW}}$ is found by considering the sum of permeation resistances for each layer, analogous to the electrical resistors in series, since the two membranes have comparable thicknesses. For this permeation flux, a diffusion-limited model has been assumed.

The objective in this section is to show the strong impact of the presence of a FW coating layer on tritium losses results, which are reported in Figure 4-10 (tritium losses) and in Figure 4-11 (total tritium inventories) by varying only the protection layer thickness Δx_{coat} in the set of input data reported in Table 4-2, Table 4-3 and Table 4-4.

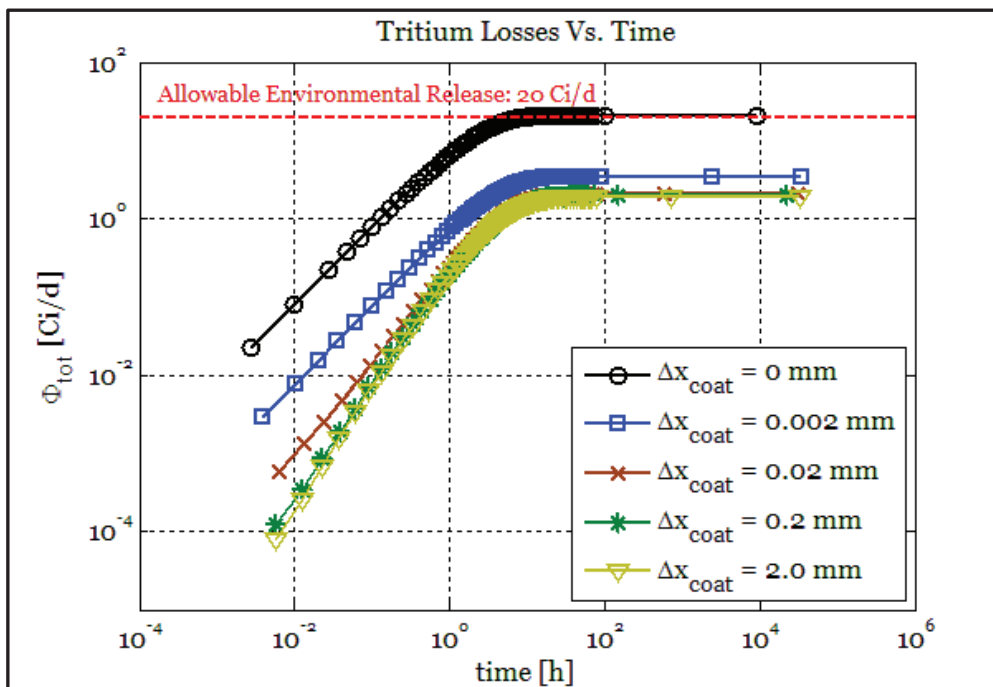


Figure 4-10 Tritium Losses Vs. Time Vs. Thickness of FW Coating Layer

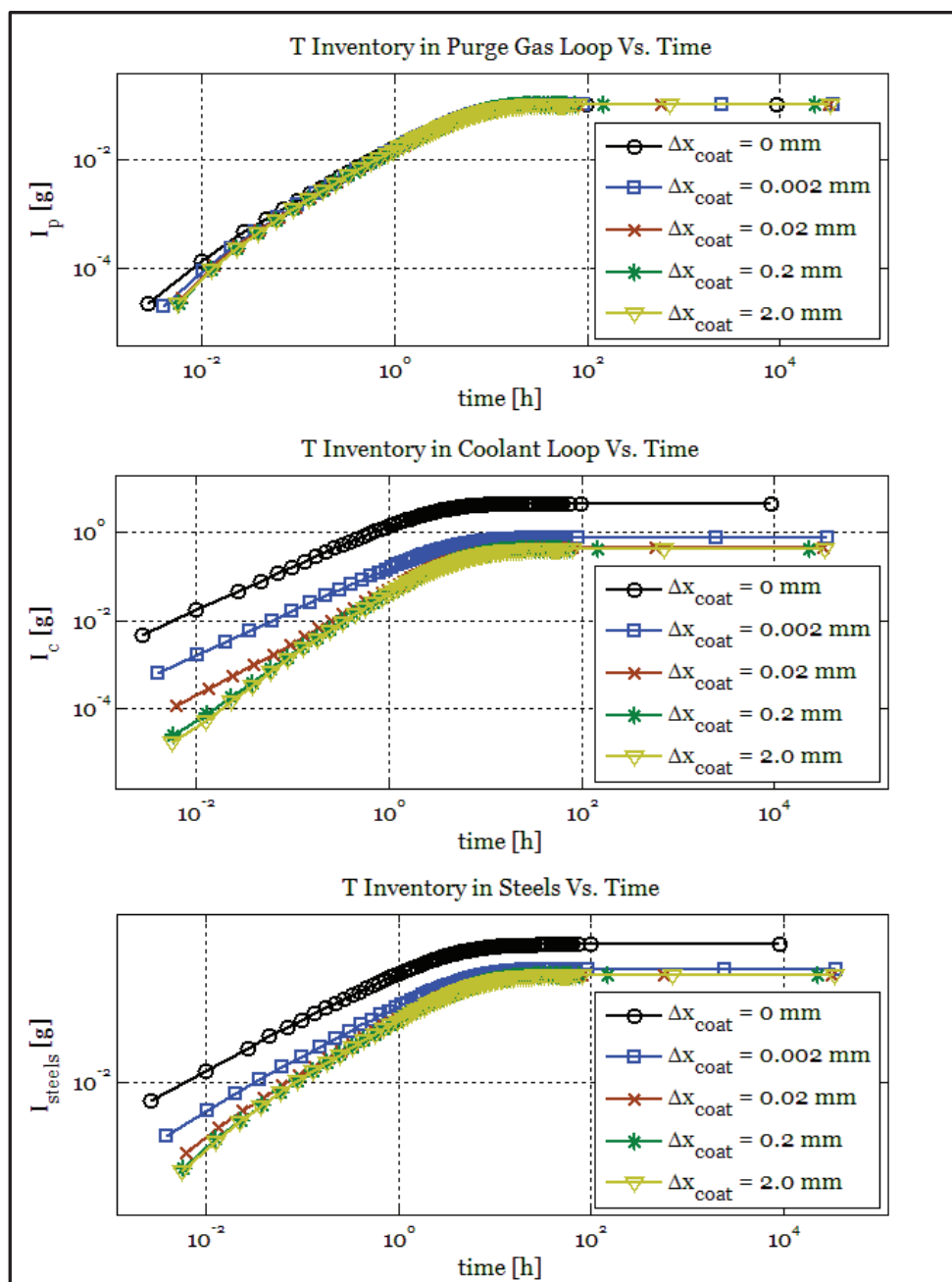


Figure 4-11 Total T Inventories Vs. Time Vs. Thickness of FW Coating Layer

Parameter	FW Coating Thickness Δx_{coat}				
	0.0 mm	0.002 mm	0.02 mm	0.2 mm	2 mm
T Losses [Ci/d]	20.82	3.468	2.09	1.944	1.929
T Inventory in Purge [g]	0.1027	0.1013	0.1010	0.1009	0.1009
T Inventory in Coolant [g]	4.42	0.7365	0.4437	0.4127	0.4096
T Inventory in Steels [g]	0.2337	0.1328	0.1172	0.1153	0.1151

Table 4-10 Steady State T Losses and Inventories Vs. Thickness of FW Coating Layer

As reported on the results, the tritium losses decrease as the FW coating layer increases, as expected, and the tritium inventories as well, since the higher thickness, the lower is the permeated flux of implanted tritons from the plasma through the FW channels.

As showed on Figure 4-10 and Figure 4-11, at a certain point, the solution tends to saturate. In other words, there is a value of Δx_{coat} beyond which tritium losses and inventories do not change with any further increase. In fact, the curves corresponding to 0.02, 0.2 and 2 mm are almost coincident either for tritium losses and tritium inventories. This is a very important result for a tritium assessment of the all blanket, because it characterizes a very precious information from the point of view of the design.

It must be pointed out also that the system is quite robust with respect the presence of a FW protection layer. As a matter of fact, the complete absence of coating ($\Delta x_{\text{coat}} = 0$ mm), i.e. the worst case in terms of tritium contamination, the tritium losses are equal to 20.82 Ci/d, which is close to the imposed allowable tritium release limit of 20 Ci/d. The tritium losses results range for about one order of magnitudes (from 20.82 to 1.93 Ci/d) as well as the total tritium inventories in coolant loop and steels (from about 4.42 g to 0.40 g for coolant and from 0.2337 g to 0.1151 g for steels). These values lead us to state that the FW coating layer might significantly impact the tritium assessment.

4.4 Main Parameters for Tritium Migration in HCPB DEMO Blanket

As performed in 2012 for the HCLL blanket configuration [37], in this section a parametric study is performed by considering five parameters of the considered tritium system (see Figure 2-2) defined by the set of input parameter listed in Table 4-2, Table 4-3 and Table 4-4 (except for the studied parameter who is ranged here), such as:

- TES Efficiency η_{TES} (see § 3.1 and Eq. (3.3));
- CPS Efficiency η_{CPS} (see § 3.1 and Eq. (3.5));
- CPS Recirculation Rate α_{CPS} (see § 3.1 and Eq. (3.5));
- PRF on CP cooling channels PRF_{CP} (see § 3.3.2 and Eq. (3.18));
- PRF on SG pipes PRF_{SG} (see § 3.3.4 and Eq. (3.24)). This is meaningful only if a diffusion limited regime through SG pipes is considered.

These parameters, after repeating several simulations, have been observed to be the most relevant ones on the overall final results (i.e. T losses and inventories) and thus are the most important ones for the blanket-related tritium system design. As a matter of fact,

this part is very important in order to address the main design guidelines toward the correct directions, and to improve the R&D efforts in the correct fields. Other parameters could be studied (e.g. temperatures in purge gas, coolants and structural materials and the flow rate in TES) but since they are fixed from the blanket design they have been considered fixed for this study.

The analysis will be carried out again by evaluating the response of the system (in terms of tritium losses and inventories), by varying these important parameters in valid and feasible ranges. The tritium inventories considered in this parametric study are simply related to: 1) tritium inventory inside the purge gas loop, 2) inside the main coolant loop and 3) inside steels, since the tritium inventories inside breeder and beryllium pebble beds, according to the model described in §§. 3.5.1.3 and 3.5.1.4, are not affected from the variation of the listed above parameters. For values of these two last tritium inventories, see Figure 4-4.

4.4.1 Tritium Losses and Inventories Vs. TES Efficiency

In Figure 4-12 are reported the steady state tritium losses and the tritium inventories for clean and oxidized SG tubes, obtained by varying the TES efficiency η_{TES} from 50 % to 100 %.

As shown in the results, the tritium losses are observed to exponentially decay vary from about 3.5 to 0.14 Ci/d with η_{TES} varying between 50 and 100 % for oxidized SG tubes, while for clean INCOLOY 800 tubes, we find much larger value between 17790 to 9140 Ci/d, confirming the trend already observed in Figure 4-6.

The same behavior with respect η_{TES} can be observed for T inventories in Purge Gas, Coolant and Steels by lowering from 0.246 to 0.082 g, from 0.715 to 0.36 g and from 0.167 to 0.106 g respectively in case of clean SG tubes. As it can be seen, in case of oxidized SG tubes the T inventory in purge gas remains totally unchanged, while T inventories in coolant and steels are increasing but maintain the same exponential decay along η_{TES} decreasing from 50 to 100 % confirming again the response of the system with respect the SG tubes conditions.

In relative terms the dumping of tritium inventory inside the purge loop is stronger than the one in HCS. This conclusion seems to be correct since the TES operates directly on purge gas loop by extracting tritium from there, thus affecting first the tritium amount present inside this system.

Anyway, according to the literature value assumed for tritium assessment either for HCLL and HCPB blanket configurations, the adopted values (such as the one adopted as a reference value in this study), are close to 90 % of TES efficiency.

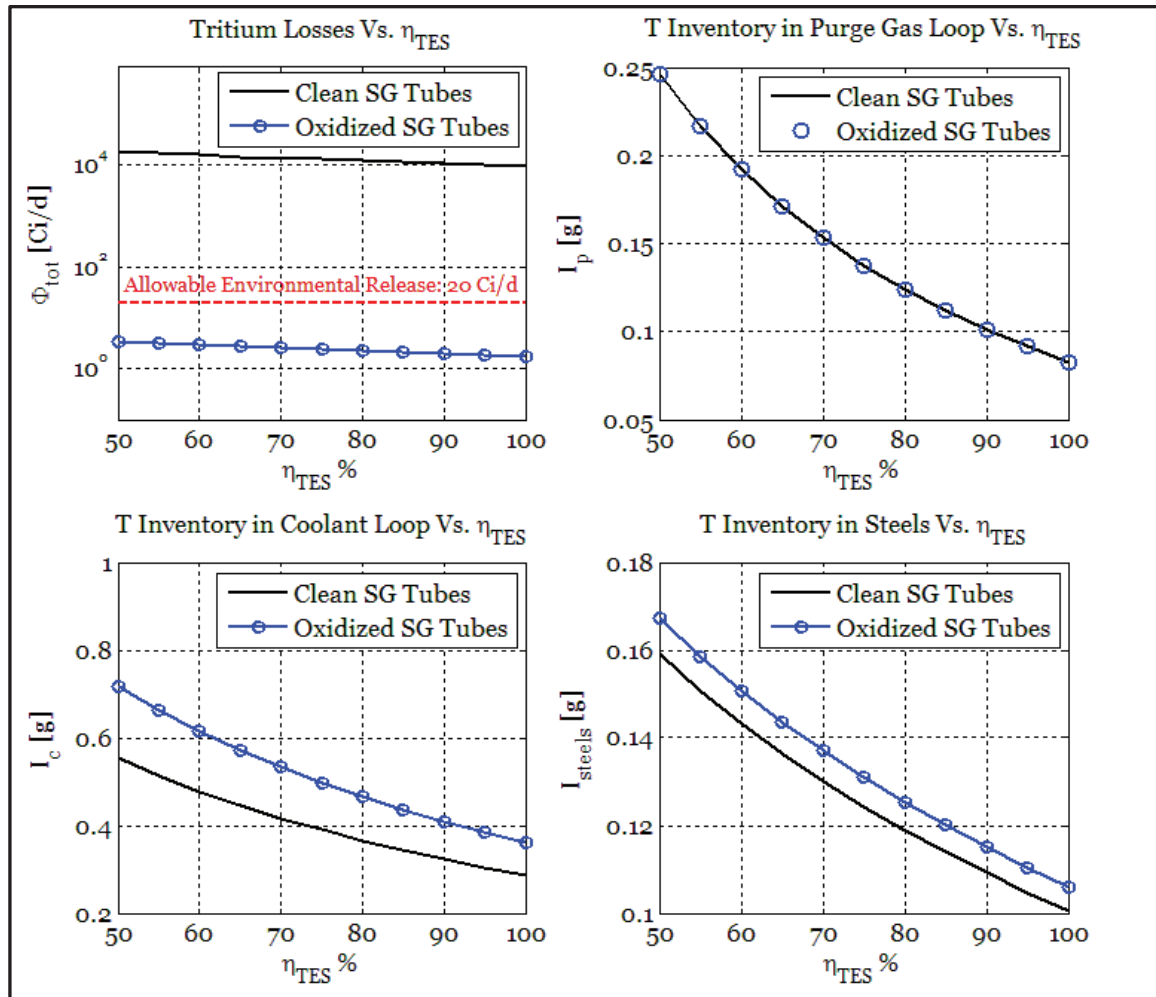


Figure 4-12 Steady State T Losses and Inventories Vs. TES Efficiency

4.4.2 Tritium Losses and Inventories Vs. CPS Efficiency

As done for TES efficiency η_{TES} , In Figure 4-13 are reported the steady state tritium losses and inventories for clean and oxidized SG tubes, obtained by varying the CPS efficiency η_{CPS} from 50 % to 100 %. The curves behaviors are apparently coincident to ones assumed in the parametric study for η_{TES} , except for the tritium inventory inside the purge gas loop which is almost constant and equal to 0.101 g either for clean and SG tubes. The tritium inventory inside the main coolant loop, as expected, dumps more significantly from 0.633 to 0.39 g and from 0.44 to 0.31 g for oxidized and clean SG tubes respectively, as the CPS efficiency increases from 50 to 100 %. This trend is well meaningful since, as η_{TES} operates directly on the purge gas loop, η_{CPS} operates on the

4. Results and Discussions

main coolant loop thus affecting mainly the tritium concentrations and partial pressures inside this loop.

Concerning the tritium losses response upon η_{CPS} variations, it is observed a dumping in the results from about 2.91 to 1.85 Ci/d in case of oxidized SG tubes and from 14100 to 10060 Ci/d in case of clean SG tubes. This leads us to conclude that the variation on CPS efficiency produce similar “effects” on T losses as those obtained by applying the same variation the TES efficiency, as reported in plot of Figure 4-12. Moreover, these results confirm the importance of assuming a correct recombination/adsorption constant between the two extreme cases adopted in this study for SG tubes surface conditions which is better discussed in the next section when dealing with the CPS recirculation rate study.

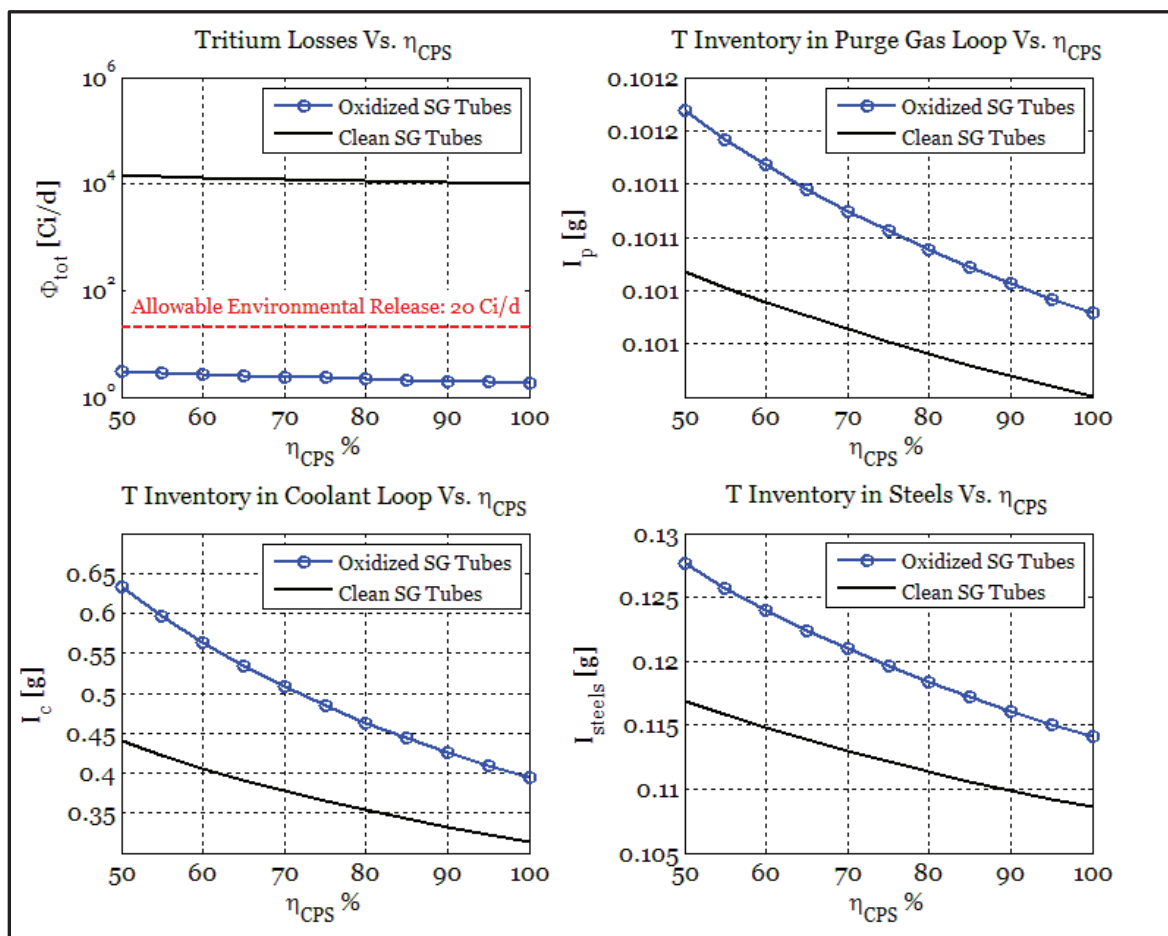


Figure 4-13 Steady State T Losses and Inventories Vs. CPS Efficiency

4.4.3 Tritium Losses and Inventories Vs. CPS Recirculation Rate

As discussed in § 3.1 a fundamental role is played by the fraction of the total coolant flowrate recirculated inside the CPS, defined as α_{CPS} . In the set of input data reported in

Table 4-4 (representing the nominal configuration of the tritium system), this parameter assumes the value of 0.1 %. This value comes also from literature values [5] and from values adopted in existing tritium assessment for HCPB blanket configuration [15]. It must be pointed out that for tritium transport analysis performed for HCLL blanket (e.g. [2], [32]) are usually adopted recirculation fractional flowrates of order of 1 %.

The objective in this section is to visualize the response of the system (in terms of tritium losses and inventories variation) if α_{CPS} ranges from 0 % (i.e. no flow rate in CPS) to 2 % (considered as the upper limit for CPS). In order to increase the overall efficiency and in order to maintain the system as much feasible as possible, this fraction must be kept as low as possible. In Figure 4-14 are reported the computed steady state tritium losses and inventories considering the CPS to be ranged from 0 to 2 % both for clean and SG tubes surface conditions (relevant for surface-limited permeation model, as adopted as the reference one in this study on this location).

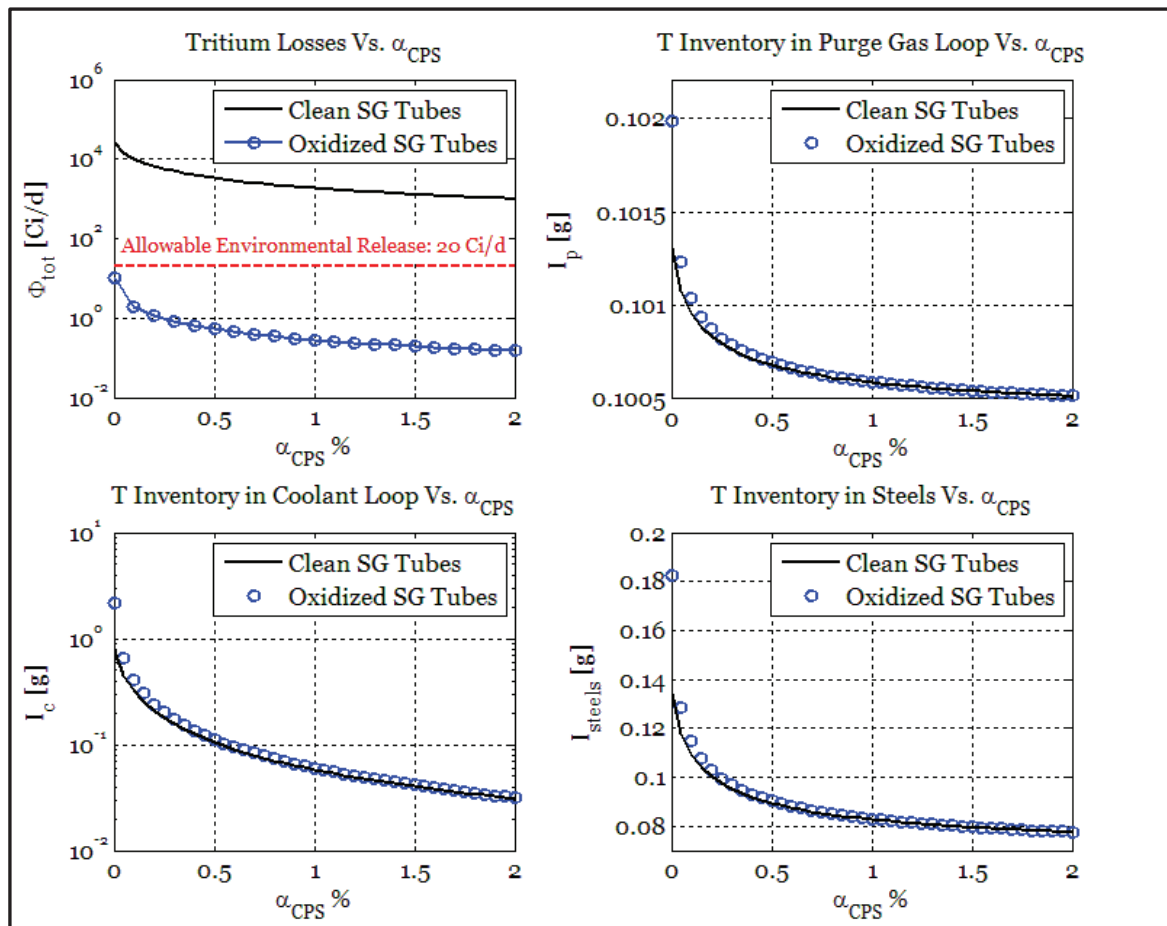


Figure 4-14 Steady State T Losses and Inventories Vs. CPS Recirculation Rate

As showed in Figure 4-14 the α_{CPS} is much more influencing the results with respect the TES and CPS efficiency, especially on T losses and T inventory in coolant loop, where the variations are wider and cover two orders of magnitude on the related plot for both SG tubes conditions. A very important aspect is remarked by the T losses results in case of oxidized SG tubes where it can be seen that even if no He coolant is recirculated inside the CPS (i.e. $\alpha_{CPS}=0$ %), the allowable environmental release limit is never reached. In fact, under these conditions the T losses are observed to vary between 7.94 to 0.15 Ci/d (for α_{CPS} equal to 0 and 2 % respectively) and T inventories inside the coolant loop and steels decay from 1.69 to 0.03 g and from 0.17 to 0.077 g respectively. T inventory inside Purge Gas Loop seems to be not affected in a relevant way from α_{CPS} as occurred for TES and CPS efficiencies. On the other hand, if assume bare INCOLOY 800 on SG pipes, we find T losses varying between 24270 and 995 Ci/d in the same operative range of α_{CPS} and the T inventories are significantly close to values reported for oxidized tubes. However, from these results it might come up stating that the CPS system is not necessary to guarantee the environmental T release below the allowable value (i.e. 20 Ci/d). Obviously this is not true, since these curves have been obtained by assuming permeation conditions which are characterized by a certain permeation regime and certain surface conditions which the given adsorption/recombination constants are corresponding to. Because of the huge gap of the recombination constant between clean and oxidized SG tubes surfaces conditions [33], the considered range for this parameter is exactly the one between the reference values for these two conditions; this is equivalent to consider oxide layers on the SG pipes surface with a different efficiency in reducing the tritium permeation flux into the HCS loop due to the change of the stability of oxide layers on the steel surface under real operating conditions [34]. Therefore, the CPS is a crucial system in compensating this degradation of the permeation barrier performed by the oxide layers during the plant operation.

In conclusion, the recirculation rate inside the CPS α_{CPS} is one of the most influencing parameter, especially in terms of tritium losses. The above plot suggests to address the effort on this system in order to mitigate tritium losses into the environment.. If these conditions are not maintained during the blanket lifetime (for instance if the coating layer formed on CPs cooling channels is being degraded by neutrons), these results might be not valid anymore as illustrated in §§ 4.3.1 and 4.3.2. Therefore, the CPS is still needed but, for economic feasibility the treated flow rate should be kept as low as possible. Another parameter, which is affecting the solution in such a relevant way is the Permeation Reduction Factor (PRF) onto CP channels, as described hereafter.

4.4.4 Tritium Losses and Inventories Vs. PRF on CPs

As reported in § 3.3.2, in order to mitigate the tritium permeation rate into the main coolant loop, it is foreseen a coating layer on the cooling channels inside the Cooling Plates (CPs), which is able (if the dominating process for the permeation is the diffusion, as assumed in this study) to provide a reduction of the permeation flux $\Phi_{\text{perm}}^{\text{CP}}$ (see Eq. (3.18)) of a factor PRF_{CP} , which is assumed until now to be equal to 10 (see Table 4-3) for the normal operative conditions.

In this section the objective is to show the influences of this parameter on tritium losses and inventories, assuming a diffusion-limited permeation regime through the CPs He channels and a surface-limited one through the SG pipes, as assumed in § 4.1.1, in which we considered this permeation asset as the reference one for the normal and the operative conditions of the our reference Tritium System, described by Figure 2-2 and by the set of features reported in Table 4-1, Table 4-2, Table 4-3 and Table 4-4. As already discussed in § 4.2.3, this PRF value is an open issue, since many values are guessed from the literature for EUROFER 97 (e.g. $15 \div 80$ [31]). Therefore, since this parameter affects both tritium losses and inventories terms with a strong impact, it is interesting to see the results obtained by varying the PRF in a reasonable range, with respect the values available from literature and from values adopted in already existing tritium assessments. In the parametric study performed in 2012 with FUS-TPC code for HCLL blanket [37], this PRF value has been ranged between 5 and 50. In this study, the range 1-100 is adopted considering the tritium permeation to be controlled by surface-limited regimes through both clean and oxidized SG tubes conditions. The results of this analysis are reported in Figure 4-15. The analysis shows that PRF_{CP} is highly affecting the solution, especially the tritium inventory inside the main coolant loop and the tritium losses, which are dumping of almost one order of magnitude for PRF_{CP} ranging between 1 to 100, whilst the tritium inventory inside the purge loop and inside the steels are not influenced in a strong way, as reported also for the parametric study of η_{CPS} and α_{CPS} (see Figure 4-13, Figure 4-14). Tritium inventory inside the purge gas loop is slightly increasing in the defined range of PRF_{CP} as expected, but as a first approximation is constant along the adopted range of PRF_{CP} (the increase is up to the 3 % of the inventory value obtained for $\text{PRF}_{\text{CP}} = 1$). The dominating tritium inventory term, as occurred also for η_{CPS} and α_{CPS} is the one inside the main coolant, which is characterized by a larger mass compared to purge gas and which is again the one responding in a much more relevant way to the considered parametric variation. Moreover, it can be noticed that in

4. Results and Discussions

case of oxidized SG tubes even for value of $PRF_{CP} = 1$ the allowable release limit of 20 Ci/d is never overcome (between 6.47 and 0.28 Ci/d), while in case of clean SG tubes we find definitively much larger values (i.e. from 39150 to 1452 Ci/d). However, as already stated in the previous section, the oxide layer on SG tubes can be degraded during the operational life of the plant and therefore the obtained T permeation flux through SG pipes might be sensitively higher. Moreover, it must be pointed out that a generic $PRF_{CP} > 1$ with the “Oxidized SG Tubes” condition are in general simultaneously satisfied, since the coating layers on SG tubes and CPs are usually supposed to be provided via chemistry control of He. Hydrogen and water are added to the coolant (with a certain molar ratio) to form this protection layer and thus to inhibit the permeation.

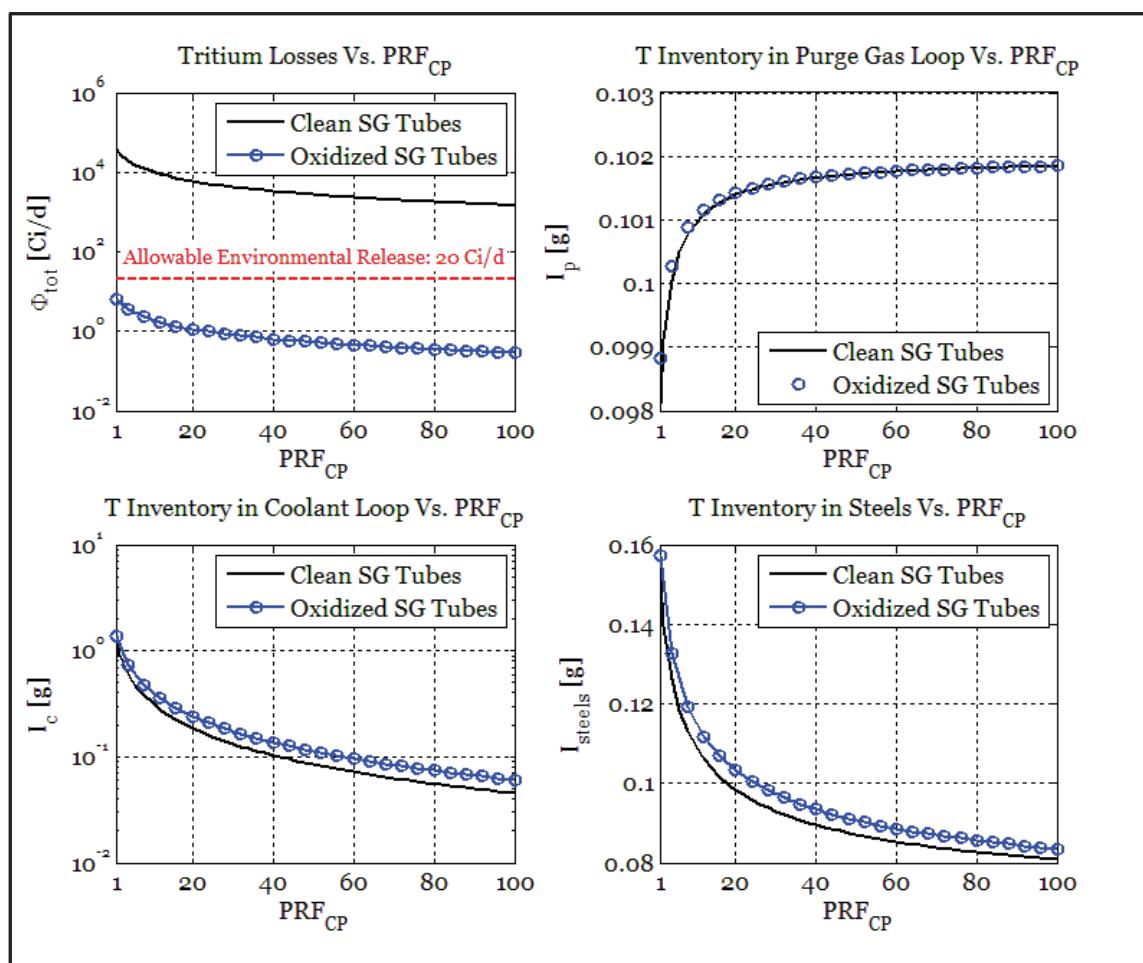


Figure 4-15 Steady State T losses and Inventories Vs. PRF on CPs

However, since the protection layer on CPs can be degraded because of severe neutronics irradiations and high temperatures conditions, thus since a $PRF_{CP} > 1$ cannot be guaranteed along the blanket lifetime, this case should be anyway considered. The oxidations layer on SG tubes is therefore assumed in this study to be less degraded

because of no-neutron fluxes and lower temperatures and able to maintain the adopted permeation regimes. In conclusion, as shown in these last two plots, the PRF on CP cooling channels is another crucial parameter for a correct tritium transport assessment, since impacts the solution in a relevant way, ranging from 5 to 50. Moreover, from the R&D point of view, some materials with more efficient PRFs should be investigated in order to reduce tritium losses lower than the safety limit even if we assume more conservative conditions (e.g. clean SG tubes surfaces).

4.4.5 Tritium Losses and Inventories Vs. PRF on SG Tubes

As discussed in § 3.3.4, the permeation flux through the SG pipes, can be described by a diffusion or a surface-limited model. In § 3.3.1 the limits of these two limiting cases have been discussed. Apparently the discriminant of the permeation model to be adopted is the tritium partial pressure involved in this process. In fact, for high values of T partial pressure, it was found that diffusion describes better the permeation phenomena, whilst for lower pressures the surface phenomena are dominating.

Since the T partial pressures involved in this study (see Figure 4-3 and Table 4-5) are lower than the one assumed to be threshold limits between the two models (about 10 Pa, as discussed in § 3.3.1), we assumed a surface-limited regime through the SG pipes until here. Moreover, we stated that at low pressures, if a diffusion model is adopted, the permeation flux is overestimated for the same value of pressure. Therefore, since the tritium partial pressures involved in tritium permeation through the CPs were close to the adopted value for threshold limit between diffusion and surface models (10 Pa), we assumed, in a conservative way, a diffusion-limited model through the CPs.

In order to complete the study and to cover all the possible cases, in this section it is assumed that the diffusion is limiting the permeation through the SG pipes. The PRF on the heat exchange pipes PRF_{SG} is studied by calculating the tritium inventories and tritium losses ranging PRF_{SG} from 1 to 400 which is assumed here to be the allowed range for this parameter. $PRF_{SG} = 400$ has been also considered in Ref. [36] as the reference value for PRF on oxidized INCOLOY 800 walls.

In plot of Figure 4-16 are visualized the results for tritium losses and inventories Vs. PRF_{SG} , obtained by considering a PRF on CPs equal to 10 and the rest of tritium system features reported in § 4.1.3. As shown on this figure, tritium losses are decreasing of about two orders of magnitudes, from 19300 to 61.5 Ci/d. These values are well above the allowed limit of 20 Ci/d. Anyway, the PRF_{CP} assumed for this simulation was equal to 10 and $\alpha_{CPS} = 0.1\%$. As reported on the top-left plot of Figure 4-16, if we adopt a $PRF_{CP} =$

4. Results and Discussions

10 and $\alpha_{CPS} = 1.0\%$, with $PRF_{SG} = 400$ tritium losses are equal to 23.69 Ci/d, which is very close to the allowable environmental release. Thereafter, if we consider to increase PRF_{CP} to 30, the T losses dump to 11.17 Ci/d for $PRF_{SG} = 400$, giving the allowable release limit of 20 Ci/d to be reached for $PRF_{SG} = 225$. However, although this set of HCPB features (i.e. CPS recirculation rate and PRF_{CP}) seems to be too stringent and optimistic to be reached, it has been already adopted in previous tritium assessments. For instance, for T assessments in HCLL DEMO blanket [32] a PRF on CPs equal to 50 has been assumed, while $PRF_{SG} = 400$ has been also reported in Ref. [36] as the reference value for tritium permeation through the Steam Generator of ceramic breeder of DEMO. Moreover, $\alpha_{CPS} = 1\%$ has been already used [2], [32] and the He operative temperatures, He inventory and mass flow rates were equal to the ones assumed for HCPB in this study (see Table 2-1, Table 4-2, Table 4-3 and Table 4-4).

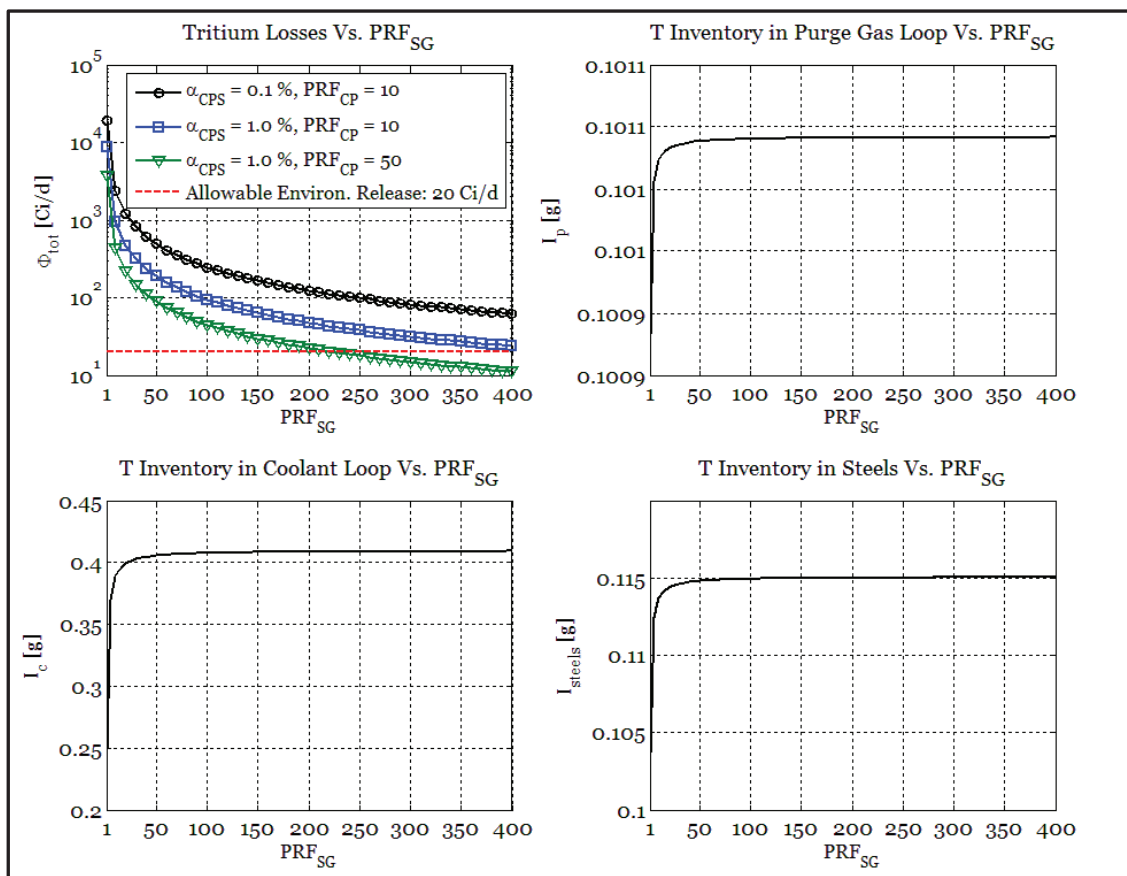


Figure 4-16 Steady State T Losses and Inventories Vs. PRF on SG Tubes (valid for diffusion-limited permeation model through SG pipes)

The tritium inventory curves reported in Figure 4-16 are quite insensitive to PRF_{SG} variations. In fact, the tritium inventory in coolant increases for the firsts PRF values included between 1 to 50 and then it stabilizes to a constant value of 0.4 g, while the

others two terms (e.g. tritium inventory inside the purge gas and inside steels) are almost constant and equal to 0.1 and 0.115 g respectively. In conclusion it can be seen that assuming a diffusion model for the permeation flux through SG tubes provides a more critical picture of HCPB blanket in terms of tritium permeation rate into the steam cycle, i.e. almost all the tritium losses. The parametric study performed in this section ends with these last results obtained for the study of PRF_{SG} . Many important parameters have been studied and analyzed in order to get a qualitative scenario of the tritium system related to HCPB blanket.

4.4.6 Overall Summary of the Parametric Study

The numerical results reported in plots from Figure 4-12 to Figure 4-16 are summarized in Table 4-11.

Ranged Parameter	Studied Parameter (<u>clean/oxidized</u> SG tubes)			
	T Losses [Ci/d]	T Invent. in Purge Gas [g]	T Invent. in Coolant [g]	T Invent. in Steels [g]
TES Efficiency				
Min. η_{TES} : 50 %	<u>17790</u> /3.37	<u>0.246</u> /0.246	<u>0.55</u> /0.71	<u>0.159</u> /0.167
Max. η_{TES} : 100 %	<u>9141</u> /1.69	<u>0.082</u> /0.082	<u>0.28</u> /0.36	<u>0.100</u> /0.105
CPS Efficiency				
Min. η_{CPS} : 50 %	<u>14100</u> /2.98	<u>0.1011</u> /0.1012	<u>0.44</u> /0.63	<u>0.116</u> /0.127
Max. η_{CPS} : 100 %	<u>10060</u> /1.85	<u>0.1010</u> /0.1010	<u>0.31</u> /0.33	<u>0.108</u> /0.114
CPS Recircul. Rate				
Min. α_{CPS} : 0.0 %	<u>24720</u> /10.21	<u>0.102</u> /0.102	<u>0.77</u> /2.169	<u>0.134</u> /0.182
Max. α_{CPS} : 2.0 %	<u>995</u> /0.15	<u>0.1005</u> /0.1005	<u>0.031</u> /0.035	<u>0.77</u> /0.77
PRF on Cooling Plates				
Min. PRF_{CP} : 1	<u>28940</u> /6.47	<u>0.098</u> /0.098	<u>1.22</u> /1.37	<u>0.151</u> /0.157
Max. PRF_{CP} : 100	<u>1452</u> /0.286	<u>0.102</u> /0.102	<u>0.062</u> /0.045	<u>0.080</u> /0.085
PRF on SG Tubes ^{††}				
Min. PRF_{SG} : 1	19300/8705	0.1009	0.25	0.103
Max. PRF_{SG} : 400	61.15/23.69	1.101	0.41	0.115

Table 4-11 Summary Results of the Sensitivity Study

Looking at the reported values, we can summarize the parametric study stating that the most relevant parameters in T migration in HCPB DEMO blanket are:

- the recombination constant on SG Tubes k_{rec}^{SG} ;

^{††} The T losses value are calculated for $\alpha_{CPS} = 0.1/1.0$ %.

4. Results and Discussions

- the recirculation flowrate in CPS α_{CPS} ;
- the Permeation Reduction Factor on Cooling Plates PRF_{CP} .

These parameters showed a deep impact on the results, as visualized in Figure 4-17, where three different values of k_{rec}^{SG} have been adopted in the reported range of α_{CPS} and PRF_{CP} .

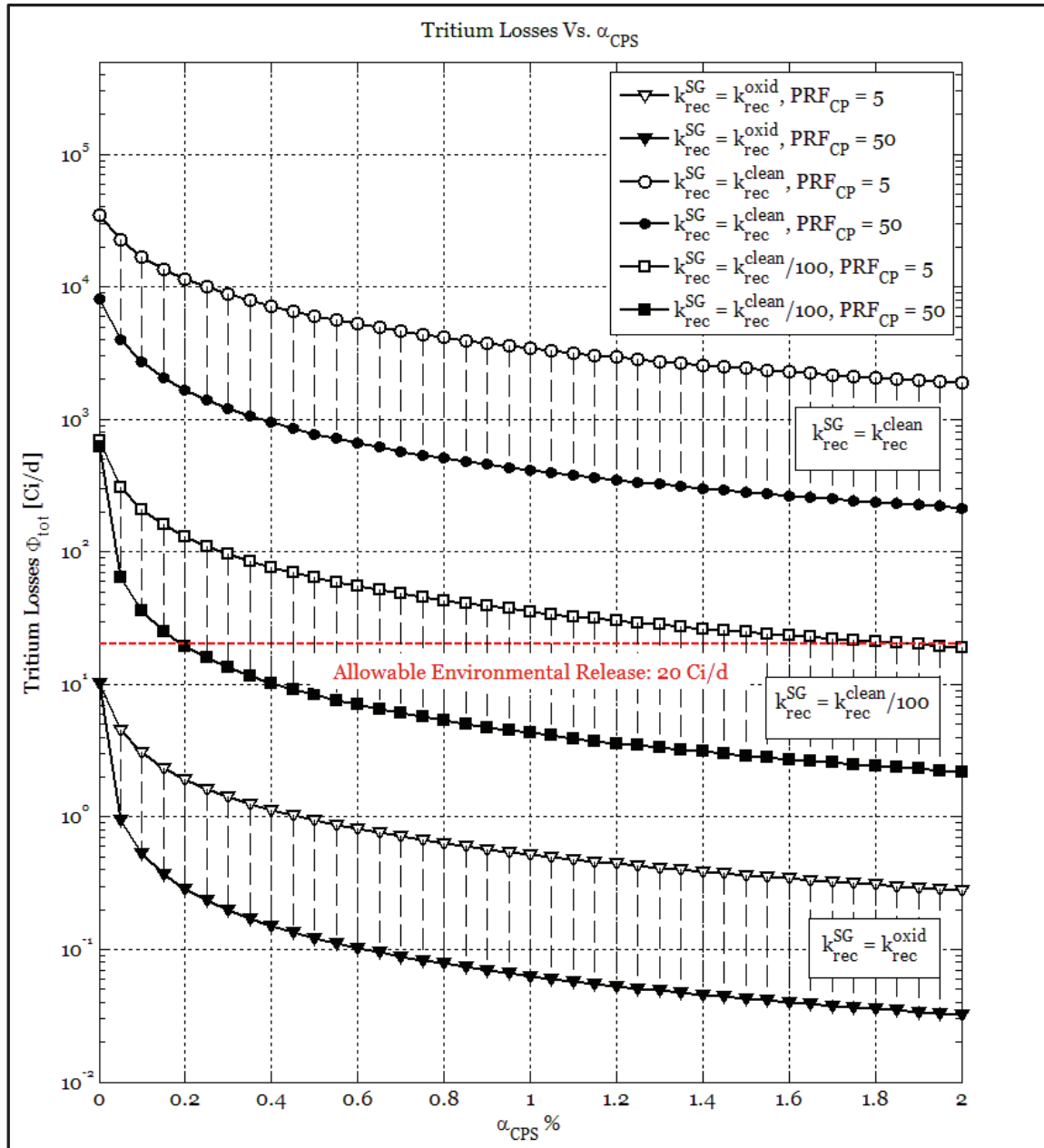


Figure 4-17 Tritium Losses Vs. α_{CPS} Vs. PRF_{CP} Vs. $T k_{rec}$. in SG tubes

As it can be seen, between the two extreme cases (i.e. clean and oxidized SG tubes) there is a huge gap in T losses results (i.e. about four orders of magnitude). If we divide

the recombination constant of clean INCOLOY 800 by 100 (i.e. $k_{\text{rec}}^{\text{SG}} = k_{\text{rec}}^{\text{clean}}/100$) we obtain the allowable environmental release limit to be reached for $\alpha_{\text{CPS}} = 0.2\%$ in case of $\text{PRF}_{\text{CP}} = 50$ and 1.9% in case of $\text{PRF}_{\text{CP}} = 5$. These results show a large sensitivity of T releases with respect the SG pipes conditions and on the “efficiency” of the oxide layer to reduce the permeation flux.

Summary and Conclusions

In this study the problem of tritium transport in Helium Cooled Pebble Bed (HCPB) DEMO blanket from the generation inside the solid breeder to the release into the environment has been studied and analyzed by means of the computational code FUS-TPC. The code has been originally developed to study the tritium transport in Helium Cooled Lead-Lithium (HCLL) blanket and it is a new fusion-devoted version of the fast-fission one called Sodium-Cooled Fast Reactor Tritium Permeation Code (SFR-TPC). The main features of the model inside the code have been described. The code has the main goal to estimate the total tritium losses into the environment and the tritium inventories inside the breeder, inside the multiplier, inside the purge gas and the main coolant loops and inside the structural materials.

This work is characterized by a brief introduction (section 1), a description of the HCPB blanket (section 2), a mathematical description of the implemented model (section 3) and by a large section dedicated to the results (section 4), in which many curves (i.e. tritium concentrations, partial pressures inventories and losses into the environment) have been reported. All of these results have been obtained considering an operative configuration of HCPB blanket, assumed to be in this study the reference one for the normal working conditions (see pars. 4.1 and 4.2). Moreover, in the same section a significant part has been dedicated to the impacts on the results of the main assumptions adopted in this study (e.g. permeation model). Finally, a parametric study has been carried out analyzing the response of has been analyzed by varying the most important HCPB blanket parameters such as: 1) the Tritium Extraction System removal efficiency η_{TES} , 2) the Coolant Purification System (CPS) efficiency η_{CPS} , 3) the recirculation rate inside the CPS α_{CPS} and the Permeation Reduction Factors (PRFs) on 4) Cooling Plates (CPs) Helium channels and on 5) Steam Generator (SG) tubes, PRF_{CP} and PRF_{SG} respectively.

In HCPB blanket tritium is generated inside the breeder in form of atomic tritium (T^-) with a local production rate \dot{G}_V^{br} and it is released into the purge gas with a time scale τ_{res} called tritium residence time; due to presence of oxygen and water inside the Li orthosilicate, tritium is assumed to be extracted from purge gas almost totally in form of tritiated water HTO (\dot{G}_{HTO}). A smaller production rate \dot{G}_V^{Be} is also present in Beryllium pebble beds, in which large amounts of tritium can be retained and only a little fraction

of produced tritium f_r is released from Be pebbles. Since HT is a gaseous (and permeable) hydrogen specie, a permeation flux (Φ_{perm}^{CP}) across the CPs, which are placed between Beryllium and breeder pebble beds, occurs as well. This permeated tritium then reaches the primary coolant system (HCS), giving thus a source term for it. Another important contribution to tritium inside the HCS might come from tritons implanted onto First Wall (FW) giving an implantation tritium flux (Φ_{imp}^{FW}). Once tritium gets into the purge gas loop, due to the presence of swamping hydrogen inside purge Helium (with a swamping ratio fixed to 0.1 %), the well-known chemical equilibrium $HT + H_2O \leftrightarrow H_2 + HTO$ takes place and a certain amount of HTO (Δ_{HTO}^P) gets converted into tritium hydride (HT), giving a source term for HT specie inside the purge loop. After getting into the purge gas, tritium is extracted in Tritium Extraction System (TES), with a certain removal efficiency η_{TES} giving a total tritium extraction rate from the purge gas $\Phi_{TES} = \Phi_{TES}^{HT} + \Phi_{TES}^{HTO}$, and characterizing two sink terms for HT and HTO tritium amounts inside the purge loop. Then, following the tritium transport paths, the permeated tritium fluxes from FW (Φ_{imp}^{FW}) and from CPs He channels (Φ_{perm}^{CP}) get in HCS, in which, due to hydrogen and water addition for the oxidation control, the isotope exchange rate from HT to HTO (Δ_{HT}^c) takes place, because of the same chemical equilibrium as considered for Δ_{HTO}^P . In HCS, the tritium fluxes Φ_{CPS}^{HT} and Φ_{CPS}^{HTO} are extracted by re-circulating inside the CPS a certain fraction of total Helium mass flow rate inside the coolant loop α_{CPS} in which the tritium fluxes Φ_{CPS}^{HT} and Φ_{CPS}^{HTO} are extracted with an efficiency η_{CPS} . Finally, a tritium permeation fluxes through the Steam Generator (SG) tubes walls (Φ_{perm}^{SG}) gets into the steam circulating the Power Conversion System (PCS), which is considered to be lost into the environment. As will be shown in the results, this tritium amount constitutes an important contribution to the total tritium losses. Finally, a certain amount of tritium released into the environment due to Helium leakage from seals and material imperfections of the coolant circuit $\Phi_{HT/HTO}^{leak}$.

A comparison between FUS-TPC results and those obtained by other authors (i.e. Ricapito [15], and Dalle Donne [23]) revealed that FUS-TPC outputs are quite satisfactory. In fact, HT and HTO steady state average concentrations inside the purge gas loop computed with FUS-TPC are observed to be 8.751 ppm for HT and 0.231 ppm for HTO. According to Eq. (3.3) and to the reference scheme visualized in Figure 2-2, these values correspond to 15.45 ppm and 0.4 ppm at TES entrance/BU outlet respectively. Therefore, it seems that the obtained concentrations are as a first

approximation quite in accordance with the ones reported by other tritium transport assessment for HCPB blanket [15] (i.e. 14.5 ppm for HT and 0.5 ppm for HTO). Moreover, the obtained molar ratio between HTO and HT species inside the purge gas loop is 2.63 %, which is quite in agreement with the value reported in Ref [15] (i.e. 3.2 %).

The steady state HT concentration in Helium Cooling System (HCS), which is equal to 0.023 ppm, appears to be in agreement with the HT concentration reported in the same tritium analysis as well (0.08 ppm for HT at SG inlet, and no HTO is assumed). In the reference study [15], the indicated average value between the inlet and the outlet Coolant Purification System (CPS) HT concentration is about 0.05 ppm, while for HTO it is assumed that no HTO is present. In our study HTO concentration is calculated, and as shown in the results, HTO is present in the HCS with an HTO/HT molar ratio equal to 5%. The foreseen HT partial pressure into the purge loop to be adopted for TES design (inlet HT partial pressure) is assumed to be 1.6 Pa, which is in accordance with the obtained results, in which the calculated inlet HT partial into TES is equal to 1.63 Pa. Concerning the HT partial pressures into HCS, the reference value reported in Ref. [15] is essentially defined as 0.6 Pa, which is, as a first approximation, close to the one calculated in this study (0.185 Pa). Moreover, two different time scales for the concentrations and partial pressures evolutions have been found for purge gas and main coolant; as a matter of fact, 4 hours and 1.6 days are needed in order to reach the steady state tritium concentrations and partial pressures into the purge gas and the main coolant loops respectively. The tritium inventories inside the different HCPB blanket locations, are well determined. The tritium inventory inside the Beryllium pebbles is a crucial point and it is still an open issue. At End Of Life (Blanket EOL = 4 years in this study) the estimated tritium inventory is close to 2.7 kg, which is a large amount. The time behavior of thus inventory term has been obtained by a linear model with a given local production rate $G_v^{Be} [T/cm^3/s]$ and a release fraction $f_r(T_{av}^{Be})$ obtained by fitting the results obtained by ANFIBE 1 code and supported by lasts experimental results (see Refs. [21] and [22]) with the average Be pebbles T_{av}^{Be} temperature. This tritium inventory term has been reported in this study just for completeness and to show anyway a conservative estimation of this quantity, but it must be pointed out that tritium and helium kinetics inside Be are quite complicated to be well described and modeled in such a simplified model.

The second important term, however, is characterized by the tritium inventory inside the ceramic breeder. At EOL, the total inventory of tritium inside the breeder is about 100 g.

Tritium inventories inside purge gas and coolant loops are important especially in case of accident (thus in case of releases). These two terms are equal to 403 mg for coolant loop and 101 mg for purge gas.

The computed tritium losses defined as the sum of total permeation rate into the steam cycle $\Phi_{\text{perm}}^{\text{SG}}$ and the tritium release rate associated to the helium leakages from the main coolant circuit $\Phi_{\text{leak}}^{\text{c}}$, are giving (assuming the same blanket-related tritium system asset) values around 1.9 Ci/d, which is lower than the safety limit fixed to 20 Ci/d. These results are quite satisfactory, either because they find some matches with the literature and because the tritium amounts involved in the different sub-systems and blanket locations are not so worrying from the radiological risks point of view.

However, before getting these results a lot of assumptions have been taken and the analysis is influenced in a strong way from them. As a matter of fact, in order to show the importance and the impacts of these assumptions on the results (essentially in terms of tritium losses and inventories inside the main blanket locations), the total tritium losses and inventories have been reported in § 4.3 by considering the following conflicts inside this tritium migration study, such as: 1) Oxidized Vs. Clean SG tubes surfaces (assuming a surface-limited permeation regime through the SG pipes); 2) Diffusion Vs. Surface-limited permeation models through CPs and SG pipes and 3) Presence Vs. Absence of a FW protection layer. The results showed that tritium losses range by almost four orders of magnitude between clean and oxidized SG tubes (from 1.93 to 10430 Ci/d), while two orders of magnitudes have been found for all the possible combinations related to the permeation models adopted for the permeation fluxes through the CPs helium channels and through the SG tubes. In fact, assuming either CPs helium channels and SG pipe being without any oxidation layer (in order to give sense to the comparison between the different models) tritium losses have been observed to range between 42427 and 913 Ci/d. Finally, one order of magnitudes in tritium losses results has been verified for the FW coating layer ranging from 0 mm to 2 mm (i.e. from 1.93 to 20.82 Ci/d).

The tritium inventories in purge gas loop are quite insensitive to all of these assumptions while the ones in coolant loop vary between 0.412 and 0.324 g for different SG tubes conditions (oxidized and clean SG tubes respectively), between 0.02846 and 1.207 g for the different permeation models options and from 4.42 to 0.4096 g for the FW coating ranging from 0 to 2 mm respectively. The response of tritium inventories in steels is as sensitive as the one in coolant loop, but with lower values (see Table 4-7, Table 4-9 and Table 4-10).

The permeation model to be adopted in the estimation of the involved permeation fluxes is a crucial point. As discussed in § 3.3.4, the permeation flux can be described by a diffusion or a surface-limited model. Apparently the discriminant is the tritium partial pressure involved in this process. As a matter of fact, for high tritium partial pressures we saw that diffusion better describes the permeation phenomena, whilst for lower pressures the surface phenomena are dominating. Anyway the first idea coming from this set of results is that the assumptions affect in a relevant manner the tritium losses rather than the tritium inventories. T inventories are representing the system response since they are immediately related to the different tritium concentrations inside the loops and locations. On the other hand, tritium losses, as a first approximation, are only representative of the HT partial pressure inside the main coolant loop and thus of the HT concentration. Therefore, the assumptions adopted in this study have a strong impact only on tritium losses, while tritium inventories in all the blanket locations are less influenced.

The last part of this work is characterized by a parametric study where several parameters have been assumed as the most relevant ones and analyzed in terms of T losses and inventories responses. The idea was to vary in a certain range a given set of parameter starting from the reference DEMO blanket configuration described by the set of data reported in Table 4-2, Table 4-3 and Table 4-4. These parameters are given by: 1) TES efficiency η_{TES} , 2) CPS efficiency η_{CPS} , 3) Recirculation Rate into CPS α_{CPS} , 4) Permeation Reduction Factor (PRF) on Cooling Plates (CPs) PRF_{CP} and 5) PRF on SG tubes PRF_{SG} . The results reported in this parametric study showed that the system response in terms of tritium inventory inside the purge gas and the main coolant loops and inside the steels is less relevant than the one of the tritium losses.

For the TES efficiency η_{TES} ranging from 50 to 100 %, the tritium losses vary from about 3.5 to 0.14 Ci/d for oxidized SG tubes and about 17700 and 9000 Ci/d in case of clean SG tubes, while the tritium inventory inside the purge gas loop dumps from 0.246 to 0.082 g and the inventory inside the HCS decreases from 0.715 to 0.36 g for both cases. Tritium inventory inside steels are not affected in a relevant way from large modifications of η_{TES} , varying between 0.167 to 0.106 g (see Figure 4-12 for results).

With the same set of assumptions, we ranged the CPS efficiency η_{CPS} in the same operative limits adopted for η_{TES} . The steady state tritium losses have been found to decrease from 2.91 to 1.85 Ci/d and from about 14000 and 10000 Ci/d in case of oxidized and clean SG tubes respectively, while the tritium inventory inside the purge gas loop has been observed to be almost constant and equal to 0.101 g. The tritium inventory inside

the main coolant loop dumps from 0.633 to 0.39 g as the CPS efficiency increases from 50 to 100 % (see Figure 4-13 for results).

The recirculation rate inside the CPS α_{CPS} is observed to be quite relevant and influencing the tritium losses and inventory inside the main coolant in a strong way. In fact for α_{CPS} ranging between 0.0 % and 2.0 %, the tritium losses have been found to decrease between 7.94 to 0.15 Ci/d for oxidized INCOLOY 800 and from around 24000 to 995 Ci/d in case of bare SG tubes, that is much more sensible with respect η_{TES} and η_{CPS} . A very important aspect is remarked by these results where it can be seen that even if no He coolant is recirculated inside the CPS (i.e. $\alpha_{CPS} = 0$ %), the allowable environmental release limit is never reached. From this statement it might come up with that the CPS system is not necessary to guarantee the environmental T release below the allowable value (i.e. 20 Ci/d). Obviously this is not true since these results have been obtained by assuming specific oxidation conditions on CPs and SG tubes. If these conditions are not maintained during the blanket lifetime (for instance if the coating layer formed on CPs cooling channels is being degraded by neutrons) these results might be not valid anymore as illustrated in §§ 4.3.1 and 4.3.2. T inventories inside the coolant loop and steels decay from 1.69 to 0.03 g and from 0.17 to 0.077 g respectively. T inventory inside Purge Gas Loop seems to be not affected in a relevant way from α_{CPS} as occurred for TES and CPS efficiencies (see Figure 4-14 for results). In conclusion, the overall results obtained by studying α_{CPS} suggest us to address the effort on improving and optimizing this parameter in order to mitigate the tritium losses into the environment.

Another highly affecting parameter is the PRF on CPs cooling channels (PRF_{CP}) especially for the tritium inventory inside the main coolant loop and the tritium losses, which are dumping of almost one order of magnitude for PRF_{CP} ranging between 1 to 100, whilst the tritium inventory inside the purge loop and inside the steels are not influenced in a strong way, as reported also for the parametric study of η_{CPS} and α_{CPS} . Tritium inventory inside the purge gas loop is slightly increasing in the defined range of PRF_{CP} as expected, but as a first approximation is constant along the adopted range of PRF_{CP} (the increase is up to the 3 % of the inventory value obtained for $PRF_{CP} = 1$). The dominating tritium inventory term, as occurred also for η_{CPS} and α_{CPS} is the one inside the main coolant which is again the one responding in a much more relevant way to the considered parametric variation. The tritium losses decrease by several orders of magnitudes lower in the indicated PRF_{CP} range (i.e. from 6.47 to 0.28 Ci/d and from

around 28000 to 1471 Ci/d for oxidized and clean SG tubes respectively). For the oxidized INCOLOY 800, it can be noticed that even for value of $PRF_{CP} = 1$ the allowable release limit of 20 Ci/d is never reached. However, as already stated in the previous section, the oxide layer on SG tubes can be degraded during the operational life of the plant and therefore the obtained T permeation flux through SG pipes might be sensitively higher. Moreover, it must be pointed out that a generic $PRF_{CP} > 1$ with the “Oxidized SG Tubes” condition are in general simultaneously satisfied, since the coating layers on SG tubes and CPs are usually supposed to be provided via chemistry control of He. Hydrogen and water are added to the coolant (with a certain molar ratio) to form this protection layer and thus to inhibit the permeation. The protection layer on CPs can be degraded by neutrons irradiations and high temperatures conditions, thus since a $PRF_{CP} > 1$ cannot be guaranteed along the blanket lifetime, the dumping of PRF_{CP} until one should be anyway considered. The oxidations layer on SG tubes is therefore assumed in this study to be less degraded because of no-neutron fluxes and lower temperatures and to be able to maintain the adopted permeation regimes (see Figure 4-15 for results).

Just for the completeness it has been assumed a diffusion-limited permeation model through the SG pipes and the PRF on the SG heat exchange pipes PRF_{SG} has been analyzed. The tritium inventories and tritium losses have been calculated by ranging the PRF_{SG} from 1 to 400, which is assumed here to be the allowed range for this parameter. $PRF_{SG} = 400$ (assumed in Ref. [36] as the reference value for PRF on oxidized INCOLOY 800 walls); it appears as a quite optimistic value. As shown on the results (see Figure 4-16) the tritium losses are decreasing of about three orders of magnitude (i.e. from 19300 to 61.5 Ci/d). These values are well above the allowed limit of 20 Ci/d. Anyway the PRF on CPs assumed for this simulation is equal to 10 and $\alpha_{CPS} = 0.1\%$. If we adopt $PRF_{CP} = 10$ and $\alpha_{CPS} = 1.0\%$, with $PRF_{SG} = 400$, tritium losses are equal to 23.69 Ci/d. For a further increase of PRF_{CP} to 50, the T losses for $PRF_{SG}=400$ are dumping to 11.17 Ci/d giving the allowable release limit of 20 Ci/d to be reached for $PRF_{SG} = 225$. However, although this set of HCPB features (i.e. α_{CPS} and PRF_{CP}) seems to be too stringent and optimistic to be reached, it has been already adopted in previous tritium assessments. For instance, for T assessments in HCLL DEMO blanket [32] a PRF on CPs equal to 50 has been assumed, while $PRF_{SG} = 400$ has been also reported in Ref. [36] as the reference value for tritium permeation through the Steam Generator of ceramic breeder of DEMO. Moreover, $\alpha_{CPS} = 1\%$ has been already used [2], [32] and the He operative temperatures, He inventory and mass flow rates were equal to the ones assumed for HCPB in this study

(see Table 2-1, Table 4-2, Table 4-3 and Table 4-4). Moreover, the diffusion model for the permeation flux through SG tubes provides a more critical picture of HCPB blanket in terms of tritium permeation rate into the steam cycle, that is almost all the tritium losses. The tritium inventories in purge gas, coolant and steels are quite insensitive to PRF_{SG} variations. In fact, the tritium inventory in coolant increases for the firsts PRF values included between 1 to 50 and then it stabilizes to a stable value of 0.4 g, while the others two terms (e.g. tritium inventory inside the purge gas and inside steels) are absolutely constant to 0.1 and 0.12 g respectively. We can summarize the parametric study stating that the most relevant parameters in T migration in HCPB DEMO blanket are:

- the recombination constant on SG Tubes k_{rec}^{SG} ;
- the recirculation flowrate in CPS α_{CPS} ;
- the Permeation Reduction Factor on Cooling Plates PRF_{CP} .

In conclusion, the tritium losses target for fusion reactor are fixed to be less than 20 Ci/d; thus, more efficient tritium permeation barriers should be performed in order to keep the tritium release into the environment as low as possible. In fact, in order to accomplish the goal of 20 Ci/d of tritium release, the best way to progress is to obtain rather good values for PRFs (in particular for blanket cooling channels) or increase the Helium coolant flow rate recirculated inside the CPS. Other parameters (such as TES and CPS efficiencies) are influencing too, but in a lighter way.

A more detailed tritium transport analysis is needed to obtain a reliable picture of tritium inventories and losses in HCPB DEMO blanket. Moreover, dedicated experimental campaigns aimed to obtain more reliable material properties are needed. In particular new experiments with tritium aimed to determine more detailed surface properties of structural materials and more reliable permeation reduction factors should be carried out. In particular, under neutrons irradiations EUROFER will degrade and the PRF on CPs might be degraded as well. Therefore, it could be useful to have a set of tritium transport properties in structural materials which are exposed to high energy neutrons fluxes. At the moment, such tritium transport properties are not available in literature.

After this analysis we might state that that tritium assessments for fusion reactors breeding blankets are affected by many uncertainties which are either parametric (e.g. tritium transport properties in materials) and related to models (e.g. surface Vs. diffusion-limited permeation models). Although these problems, the HCPB blanket seems to be quite robust in terms of tritium radiological risk.

References

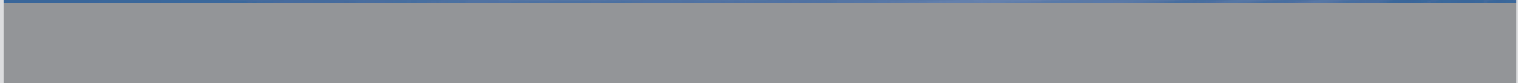
- [1] J. Freidberg, Plasma Physics and Fusion Energy. 2007. ISBN-13 978-0-521-85107-7.
- [2] F. Franza, A. Ciampichetti, I. Ricapito, M. Zucchetti. A model for tritium transport in fusion reactor components: The FUS-TPC code. Fusion Engineering and Design, 87 (2012) 299– 302.
- [3] F. Franza, Tritium Transport Analysis in Advanced Sodium-Cooled Fast Reactors, Thesis for a Master Degree in Nuclear Engineering, Politecnico di Torino, Italy (2011).
- [4] L.V. Boccaccini et al. Materials and Design of the European DEMO Blankets. Journal of Nuclear Materials, 329-333 (2004) 148-155.
- [5] M. Dalle Donne et al., Demo-relevant Test Blanket for NET/ITER. BOT Helium Cooled Solid Breeder Blanket, Kernforschungszentrum Karlsruhe, Report Kfk 4928 and 4929, October 1991.
- [6] S. Hermsmeyer, U. Fischer, M. Fütterer, K. Schleisiek, I. Schmuck, H. Schnauder, An improved European helium cooled pebble bed blanket, Fusion Engineering and Design, Volumes 58-59, November 2001, Pages 689-693.
- [7] S. Hermsmeyer et al., Lay-out of the He-cooled solid breeder model B in the European power plant conceptual study, Fusion Engineering and Design 69 (2003) 281-287.
- [8] A. Li Puma. Helium cooled lithium-lead blanket module for DEMO. Design and analyses. Report of EFDA Task Tw2-TTBC-001 D01, 2003.
- [9] Chang H. Oh, Eung S. Kim. Development and Verification of Tritium Analyses Code for a Very High Temperature Reactor. September 2009. INL/EXT-09-16743.
- [10] C. Boyer, L.Vichot , M.Fromm, Y.Losset, F.Tatin-Frouxa, P.Guétat, P.M.Badot. Tritium in plants: A review of current knowledge. Environmental and Experimental Botany. 67 (2009) 34–51.
- [11] H.D. Rohrig, R. Hecker, J. Blumensaat. J. Schaefer. Studies on the permeation of hydrogen and tritium in nuclear process heat installations Nuclear Engineering and Design 34 (1975) 157-167.

- [12] C. San Marchi, B.P. Somerday, S.L. Robinson. Permeability, solubility and diffusivity of hydrogen isotopes in stainless steels at high gas pressures. *International Journal of Hydrogen Energy* 32 (2007) 100 – 116.
- [13] A. S. Zarchy, R. C. Axtmann. Tritium permeation through stainless steel at ultra-low pressures. *Journal of Nuclear Materials*, 74 (1979) 110-117.
- [14] Bojan Zajec, Vincenc Nemanic, Cristian Ruset. Hydrogen diffusive transport parameters in W coating for fusion applications. *Journal of Nuclear Materials* 412 (2011) 116-122.
- [15] I. Ricapito Tritium recovery in the HCPB blanket for ITER and DEMO reactors EAS S.A.S. report, 325/20260378/HVT FZK, Germany, April (2004).
- [16] L.A.Sedano, Tritium Cycle Design for He-cooled blankets for DEMO, Report for TASK of the EFDA Technology Programme TW4-TTB-COMPU. January 2006.
- [17] J.L. Berton, Helium and tritium leaks in the PPCS BKT & DV cooling circuits CEA Technical document DTN/STP/LTCG/2004/032.
- [18] L.V. Boccaccini, U. Fischer, S. Malang, P. Norajitra, G. Piazza, J. Reimann, K. Schleisiek, H. Werle. Importance of Ceramic Pebble Bed Density and Tritium Residence Time for the HCPB Blanket Design in a Power Reactor. CBBI-7 Presentations at Seventh International Workshop on Ceramic Breeder Blanket Interactions, September 14-16, Petten, Netherlands.
- [19] L.V. Boccaccini, L. Giancarli, G. Janeschitz, S. Hermsmeyer, Y. Poitevin, A. Cardella, E. Diegele. Materials and design of the European DEMO blankets. *Journal of Nuclear Materials* 329–333 (2004) 148–155.
- [20] E. Rabaglino, J.P. Hiernaut, C. Ronchi, F. Scaffidi-Argentina. Helium and tritium kinetics in irradiated beryllium pebbles. *Journal of Nuclear Materials*, 307–311 (2002) 1424.
- [21] Elisa Rabaglino. Helium and Tritium in neutron-irradiated beryllium. PhD Thesis, Forschungszentrums Karlsruhe GmbH, Karlsruhe. July 2004. ISSN 0947-8620.
- [22] Scaffidi-Argentina, M. Dalle Donne, C. Ronchi, C. Ferrero. ANFIBE: a comprehensive model for swelling and tritium release from neutron irradiated beryllium – II: comparison of models predictions with experimental results. *Fusion Technology*, 33 (1998) 146-163.
- [23] M. Dalle Donne, S. Dorner. Some Consideration on Tritium Control in a Helium Cooled Ceramic Blanket for the NET Reactor. KfK 3765, EUR 7993e. June 1984.
- [24] E. Serra, A. Perujo. The surface rate constants of deuterium in the martensitic steel DIN 1.4914 (MANET). *Journal of Nuclear Materials* 223 (1995) 157-162.

-
- [25] E. Serra, G. Benamati, O.V. Ogorodnikova. Hydrogen isotopes transport parameters in fusion reactor materials. *Journal of Nuclear Materials* 255 (1998) 105–115.
- [26] R. Lässer, G. L. Powell. Solubility of protium, deuterium and tritium in palladium-silver alloys at low hydrogen concentrations. *Journal of the Less-Common Metals*, 130 (1987) 387 – 394.
- [27] O. V. Ogorodnikova, X. Raepsaet, M. A. Fütterer. Tritium permeation through the first wall of the EU-HCPB blanket. *Fusion Engineering and Design* 49–50 (2000) 921–926.
- [28] Z. Xu, J. Rey, U. Fisher, A. v.d. Weth, C. Polixa. Development of a DEMO Helium Cooled Pebble Bed (HCPB) Breeder Unit Featured in Flat Plates with Meandering Channels. Report FZKA 7181, Forschungszentrum Karlsruhe, 2006.
- [29] Y. Chen, U. Fischer, P. Pereslavytsev and F. Wasastjerna. The EU Power Plant Conceptual Study – Neutronic Design Analyses for Near Term and Advanced Reactor Models. Report FZKA 6763, Forschungszentrum Karlsruhe, 2002.
- [30] S. Hermsmeyer et al. Improved Helium Cooled Pebble Bed Blanket. Report FZKA 6399, Forschungszentrum Karlsruhe, 1999.
- [31] G.W.Hollenberg, E.P.Simonen, G.Kalinin, A.Terlain. Tritium/hydrogen barrier development. *Fusion Engineering and Design* . 28 (1995) 190-208.
- [32] O.Gastaldi, N.Ghirelli, F.Gabriel, L.Giancarli, J.F.Salavy. Tritium transfers and main operating parameters impact for demo lithium lead breeding blanket (HCLL). *Fusion Engineering and Design*, 83 (2008) 1340–1347.
- [33] G.A. Esteban, A. Perujo, L.A. Sedano, F. Legarda, B. Mancinelli, K. Douglas. Diffusive Transport Parameters and Surface Rate Constants of Deuterium in Incoloy 800. *Journal of Nuclear Materials* 300 (2002) 1-6.
- [34] A. Perujo, J. Reimann, H. Feuerstein, B. Mancinelli. The oxidation kinetics of Incoloy 800 and its deuterium. *Journal of Nuclear Materials*, 283-287 (2000) 1292-1296
- [35] W. Farabolini et al. Tritium control modelling for a helium cooled lithium–lead blanket of a fusion power reactor. *Fusion Engineering and Design* 81 (2006) 753–762.
- [36] M.A.Futterer, X.Raepsaet, E.Proust. Tritium permeation through helium-heated steam generators of ceramic breeder blankets for DEMO. *Fusion Engineering and Design* 29 (1995) 225-232.

References

- [37] F. Franza, A.Ciampichetti, I.Ricapito, M. Zucchetti. "Sensitivity Study for Tritium Permeation in Helium-Cooled Lithium-Lead DEMO Blanket with the FUS-TPC code", ANS Topical Meeting on the Technol. of Fusion Energy, Nashville, August 2012 (To be published on Fusion Science and Technology (2013)).



ISSN 1869-9669
ISBN 978-3-7315-0012-4

